Identification and characterization of rickettsial proteins at the host-pathogen interface

by

Allen Garrett Sanderlin

B.A. Neuroscience
Kenyon College, 2015

SUBMITTED TO THE DEPARTMENT OF BIOLOGY
IN PARTIAL FULFILLMENT OF THE REQUIREMENTS FOR THE DEGREE OF

DOCTOR OF PHILOSOPHY IN BIOLOGY

AT THE
MASSACHUSETTS INSTITUTE OF TECHNOLOGY

JUNE 2024

Authored by: Allen G. Sanderlin
Department of Biology
May 13, 2024

Certified by: Rebecca L. Lamason
Associate Professor of Biology
Thesis Supervisor

Accepted by: Mary Gehring
Professor of Biology
Member, Whitehead Institute
Director, Biology Graduate Committee

Identification and characterization of rickettsial proteins at the host-pathogen interface

by

Allen Garrett Sanderlin

Submitted to the Department of Biology on May 13, 2024 in Partial Fulfillment of the Requirements for the Degree of Doctor of Philosophy in Biology

ABSTRACT

Bacterial pathogens subvert host cell processes during infection by secreting protein effectors that manipulate host machinery. Cataloging such effectors has enabled a deeper exploration of the molecular basis of disease for numerous pathogens. Members of the *Rickettsia* genus are obligate intracellular bacteria that pose a growing threat to human health, but their complete dependence on the host cell niche has precluded a thorough investigation of the bacterial factors acting at the host-pathogen interface. Accurately identifying and characterizing these proteins will provide a necessary framework for understanding rickettsial biology and disease.

In this work, I demonstrate that the conserved rickettsial protein RARP-1 is not a *bona fide* secreted effector, as had been previously suggested. Instead, I found that *Rickettsia parkeri* RARP-1 localizes to the periplasm where it supports the rickettsial life cycle by promoting host cell invasion and intracellular growth. Motivated by this discrepancy, I developed a cell-selective proteomic screen to identify effectors secreted during *R. parkeri* infection. In addition to several known secreted effectors, my approach revealed the novel secreted rickettsial factors SrfA–G. Notably, these Srfs include *Rickettsia*-specific proteins of unknown function that are structurally diverse, variably conserved, and targeted to distinct host cell compartments. I further demonstrate that one of these effectors, SrfD, localizes to the endoplasmic reticulum where it interacts with the host Sec61 translocon. Taken together, this work highlights the elusive nature of rickettsial effectors while offering new ways to probe the unique biology of these bacterial pathogens.

Thesis Supervisor: Rebecca L. Lamason
Title: Associate Professor of Biology

ACKNOWLEDGEMENTS

To my advisor: Becky, thank you for helping me become a better scientist and communicator. You gave me the independence to develop my wild ideas and the support for when the science inevitably had other plans in mind. You always kept an open door for brainstorming, gave quick and insightful feedback, and offered an optimistic view to counter my trademark pessimism. Your passion for interesting biology is contagious, and you have assembled an awesome team doing equally amazing work. I am incredibly fortunate to have had you as my mentor along this journey.

To my committee: Thank you for your support and feedback from day one. You challenged me to think deeply and see my work from different angles. Mike, thank you for taking a chance on me all those years ago; the lessons I learned from your lab were the best preparation for grad school I could have. Sebastian, thank you for your encouragement when dealing with the unknown and for reminding me to be kinder to myself. And thank you to Ralph for taking the time to serve on my defense committee.

To my undergraduate mentor: Harry, thank you for seeing my interest and helping me become a part of the scientific process. I fondly remember coating slides with egg whites and the thrill of capturing my first micrograph. Your advice on balancing work and life may not have been heeded at times, but it was always appreciated.

To the Lamason lab: Thank you for being such wonderful colleagues. Your compassion, curiosity, and dedication have no rival. Special thanks to the founding cohort – Cassandra, Jon, and Yami – for being there for me whenever I needed a laugh or a shoulder to lean on. Thank you all for the wonderful conversations about science and life and the many, many trips to Area Four.

To the Building 68 community past and present: Thank you for nearly nine (!) years of hallway banter and technical support. It has been an absolute pleasure working alongside such talented and caring people.

To my friends in Boston, Columbus, and beyond: Thank you for always being there and telling me when I needed to slow down. Special thanks to James for your wisdom, enlightening me about all things pop culture, and showing me the light at the end of the tunnel; Mary for the hilarious birthday cards and many a conversation over drinks; the D&D crew for the ridiculous antics and much-needed escapism; and Tyler for your humor and bringing out the best in me since we were kids.

To my family: Thank you for your unceasing love and support. None of this would have been possible without you, and I could always count on you being my personal cheer squad. Thank you for instilling a strong work ethic in me and fostering my curiosity from the very beginning.

And to my partner: Michael, thank you for everything. I could not have asked for a more supportive companion all these years. You keep me centered when I lose sight of what matters, and you inspire me to be my best self. We met over a decade ago doing science – may we continue our journey of learning, growth, and love for decades to come.

TABLE OF CONTENTS

ABSTRACT **3**
ACKNOWLEDGEMENTS **4**
TABLE OF CONTENTS **5**
LIST OF FIGURES **7**
CHAPTER 1: INTRODUCTION **9**
Overview 10
Rickettsiosis: a growing global health threat 10
Evolution and diversity of *Rickettsia* spp. 12
Manipulating rickettsiae: advances and limitations 14
Host cell entry 15
Life in the host cytoplasm 17
Dissemination 23
Interactions with the vector cell 25
Rickettsial secretion systems 25
Sec61 34
Conclusion 37
References 37
CHAPTER 2: THE ANKYRIN REPEAT PROTEIN RARP-1 IS A PERIPLASMIC FACTOR THAT SUPPORTS *RICKETTSIA PARKERI* GROWTH AND HOST CELL INVASION **50**
Abstract 51
Introduction 51
Results 53
Discussion 71
Methods 77
References 90
CHAPTER 3: CELL-SELECTIVE PROTEOMICS REVEAL NOVEL EFFECTORS SECRETED BY AN OBLIGATE INTRACELLULAR BACTERIAL PATHOGEN **94**
Abstract 95
Introduction 95
Results 98
Discussion 111
Methods 116
References 130
CHAPTER 4: DISCUSSION **136**
RARP-1 as a periplasmic regulator of the rickettsial life cycle 137
BONCAT: optimization and future uses 143
Exploring Srf function 145
SrfD as a regulator of Sec61 activity 149

References.. 155

LIST OF FIGURES

Figure 1.1 – Rickettsial transmission cycle **11**
Figure 1.2 – Schematic cladogram of *Rickettsia* spp. groupings **14**
Figure 1.3 – *R. parkeri* life cycle during vertebrate host infection **15**
Figure 1.4 – Rickettsial secretion systems **26**
Figure 1.5 – Putative Sec-TolC pathway for RARP-1 ..... **29**
Figure 1.6 – Candidate rickettsial secreted effectors **33**
Figure 1.7 – Sec61 and the secretory pathway **35**
Figure 2.1 – Transposon mutagenesis of *rarp-1* impairs *R. parkeri* infection **55**
Figure 2.2 – RARP-1 supports bacterial growth and is dispensable for cell-to-cell spread **57**
Figure 2.3 – RARP-1 is dispensable for bacterial viability **59**
Figure 2.4 – RARP-1 is dispensable for evasion of host cell autophagy and supports host cell invasion **61**
Figure 2.5 – RARP-1 is not secreted **63**
Figure 2.6 – Tagged RARP-1 constructs and endogenous RARP-1 are not secreted **64**
Figure 2.7 – RARP-1 resides within *R. parkeri* **68**
Figure 2.8 – Inputs and eluates from co-immunoprecipitation of lysozyme-permeabilized bacteria **69**
Figure 2.9 – Co-immunoprecipitation of lysozyme-permeabilized bacteria reveals that RARP-1 interacts with other bacterial factors that access the periplasm **70**
Figure 2.10 – RARP-1 does not regulate the abundance or localization of Sca2 ..... **71**
Figure 3.1 – BONCAT permits selective labeling of rickettsial proteins **99**
Figure 3.2 – BONCAT identifies novel secreted rickettsial factors (Srfs) that are structurally diverse and variably conserved **101**
Figure 3.3 – Tryptic peptides mapping to autotransporter proteins Sca1 and OmpA **102**
Figure 3.4 – Genomic positions of *srf* loci **103**
Figure 3.5 – Srfs are secreted by *R. parkeri* into the host cell during infection **104**
Figure 3.6 – GSK-tagged SrfB and SrfE are not obviously expressed by *R. parkeri* **105**
Figure 3.7 – Srfs exhibit diverse subcellular localization patterns **108**
Figure 3.8 – SrfD interacts with host Sec61 and localizes to the ER via multiple domains **109**
Figure 3.9 – SrfD does not impact secretion of *Gaussia* luciferase **110**
Figure 4.1 – RARP-1 conservation and ANKs **139**
Figure 4.2 – Cell-selective BONCAT using PheRS* **144**

Figure 4.3 – Future uses for cell-selective BONCAT 145
Figure 4.4 – Srf AlphaFold models 147
Figure 4.5 – SrfG has putative structural homology to GAPs 148
Figure 4.6 – Sec61 spectral counts from Sec61β co-IP/MS 151
Figure 4.7 – AlphaFold model of SrfD with Sec61 152
Figure 4.8 – IRE1 reporter activity in SrfD-expressing cells 153
Figure 4.9 – Yeast toxicity assay for SrfD 154
Figure 4.10 – Infectious focus assays with ipomoeassin F treatment 155

CHAPTER 1: INTRODUCTION

Overview

Pathogens are expert cell biologists. Diverse bacteria, viruses, and eukaryotes have evolved numerous strategies to influence their hosts and drive infection (1). To do so, they deploy an arsenal of small molecules, surface proteins, and secreted protein effectors to subvert host cell machinery. No host cell function is safe: microbial factors have been found to target cytoskeletal dynamics, membrane trafficking, metabolism, processes of the central dogma, cell signaling, and more. Studying this host-pathogen interface has provided a wealth of knowledge about both microbial and host cell biology, and with each new molecular saboteur comes a clearer understanding of pathogenesis.

Rickettsia spp. are Gram-negative obligate intracellular bacteria that are carried by arthropod vectors and can be transmitted to vertebrate hosts (2). Members of this genus include the causative agents of serious human diseases, such as typhus and Rocky Mountain spotted fever. Rickettsiae are completely dependent on their hosts for survival and have evolved unique strategies to thrive within the host cell niche (3). Nevertheless, this obligate intracellular lifestyle has hindered progress towards a molecular understanding of rickettsial biology and pathogenesis (4). The identities and host cell targets of the full suite of rickettsial secreted effectors have remained particularly elusive. In the following chapter, I discuss what is known about the rickettsial life cycle and secretion as well as highlight open questions in the field.

Rickettsiosis: a growing global health threat

Pathogenic rickettsiae are carried by blood-feeding arthropods (*e.g.*, ticks, lice, fleas, and mites) and can be transmitted vertically and horizontally (Figure 1.1) (2). In the former route, rickettsiae within the eggs can be passed from mother to offspring (transovarial transmission)

and, if infecting other vector cells, can be maintained during molting (transstadial transmission). In the latter route, rickettsiae from the salivary glands and midgut can infect a vertebrate reservoir (*e.g.*, mammals, birds, reptiles, and amphibians) by regurgitation during the bloodmeal or through inoculation of a wound or mucous membranes with excretions (2, 5, 6); from there, they can be transmitted to a new vector during its bloodmeal. Except for *R. prowazekii* (discussed below), humans are considered incidental hosts for rickettsiae as they do not contribute to transmission (7).

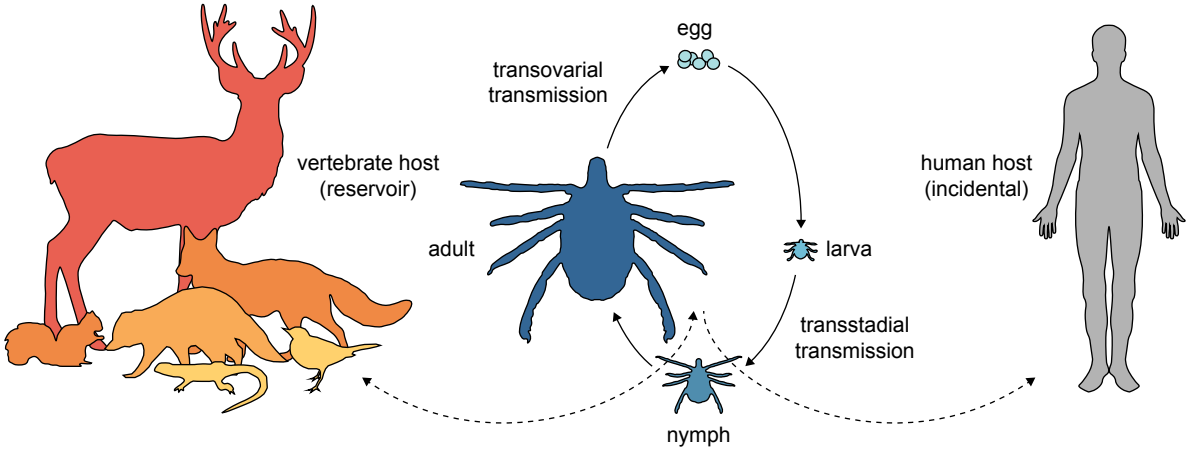

Figure 1.1 – Rickettsial transmission cycle. Rickettsiae can be maintained in an arthropod host (*e.g.*, ticks) through vertical transmission and can be transmitted horizontally during bloodmeals from a vertebrate host. For most rickettsial diseases, humans do not serve as reservoirs and are instead incidental hosts.

Within the vertebrate host, rickettsiae primarily infect the vascular endothelium but can also infect other cell types, such as macrophages, monocytes, and hepatocytes (8). Although symptoms of infection vary between species, rickettsioses frequently present with fever, headache, nausea, and myalgia (9). Such non-specific symptoms can complicate diagnosis, and serological detection of rickettsiae is generally not possible until the second week of infection. Endothelial cell death and permeabilization of the vasculature during infection with certain *Rickettsia* spp. can nevertheless provide useful diagnostic clues in the form of necrosis at the bite

site (eschar) and a systemic rash. No vaccines are available for preventing infection, but treatment with tetracyclines and chloramphenicol can be effective (10). Absent timely treatment, however, some rickettsioses can have fatality rates approaching 60–80% (11, 12).

Rickettsial diseases have been entangled with human history for centuries (13). Outbreaks of epidemic typhus, transmitted by lice carrying *R. prowazekii*, have often accompanied war and crowded, unsanitary conditions. Indeed, *R. prowazekii* has been detected in mass graves dating to the War of the Spanish Succession (1701–1714) and Napoleon's ill-fated retreat from Russia (1812), and typhus is one candidate for the plague that killed a quarter of the besieged Athenian population during the Peloponnesian War (431–404 BCE) (13–15). Although typhus is now rare in the United States, this disease still afflicts prisons, refugee camps, and marginalized communities around the world (16). Spotted fever rickettsioses (from tick bites with *e.g.*, *R. rickettsii* or *R. conorii*) likewise pose a global health threat, especially for impoverished rural and agricultural communities. In the United States alone, the incidence of spotted fever rickettsioses tripled between 2010 and 2017 (17). Changes in both climate and land use patterns have the potential to expand the habitable range for ticks and bring them in closer proximity to humans, thus exacerbating the issue (18).

Evolution and diversity of *Rickettsia* spp.

The *Rickettsia* genus is part of the α-proteobacterial order Rickettsiales, which also includes genera of ubiquitous invertebrate endosymbionts (*Wolbachia*) and other zoonotic pathogens (*Ehrlichia*, *Anaplasma*, *Orientia*). The genome reduction and metabolic parasitism (discussed below) characteristic of the Rickettsiales have drawn attention to these bacteria as close relatives of mitochondria; indeed, various phylogenomic reconstructions have placed the

mitochondrial progenitor within or basal to Rickettsiales (19–21). Nevertheless, recent analyses incorporating newly sampled genomes (*e.g.*, of putative free-living clades of Rickettsiales) have suggested that the mitochondrial ancestor diverged prior to the α-proteobacteria (22, 23), evolving host dependency independently of the Rickettsiales.

Rickettsia spp. have been classically divided into four groups of variable pathogenicity and vector tropism: the Spotted Fever (SFG), Transitional (TRG), Typhus (TG), and Ancestral (AG) Groups (24). The SFG includes tick-borne pathogens like *R. parkeri* (spotted fever rickettsiosis; studied in this work), *R. conorii* (Mediterranean spotted fever), and *R. rickettsii* (Rocky Mountain spotted fever). The TRG includes the flea-borne *R. felis* (flea-borne typhus) and mite-borne *R. akari* (rickettsialpox), and the TG includes louse-borne *R. prowazekii* (epidemic typhus) and flea-borne *R. typhi* (murine typhus). Finally, the AG includes tick-borne *R. canadensis* and *R. bellii*, which have unknown pathogenicity. Recent phylogeny estimates suggest that *R. canadensis* and *R. bellii* represent discrete clades and identify a Tamurae/Ixodes Group (TIG) that is distinct from the remaining SFG rickettsiae (Figure 1.2) (25, 26). Although all known human pathogens within the *Rickettsia* genus are carried by blood-feeding arthropods, rickettsiae have also been identified in association with plant-feeding arthropods as well as annelids, amoebae, and plants (27–31). Given our limited understanding of rickettsial biology within these contexts, however, the following discussion will focus primarily on infection of vertebrate hosts.

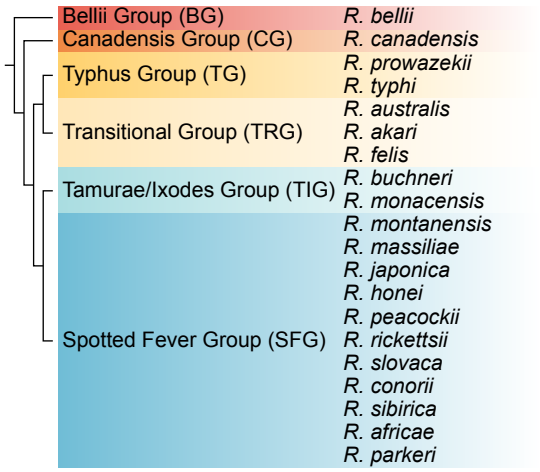

Figure 1.2 – Schematic cladogram of *Rickettsia* spp. groupings. Select species are listed for each group.

Manipulating rickettsiae: advances and limitations

The development of genetic tools for studying rickettsiae has lagged far behind that of model bacteria (*e.g.*, *Escherichia coli* and *Bacillus subtilus*) and even other intracellular bacterial pathogens (*e.g.*, members of the *Listeria*, *Salmonella*, and *Legionella* genera). Rickettsiae cannot yet be cultured axenically, and thus any attempt to study these obligate intracellular bacteria must be made within the context of a host cell. Genetic manipulation of isolated rickettsiae was first described less than three decades ago and is still plagued by low transformation efficiencies (32, 33); indeed, transposon- and plasmid-based complementation of rickettsial mutants only joined the toolkit in 2011 and 2016, respectively (34, 35). Targeted mutagenesis of rickettsiae is still in its infancy, with single reports of successful mutant generation by allelic exchange or intron retrohoming (36, 37). Instead, random mutagenesis using transposons has provided the greatest wealth of rickettsial mutants (38, 39). Studying these mutants has offered much-needed insight into the molecular underpinnings of infection. Genome-wide coverage has not yet been achieved, however, and robust systems for conditional expression or knockdown of essential genes have yet to be developed. Such advances will be critical for a more comprehensive view of rickettsial biology.

Host cell entry

Invasion

The rickettsial life cycle begins with adhesion of extracellular rickettsiae to the host cell surface (Figure 1.3). Rickettsiae use a zipper mechanism of host cell entry wherein rickettsial surface proteins engage host receptors to induce phagocytosis (40). The outer membrane protein OmpA (Sca0) binds host adhesion receptor α2β1 integrin and may also interact with fibroblast growth factor receptor FGFR1 (41, 42). Similarly, OmpB (Sca5) has been shown to bind a surface-displayed form of the DNA repair protein Ku70 (43, 44). Other rickettsial surface proteins, such as Sca1 and Sca2, have also been implicated in invasion, but their host receptors are unknown (45, 46). Interestingly, rickettsial mutants lacking any one of these proteins are still competent for invading a variety of cell types (37, 47–49), suggesting that rickettsiae use redundant strategies for entry.

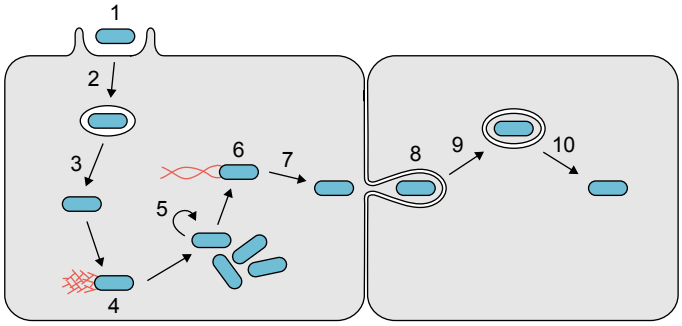

Figure 1.3 – *R. parkeri* life cycle during vertebrate host infection. 1, adhesion; 2, invasion; 3, primary vacuole escape; 4, early actin-based motility; 5, replication; 6, late actin-based motility; 7, loss of actin tail; 8, protrusion; 9, engulfment; 10, secondary vacuole escape.

Host receptor binding initiates a signaling cascade culminating in Arp2/3-mediated actin polymerization and membrane rearrangements at the contact site and subsequent bacterial engulfment (50). Plasma membrane deformation by clathrin and caveolins also supports

endocytic uptake of rickettsiae (44). Furthermore, manipulation of host membrane phosphatidylinositides by rickettsial effectors is suggested to facilitate invasion. The candidate effector RalF activates the small GTPase Arf6 (51, 52), which may ultimately lead to the generation of $PI(4,5)P_2$ and recruitment of endocytic regulators (53). Likewise, the secreted phosphatidylinositol 3-kinase effector Risk1 converts $PI(4,5)P_2$ to $PI(3,4,5)P_3$ (54), which may recruit additional factors to promote extension and eventual scission of the nascent vacuole (55). Based on what is known about the rickettsial secretion machinery (discussed below), it seems unlikely that effectors are delivered by extracellular rickettsiae piercing the plasma membrane. Instead, RalF and Risk1 secreted from rickettsiae already in the cytoplasm may prime the host plasma membrane to facilitate subsequent invasion events. Absent *ralF* or *risk1* mutants, however, the contribution of these two proteins to invasion remains to be determined.

Vacuole escape

Within minutes of contact (56), rickettsiae are internalized and rapidly escape to the host cytoplasm. *Rickettsia* spp. encode several putative membranolytic proteins that may prevent entrapment by lysing the endocytic vacuole: predicted hemolysins TlyA and TlyC (57), phospholipase D (Pld) (36), and patatin-like phospholipase A_2 enzymes Pat1 and Pat2 (58). Nevertheless, Pld is dispensable for vacuole escape (36), and only Pat1 and Pat2 have been demonstrated to be secreted during infection (58). Recent work has shown that rickettsiae lacking Pat1 are less efficient at rupturing the vacuole, which eventually matures into a degradative lysosome (59, 60). Moreover, rickettsiae still trapped within damaged vacuoles can be targeted for autophagy (discussed in more detail below) through the marking of exposed host

glycans by galectins (59). Again, the fact that *pat1* mutants are still competent for vacuole escape suggests that there are redundant mechanisms for accessing the cytoplasm.

Life in the host cytoplasm

Evasion of host defenses

Liberation from the vacuole may allow rickettsiae to bypass endolysosomal destruction, but other host defenses remain. For example, host cells can target intracellular bacteria for antimicrobial autophagy. Briefly, host E3 ligases decorate the bacterial surface with ubiquitin, ubiquitin is recognized by receptors (*e.g.*, p62 and NDP52), and these receptors in turn recruit LC3 attached to ER-derived phagophores (47, 61). Elongation and closure of the double-membrane phagophore traps bacterial cargo in an autophagosome, which can be subsequently destroyed by fusion with lysosomes.

Recent work has demonstrated that SFG member *R. parkeri* evades autophagic detection by methylating a subset of surface proteins, including the aforementioned OmpB (47). Methylation of surface-exposed Lys on these proteins precludes conjugation of ubiquitin, and rickettsiae lacking the methyltransferases PKMT1 and PKMT2 are readily polyubiquitinated by the host (62). Rickettsiae lacking OmpB are likewise polyubiquitinated and targeted for autophagy (47); genetic ablation of host Beclin-1 or ATG5, which are respectively involved in the nucleation and elongation of the phagophore (61), rescues growth of *ompB* mutant rickettsiae in macrophages (47). How OmpB shields the surface proteome from ubiquitination is unclear. OmpB may recruit host proteins that block ubiquitination or, by virtue of being the most abundant rickettsial outer membrane protein (63), it may simply camouflage the rest of the bacterial surface. Rickettsiae lacking the O-antigen, the outermost moiety of the major outer

membrane component lipopolysaccharide (LPS), are also polyubiquitinated during infection (62). It is possible that the O-antigen polysaccharide sterically occludes rickettsial surface proteins from ubiquitination. Since O-antigen mutants express elevated levels of OmpB (39), it is tempting to speculate that this is a compensatory mechanism to limit surface protein ubiquitination. Alternatively, since the lipid A anchor of LPS can serve as a non-proteinaceous target for ubiquitination in the absence of O-antigen (64), the O-antigen may protect rickettsiae from ubiquitination of LPS itself.

Interestingly, this autophagy avoidance strategy does not appear to be conserved across the genus or even among other SFG rickettsiae. TG member *R. typhi* and SFG member *R. rickettsii* str. Sheila Smith both become ubiquitinated during infection and even associate with LC3 (65), indicating autophagic capture. Nevertheless, these bacteria do not associate with the lysosomal marker LAMP2, suggesting that autophagosomal maturation is incomplete. Strikingly, the growth of these species and TRG member *R. australis* is crippled in ATG5-null macrophages (66), and thus they may benefit from induction of autophagy (in contrast to *R. parkeri*). Although many vacuolar bacterial pathogens hijack autophagy to bolster their replicative niche (67), the mechanisms by which autophagy could support the growth of cytosolic rickettsiae are unknown. Furthermore, it is unclear how closely related *Rickettsia* spp. have evolved such divergent behaviors.

In addition to autophagy, other cellular defenses combat rickettsial infection. Rickettsial growth is halted in macrophages stimulated with type I (IFN-α/β) or type II (IFN-γ) interferons, and this effect appears to be mediated in part by guanylate-binding proteins (GBPs) and inducible nitric oxide synthase (iNOS) (68). GBPs are GTPases that can target and lyse bacterial membranes (69), and the reactive nitrogen species generated by iNOS can damage bacterial

macromolecules (70). Additional anti-rickettsial defense mechanisms, such as production of reactive oxygen species and Trp deprivation, have been described (71).

Metabolic parasitism

Rickettsiae are metabolic parasites, siphoning nutrients from the host cytoplasm to support their growth. A slew of metabolic studies have shown that rickettsiae import a variety of metabolites from the host, including ATP, ribonucleotides, a majority of the proteinogenic amino acids, glycerophospholipid precursors, and enzyme cofactors (72). Moreover, rickettsial transporters for several of these metabolites have been identified and functionally validated in heterologous systems (73, 74). Comparative genomics have expanded this list of host-acquired metabolites (72), suggesting that rickettsiae also pilfer host pyruvate, flavin nucleotides, biotin, isoprenoids, glutathione, and more.

With access to such a bounty of host nutrients, these bacteria have undergone dramatic genome reduction, with genomes of approximately 1.1–1.5 Mbp (19). Rickettsial genomes contain gaps in several biosynthetic processes and have even lost entire pathways, such as glycolysis/gluconeogenesis, the pentose phosphate shunt, and biosynthesis pathways for most amino acids (72). A full characterization of these auxotrophies has important implications for both the study of rickettsial biology and the treatment of rickettsial infections. Following in the footsteps of the once-unculturable obligate intracellular pathogen *Coxiella burnetii* (75), an axenic medium for *Rickettsia* spp. would greatly facilitate the culture and genetic manipulation of these bacteria. On the other hand, recent work has highlighted how rickettsial metabolic vulnerabilities can be exploited with host-targeted therapeutics. Rickettsiae likely rely on host isoprenoids for the synthesis of peptidoglycan and ubiquinone (72); as a result, blocking host

isoprenoid biosynthesis with statins leads to rickettsial cell wall defects and growth arrest (76). Similarly, depletion of host glutathione impedes rickettsial division, actin-based motility (discussed below), and evasion of autophagy (77).

Actin-based motility

All *Rickettsia* spp. lack flagellae (78), and yet some species hijack host actin polymerization to move around the cytoplasm (79). This actin-based motility is uniquely biphasic and conferred by the polar surface proteins RickA and Sca2 (49). RickA mimics the host actin nucleation promoting factor WASP to activate Arp2/3 (80, 81); this generates a short, curved tail at the rickettsial pole consisting of a branched actin network. In contrast, Sca2 mimics host formins to directly nucleate and polymerize actin at the rickettsial pole (82, 83); this generates a long, straight tail consisting of a bundled actin network. RickA tails provide slow motility and are present during the first 2 h of infection, whereas Sca2 tails provide fast motility and are present after 8 h of infection (49). Actin-based motility is supported by a number of host actin regulators, including profilin, fimbrin, capping protein, and cofilin (84). The bacterial and/or host factors that govern the display of RickA and Sca2 are largely unexplored, but recent work identified the rickettsial cytoplasmic factor RoaM as a negative regulator of motility (85).

SFG rickettsiae are noteworthy for using two forms of actin-based motility, and it is unclear if or how this is advantageous for infection. Both RickA and Sca2 are dispensable (49), but their absence has different impacts on *R. parkeri* cell-to-cell spread (discussed below). TG rickettsiae lack RickA (81), but *R. typhi* encodes a divergent Sca2 and exhibits short, curved tails with frequent directional changes (86, 87). Although its motility has not yet been quantitively compared to that of SFG rickettsiae, *R. bellii* encodes RickA and a divergent Sca2 (83).

Interestingly, RoaM is encoded by many isolates across the genus, but it is rapidly selected against with extended passage *in vitro* (85). Future studies may shed light on how diversification of RickA, Sca2, and RoaM influences the actin-based motility of these bacteria.

Interactions with host organelles

SFG rickettsial infection is correlated with dramatic changes in host cell morphology (88). Infected cells exhibit dilation of the rough ER and outer nuclear envelope, mitochondrial swelling, and loss of Golgi apparatus organization. Such changes are notably absent from infection with TG rickettsiae (89), and limited progress has been made identifying the sources and consequences of these morphological alterations. Nevertheless, recent work implicated the secreted effector RARP-2 in disruption of the Golgi apparatus (90). Although the *cis*-Golgi is unaffected by *R. rickettsii* infection, the *trans*-Golgi is fragmented in a RARP-2-dependent manner. Moreover, dispersal of the *trans*-Golgi is associated with defective trafficking of membrane proteins to the host cell surface. RARP-2 is an ankyrin repeat protein with predicted cysteine protease activity (91), and the *trans*-Golgi phenotype is dependent on both its ankyrin repeats and putative catalytic Cys (90). Furthermore, RARP-2 induces and localizes to multilamellar structures harboring ER markers through its ankyrin repeats (91). Although the host cell target for RARP-2 is unknown, it is possible that RARP-2-mediated cleavage of an ER protein is responsible for its effects on the ER, Golgi, and, ultimately, protein trafficking.

Recent work has demonstrated that rickettsiae also interact directly with the ER. Non-motile WT *R. parkeri* have been observed tightly wrapped within rough ER membranes at low (1-2%) frequencies (92), increasing nearly 25-fold for *R. parkeri* lacking Sca2. This behavior is distinct from autophagic capture since *sca2* rickettsiae are not defective for growth and are not

readily targeted for autophagy (47). Furthermore, this behavior seems to be unique to rickettsiae since *L. monocytogenes* and *Shigella flexneri* mutants incapable of actin-based motility do not display ER wrapping (92). These ER structures are notably stable, lasting for at least one hour, and cover more than half of the rickettsial surface. Such bacterial-ER contact sites (BERCs) are reminiscent of membrane contact sites (MCSs) observed between ER and mitochondria (93, 94). Similar to MCSs, electron-dense structures appear to link ER and rickettsial surfaces (92), although the identity of these putative tethers are unknown. Depletion of two host ER tethering proteins, VAPA and VAPB, reduces BERC formation, but it is unclear if this effect is direct or indirect. It is possible that BERCs play a role in signaling or metabolic exchange between host and pathogen, as has been demonstrated for ER-organelle MCSs (93, 94). Future studies may reveal the molecular basis and functional consequences of BERC formation.

How the host cell tolerates such insults requires further investigation. In theory, prolonged disruption of cellular homeostasis by infection should trigger programmed cell death by apoptosis (95). During apoptosis, activation of proteolytic caspases results in the degradation of the cytoskeleton, fragmentation of DNA, exposure of plasma membrane phosphatidylserine to the outer leaflet, and the formation of apoptotic bodies for clearance by neighboring phagocytes (95, 96). This strategy has the dual benefit of destroying the infectious niche while preventing the release of inflammatory cytoplasmic content (95). Intriguingly, SFG rickettsiae appear to block apoptosis by activating NF-κB (97), a transcription factor that regulates expression of a number of anti-apoptotic genes (98). In contrast to uninfected cells, inhibition of NF-κB signaling during infection rapidly induces apoptosis (97). Although the bacterial factors responsible for NF-κB activation are unknown, overriding host apoptosis could extend the window for rickettsial growth leading up to the hallmark necrotic cell death described above.

Dissemination

Cell-to-cell spread

Rickettsiae use two strategies to disseminate to new host cells (71): cell-to-cell spread (used by SFG rickettsiae) and host cell lysis (used by TG rickettsiae). In cell-to-cell spread, SFG rickettsiae in the cytoplasm approach the donor cell membrane, form a short protrusion that is quickly engulfed by the recipient cell, and escape the resulting double-membrane vacuole (35). It is assumed that the same membranolytic proteins that promote release from the single-membrane endocytic vacuole during invasion also support escape from this secondary vacuole; indeed, rickettsiae lacking Pat1 exhibit reduced cell-to-cell spread (59). Curiously, and in contrast to *L. monocytogenes* and *S. flexneri* undergoing cell-to-cell spread (79), rickettsiae lose their actin tails prior to protrusion initiation (35). It is unclear how rickettsiae can form protrusions without the force from actin-based motility, and the host factors supporting rickettsial protrusion formation are unknown. This observation might suggest that motility is dispensable for rickettsial cell-to-cell spread but, paradoxically, rickettsiae lacking Sca2 are unable to spread (49). Since *rickA* mutant rickettsiae are still capable of cell-to-cell spread, the latter phase of actin-based motility provided by Sca2 seems to drive spread, possibly by positioning rickettsiae proximal to the site of protrusion formation. Future work is needed to determine if the cell-cell junctions of infected cells are permissive to rickettsial spread in the absence of Sca2 tails.

Recent work identified the secreted effector Sca4 as a mediator of protrusion engulfment (35). Sca4 harbors two vinculin binding sites (VBSs) through which it binds and inhibits the host actin adaptor protein vinculin at adherens junctions (35, 99). At adherens junctions, a ternary complex of the cadherin cytoplasmic domain, β-catenin, and α-catenin mechanically couples

cell-cell adhesion to the actin cytoskeleton (100). Pulling forces expose a VBS within α-catenin, thereby recruiting vinculin-actin to reciprocate tension at the junction. By binding vinculin, Sca4 competes with α-catenin and thus decreases junctional stiffness (35). Since Sca4 acts specifically in the donor cell, unequal tension at the junction facilitates protrusion engulfment. Rickettsiae lacking Sca4 spend more time in protrusions and exhibit defective cell-to-cell spread that can rescued by inhibition of actomyosin contractility. The fact that *sca4* mutant rickettsiae can still spread suggests that additional factors support this process. Interestingly, Sca4 and its VBSs are conserved across the *Rickettsia* genus (99), even among rickettsiae that do not undergo cell-to-cell spread. Sca4 may therefore play other roles during infection that are independent of spread.

Extracellular rickettsiae

By spreading between host cells, SFG rickettsiae can maintain relatively low burdens across a wide infectious focus and shelter within the host cell niche (3). In contrast, TG rickettsiae (and late-stage SFG rickettsiae) accumulate to high densities within a given host cell, eventually leading to cell lysis and release of the bacteria to the extracellular space. Although this strategy permits invasion of new host cells by the processes described above, it also exposes rickettsiae to the humoral immune system. In particular, the complement system should pose a threat to circulating rickettsiae. Recognition of bacterial surface molecules by complement leads to the activation of a proteolytic cascade culminating in opsonization and the formation of pores in the bacterial membrane (101). Rickettsiae are resistant to pre-immune serum (102), suggesting that they can evade destruction by complement. Heterologous expression studies have implicated several outer membrane proteins in this behavior: OmpB and Adr1/2 can respectively recruit the complement regulators factor H and vitronectin to the bacterial surface, thereby interrupting the

complement cascade (103–105). Nevertheless, avoidance of complement by *ompB* mutant rickettsiae has not been studied and, absent *adr* mutants, the contribution of these proteins to the survival of extracellular rickettsiae remains to be determined.

Interactions with the vector cell

Much of the above discussion has centered on the molecular details of vertebrate host cell infection. Nevertheless, rickettsiae also occupy arthropod vector cells during their life cycle, with reports characterizing these bacteria as anything from mutualists to parasites (106). Far less is known about this vector-pathogen interface, but recent work has highlighted ways in which rickettsial behavior is similar and different between the two niches. For example, Sca1 and OmpB have been implicated in flea and tick cell invasion, respectively, but with histone H2B as the putative cell surface ligand for OmpB (48, 107). Relatedly, invasion of tick tissues is sensitive to inhibition of Arp2/3 (108). SFG rickettsiae exhibit biphasic actin-based motility in cultured tick cells, but RickA and Sca2 are dispensable for dissemination between tick tissues (109). Finally, conflicting reports suggest that rickettsiae either inhibit or induce tick cell apoptosis to support their growth (110, 111). Clearly the lessons learned from researching vertebrate cell infection do not necessarily extend to the arthropod cell niche.

Rickettsial secretion systems

Across the inner membrane

Rickettsia spp. are Gram-negative bacteria and thus contain an inner membrane, dividing the rickettsial cytoplasm from the periplasm, and an outer membrane, dividing the periplasm from the extracellular space (*e.g.*, host cytoplasm). Delivering proteins to these various

compartments requires dedicated secretion systems and recognition signals (Figure 1.4). The following discussion highlights general features of these systems learned from studying other bacteria and what is known about their rickettsial counterparts; a more comprehensive review is provided by Gillespie *et al*. (112).

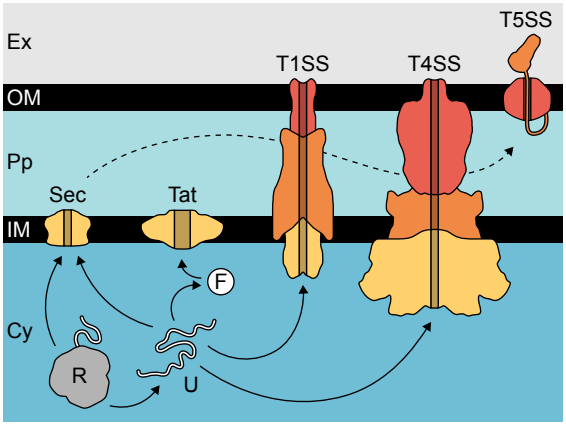

Figure 1.4 – Rickettsial secretion systems. Rickettsiae encode various machinery for delivering proteins from the cytoplasm (Cy) across the inner membrane (IM) to the periplasm (Pp) and across the outer membrane (OM) to the extracellular space (Ex). Substrates can be co-translationally (R, ribosome) or post-translationally (U, unfolded protein) translocated using the Sec system. Folded proteins (F) can be translocated to the periplasm using the Tat system. Unfolded proteins can be translocated to the extracellular space using the type I (T1SS) and type IV (T4SS) secretion systems. The putative T1SS consists of an IM ATPase (yellow), a membrane fusion protein (orange), and an OM porin (red). The T4SS includes ATPases (yellow) that face the cytoplasm, additional IM complex components (orange), and OM core complex components (red). The type V secretion system (T5SS) consists of Sec substrates whose autotransporter domains (red) serve as porins for delivery of their passenger domains (orange) to the rickettsial surface. Accessory factors supporting these systems are omitted for clarity.

Rickettsiae encode two secretion systems for exporting proteins across the inner membrane: the Sec translocon and the twin-arginine translocation (Tat) system. The Sec translocon, homologous to the eukaryotic Sec61 translocon (described below), contains a core translocation complex (SecYEG) and is supported by accessory factors in both the inner membrane (SecDF, YajC, YidC, FtsY) and cytoplasm (SecAB, SRP, TF) (113). Many proteins targeting the inner membrane, periplasmic space, and outer membrane are Sec substrates, and these proteins can be translocated co-translationally or post-translationally. Most inner membrane proteins use the former pathway, whereas most proteins destined for the periplasm

and outer membrane use the latter. During translation, a Sec signal sequence (described below) is exposed and recognized by either SRP (co-translational) or TF (post-translational) (113, 114). SRP binding temporarily halts translation, the SRP/ribosome/pre-protein complex is targeted to SecYEG by docking at the SRP receptor FtsY, and translation resumes to drive the pre-protein through the translocon. In the absence of a Sec signal sequence, an internal transmembrane helix (signal anchor) can be recognized by SRP (115). Insertion of inner membrane proteins occurs through a lateral gate of the SecY channel and is facilitated by YidC (113), although YidC can sometimes act autonomously to insert these proteins without the translocon or SRP. Conversely, TF binding does not halt translation and, instead, likely shields the signal sequence from SRP during elongation; after elongation, the chaperone SecB keeps the protein unfolded and delivers it to its receptor SecA, which uses ATP hydrolysis to drive protein translocation through SecYEG.

The canonical Sec signal sequence is a 20–30 amino acid N-terminal tag consisting of a basic N-terminal region, a hydrophobic core, and a cleavage motif. Although most inner membrane proteins retain their signal sequences, the signal sequences of periplasmic and outer membrane proteins are usually recognized and cleaved by signal peptidases. Autotransporter proteins (discussed below) sometimes contain elongated signal sequences (116), and lipoproteins harbor a unique cleavage motif containing a terminal Cys for conjugation of a lipid anchor (117). The Sec signal sequence is readily identifiable by *in silico* tools (118), although the AT-rich genomes of *Rickettsia* spp. appear to bias the cleavage motif amino acid composition away from the canonical sequence (119).

In contrast to the Sec system, the Tat system governs translocation of folded substrates (120). Here, TatC recognizes the Tat signal sequence and, as the TatABC complex, uses the

proton motive force to drive translocation across the inner membrane. The Tat signal sequence is a 30–40 amino acid N-terminal tag consisting of a basic N-terminal region containing the eponymous Arg-Arg motif, a comparably less hydrophobic core, and a cleavage motif often flanked by basic residues. *In silico* tools predict only a single Tat substrate conserved across *Rickettsia* genomes (112), suggesting that the putative rickettsial Tat system is victim to reductive evolution in these bacteria or that the amino acid composition of rickettsial Tat signals is highly divergent.

Across the outer membrane

Rickettsiae encode three secretion systems for protein delivery across the outer membrane: the type I (T1SS), IV (T4SS), and V (T5SS) secretion systems. The putative rickettsial T1SS consists of the inner membrane ATP-binding cassette transporter AprD, the periplasmic membrane-fusion protein AprE, and the outer membrane porin TolC (112, 121). ATP hydrolysis by AprD would thereby drive translocation of unfolded proteins through AprE/TolC to the extracellular space. Excluding the peptide bacteriocins, the signal sequence for T1SS substrates in other bacteria is a 50–100 amino acid C-terminal tag of variable composition that is preceded by Gly-rich repeat motifs (122, 123); these repeat motifs bind calcium to facilitate secretion and folding upon exposure to a calcium-rich extracellular environment. No T1SS substrates have been predicted for *Rickettsia* spp. (112), and it is unclear how Gly-rich motifs would support these substrates in the calcium-poor host cytoplasm (124).

A study by Kaur *et al*. (121) suggested that *Rickettsia* spp. use a non-canonical Sec-TolC pathway to export the ankyrin repeat protein RARP-1 first to the periplasm and then to the host cytoplasm (Figure 1.5). This secretion route has thus far only been shown for the small

enterotoxins STI and STII produced by pathogenic *E. coli* (125, 126). In this work (Chapter 2), I demonstrate that RARP-1 is not a *bona fide* secreted effector and instead remains in the rickettsial periplasm as a canonical Sec substrate.

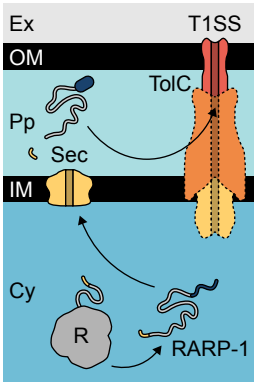

Figure 1.5 – Putative Sec-TolC pathway for RARP-1. Model proposed by Kaur *et al.* (121) wherein RARP-1 is translocated to the periplasm by the Sec system and is then secreted by TolC (red) with or without support from the rest of the T1SS apparatus. RARP-1 Sec secretion signal (yellow), intrinsically disordered region (grey), and ankyrin repeats (dark blue) are indicated. Abbreviations are the same as in Figure 1.4.

All sequenced *Rickettsia* spp. encode homologs of the *Agrobacterium tumefaciens vir* P-type T4SS for export of unfolded proteins to the extracellular space (127–130). Following the *vir* system nomenclature, the rickettsial T4SS consists of the cytoplasm-facing ATPases RvhB4, RvhB11, and RvhD4; additional inner membrane complex components RvhB3, RvhB6, and RvhB8; outer membrane core complex components RvhB7, RvhB9, and RvhB10; periplasmic lytic transglycosylase RvhB1; and major pilus subunit RvhB2. Rickettsiae do not encode a homolog of the essential minor pilus subunit VirB5 and do not appear to extend a pilus for protein delivery (112, 127). Instead, protein substrates presumably exit through the outer membrane pore. Remarkably, and despite considerable genome reduction, *Rickettsia* spp. encode paralogs of several *rvh* T4SS components (127). The *rvhB4*, *rvhB8*, and *rvhB9* genes are duplicated (a and b), with one paralog of each set deviating considerably from its *vir* counterpart. RvhB4b contains mutations in its ATPase active site and is likely catalytically inert. RvhB8a

contains mutations along its periplasmic dimerization interface and, while able to form homodimers *in vitro*, is not predicted to form a heterodimer with RvhB8b (131). Rvh9b is missing its C-terminal domain predicted to mediate interactions with RvhB7 and RvhB10 in the core complex (127). Even more strikingly, *rvhB6* is present as five highly divergent copies (a–e). RvhB6a–e contain N- and C-terminal extensions of variable length and are only unified by their multiple transmembrane helices and conserved central cytoplasmic loop. Despite evidence for surface exposure of RvhB6a (132), the topology and function of these extensions are unknown. More generally, how *rvh* gene expansion impacts the assembly and function of the T4SS remains to be determined. Although all *rvhB4*, *rvhB8*, and *rvhB9* paralogs are simultaneously transcribed during infection (127), protein expression for these and expression patterns for the *rvhB6* paralogs are unknown. Assuming some or all of these paralogs are translated, it is tempting to speculate that different T4SS assemblies govern the secretion of different substrates or are active under different conditions.

Of the secretion signals described thus far, the T4SS signal sequence is the most enigmatic. In many T4SS effectors, the last 20–100 amino acids are sufficient for translocation, but these C-terminal tails can have basic, acidic, or hydrophobic character (133–136). For other effectors, however, an additional intrinsic (*e.g.*, bipartite signal sequence) or extrinsic (*e.g.*, adaptor protein) component is required for efficient secretion (137, 138). Various score-based and machine-learning algorithms have been developed for *in silico* T4SS effector prediction (139–141). These predictions consider C-terminal amino acid composition as well as homology to known T4SS effectors (biased towards the large effector repertoire of *Legionella pneumophila*), the presence of eukaryotic-like features (*e.g.*, localization signals or interaction motifs), and the presence of cognate DNA sequence features (*e.g.*, AT skew or regulatory motifs

found in the promoters of known effectors). In my experience searching the *R. parkeri* proteome, such *in silico* tools generate effector lists replete with false positives (*i.e.*, cytoplasmic housekeeping proteins are called as secreted) and potential false negatives (*i.e.*, "known" effectors are called as non-secreted). Regarding false negatives, pull-downs with the RvhD4 coupling protein suggest that RalF, Risk1, Pat2, and RARP-2 are T4SS effectors (51, 54, 91); absent a *rvh* secretion mutant, however, the status of these proteins as *bona fide* T4SS effectors is unclear.

Although not the focus of this work, certain *Rickettsia* spp. harbor homologs of the *E. coli tra* F-type T4SS (112, 142). Encoded within the *Rickettsiales* amplified genetic element (RAGE), a predicted integrative and conjugative element, this T4SS is found intact in the genomes and/or plasmids of *R. bellii*, *R. felis*, *R. massiliae*, and *R. buchneri* (143). Apart from the TraI relaxase, however, the RAGE T4SS is assumed to mediate conjugative delivery of DNA and not protein secretion (142). Intriguingly, long pili-like structures joining pairs of bacteria have been documented for *R. bellii* (144), and these are presumably composed of the rickettsial TraA homolog.

Finally, the T5SS in *Rickettsia* spp. consists of autotransporter proteins, which mediate their own exposure to the extracellular space (112). Rickettsial autotransporter proteins contain an N-terminal Sec signal sequence, a central passenger domain, and a C-terminal autotransporter domain consisting of a β-barrel. After passing through the Sec translocon, these proteins are likely kept in an unfolded state by periplasmic chaperones (SurA, Skp, DegP) before outer membrane insertion of the autotransporter domain by the BAM complex. This β-barrel serves as a porin for translocating the passenger domain to the rickettsial surface. Most rickettsiae encode at least four autotransporter proteins – OmpA, OmpB, Sca1, and Sca2 – and their surface-

exposed passenger domains are involved in several aspects of the life cycle described above. Passenger domain cleavage has been described for these proteins, with OmpA and OmpB being substrates of the periplasmic protease RapL (145). The fact that the passenger domain of OmpB remains non-covalently associated with its autotransporter domain suggests that these cleaved domains may still function on the rickettsial surface if they are not shed into the host cytoplasm (146).

Evidence for rickettsial effector secretion

As discussed above, the toolkit for studying rickettsial biology is extremely limited; experimental validation of rickettsial effectors is therefore non-trivial. Traditional methods of effector identification, like genome-wide tagging or proteomic analysis of axenic culture broth, cannot be extended to these bacteria (147, 148). Instead, evidence for secretion has come from either heterologous expression systems or detection of rickettsial effectors *in situ*. In the former approach, rickettsial effectors are expressed in genetically tractable bacteria and assessed for their ability to be secreted or otherwise confer an effector phenotype (*e.g.*, vacuole escape by *Salmonella enterica*) (57, 121, 149). Although the results from these experiments are suggestive, they do not demonstrate effector secretion during rickettsial infection. In the latter approach, effectors are detected during infection either with antibodies or by fusion to secretion reporter constructs. Using such antibodies, RalF has been detected on the rickettsial surface (51), but only Pat1, Pat2, Sca4, Risk1, and RARP-2 have been observed in the host cytoplasm (35, 54, 58, 91). Additional evidence for Sca4 and RARP-2 secretion comes from fusions with the β-lactamase TEM-1 and the glycogen synthase kinase (GSK) tag, respectively (35, 91). Here, release to the cytoplasm is demonstrated by cleavage of the cell-permeable FRET sensor CCF4/AM by TEM-1

or phosphorylation of the GSK tag by host cytoplasmic kinases (150, 151). As described above, interactions with RvhD4 may also provide support for secretion by the T4SS, but they are not definitive proof. A summary of candidate secreted effectors discussed in this chapter and the evidence for their secretion is provided below (Figure 1.6). If detection in the infected host cytoplasm is considered a necessary criterion for calling an effector as secreted, only five rickettsial secreted effectors have been experimentally validated.

Hit	Evidence				References
	SL	RF	IP	Other	
TlyA					
TlyC				Complements hemolysin-null *Proteus mirabilis*; expression in *S. enterica* increases vacuole escape	(57, 149)
Pat1	+				(58)
Pat2	+		+		(54, 58)
Pld				Ab treatment reduces cytotoxicity (non-target Ab control not provided); expression in *S. enterica* increases vacuole escape	(57, 152)
Sca4		+		Found on surface and in host cytoplasm by IF	(35)
Risk1	+		+	Found on surface by IF; sensitive to protease K treatment; Ab treatment reduces invasion efficiency	(54)
RalF			+	Found on surface by proteomics and IF; sensitive to protease K treatment; Ab treatment reduces invasion efficiency	(51, 54, 132)
RARP-1	+*			Secreted by *E. coli* in a TolC-dependent manner*	(121)
RARP-2		+	+	Colocalizes with host ER markers by IF	(91)

Figure 1.6 – Candidate rickettsial secreted effectors. Experimental evidence for (or against) secretion is indicated. No evidence has been provided for secretion of TlyA. Asterisks indicate findings refuted by this work. SL, selective lysis immunoblotting; RF, secretion reporter fusion; IP, co-immunoprecipitation with RvhD4; Ab, antibody; IF, immunofluorescence microscopy.

An unexplored secretome

Each of the candidate effectors above was identified *in silico* by virtue of a putative enzymatic or protein interaction domain. RalF, for example, was flagged because it contains a Sec7 guanine nucleotide exchange factor domain similar to that of the *L. pneumophila* effector RalF (51). Likewise, Sca4 was identified in a search for VBSs encoded by rickettsiae several years before confirmation of its secretion (35, 99). These putative effector domains may be low-hanging fruit, but they should not be the sole source of rickettsial effector discovery. On the one

hand, the presence of a suggestive domain does not guarantee that a candidate effector is, in fact, secreted; as discussed in this work (Chapter 2), the ankyrin repeat protein RARP-1 is not a secreted effector. On the other hand, such domain searches are myopic given the extraordinary diversity of effectors employed by other intracellular bacterial pathogens. For example, *L. pneumophila* RavC, *S. enterica* SteA, *C. burnetii* MceA, and *Chlamydia trachomatis* CteG all lack known effector domains (153–156).

Rickettsiae, with their streamlined genomes, are likely not as prolific as *L. pneumophila*, which secretes over 300 effectors, many of which are redundant (153). The predicted effector repertoires for other bacteria range from several dozen (*e.g.*, *S. flexneri* (157), *S. enterica* (158), and *C. trachomatis* (159)) to more than one hundred (*e.g.*, *C. burnetii* (160)). And yet, the single digit list of experimentally validated rickettsial effectors is still woefully short of what we might expect from a pathogen that must interact with the host cell at every step of its life cycle. Given the limitations of genetic and *in silico* approaches for effector identification in *Rickettsia* spp., alternative strategies – such as the proteomic screen discussed in this work (Chapter 3) – are required to reveal new secreted effectors.

Sec61

In this work (Chapter 3), I identify host Sec61 as an interaction partner for the novel secreted rickettsial factor SrfD. Although the impact of the SrfD-Sec61 interaction is not yet determined, a brief discussion of Sec61 as a site of interest along the host-pathogen interface is warranted. Homologous to bacterial SecYEG described above, the Sec61αβγ heterotrimer complex is the core of the eukaryotic translocon and resides in the ER membrane (Figure 1.7)

(161). Many proteins destined for the secretory pathway pass through Sec61, and these proteins can be translocated co-translationally or post-translationally.

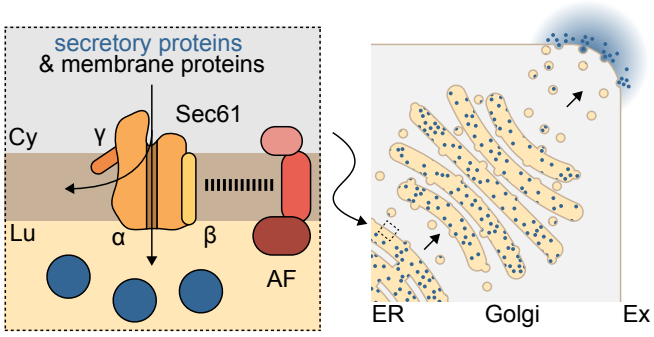

Figure 1.7 – Sec61 and the secretory pathway. Sec61 is a heterotrimer (light orange, α; yellow, β; dark orange, γ) that mediates translocation of proteins into or across the ER membrane (Cy, cytoplasm; Lu, lumen). Sec61 is supported by various accessory factors (AF) that together form the eukaryotic translocon. From the ER, secretory proteins (blue) and membrane proteins can be trafficked by vesicle-mediated transport to the Golgi and ultimately to the cell exterior (Ex).

In higher eukaryotes, co-translational translocation is used for most Sec61 substrates whereas post-translational translocation is reserved for short (≤ 100 amino acids) secretory proteins. During co-translational translocation, just like in bacteria, exposure of an N-terminal signal peptide or internal signal anchor during translation is recognized by SRP. SRP binding temporarily halts translation, the SRP/ribosome/pre-protein complex is targeted to Sec61 by docking at the SRP receptor SR, and translation resumes to drive the pre-protein through the translocon. Insertion of ER membrane proteins occurs through a lateral gate of the Sec61α channel and may be facilitated by a YidC homolog. The YidC homolog TMCO1 (together with OPTI and the PAT and BOS complexes) associates with Sec61 to promote insertion of multi-pass transmembrane proteins (162, 163); another YidC homolog, EMC3 (as part of the ER membrane complex), may also support insertion of some single- and multi-pass transmembrane proteins (164–166), but a direct interaction with Sec61 has not yet been identified. Co-translational translocation is also supported by Sec61 interactions with the TRAP (which facilitates ribosome

docking, signal peptide insertion, and nascent protein folding in the lumen) and TRAM1 (which may support passage through the lateral gate) complexes in the ER membrane (167, 168).

Short secretory proteins, which are synthesized too quickly for efficient SRP targeting, are maintained in an unfolded by cytosolic chaperones (mainly calmodulin) and traverse the Sec61 post-translationally (169, 170). Interaction between Sec61 and a dimer of Sec62 and Sec63 appears to be mutually exclusive of ribosome binding (161, 171), and this complex likely recruits ER lumenal chaperones such as BiP to ratchet unfolded proteins through the translocon using the energy from ATP hydrolysis (161, 170, 172).

Other accessory factors associate with the Sec61 translocon to influence secretory protein biogenesis and ER homeostasis. For example, SPC cleaves signal peptides, OST N-glycosylates nascent glycoproteins, and the lectin chaperones malectin and calnexin facilitate glycoprotein folding (161). Aside from their aforementioned chaperone roles, calmodulin and BiP can respectively interact with the cytoplasmic and lumenal faces of Sec61 to close the channel after protein translocation and thus limit calcium leakage from the ER (173, 174). Moreover, recent work identified an interaction between Sec61 and the ER stress sensor IRE1 (175, 176); disruption of the Sec61-IRE1 interface leads to premature IRE1 activation and prevents its attenuation during sustained ER stress (175, 176).

Although Sec61 was not previously known as a target for protein effectors, some naturally-occurring small molecule Sec61 inhibitors have been characterized (177, 178). These include fungal cotransin and decatransin, plant ipomoeassin F, cyanobacterial apratoxin A and coibamide A, and the human pathogen *Mycobacterium ulcerans* toxin mycolactone. Interestingly, these inhibitors bind at the lateral gate of Sec61α and stabilize the channel in a closed state, with different inhibitors exhibiting broad or client-selective effects. Mycolactone is

particularly noteworthy, since its inhibitory effect on Sec61 appears to mediate the immune signaling suppression and endothelial dysfunction observed during infection with *M. ulcerans* (179, 180). It is tempting to speculate that modulation of Sec61 activity is a widely distributed strategy to subvert fundamental cell biological processes.

Conclusion

Despite the challenges associated with studying *Rickettsia* spp., we are steadily uncovering how these bacteria have mastered their intracellular niche. They thwart host defenses, commandeer host nutrients, and sculpt host structures for their own ends. At the heart of this biological puppetry is an array of surface proteins and secreted protein effectors dedicated to manipulating host cell processes. A deeper investigation of such molecular weaponry will be crucial to understanding rickettsial biology and pathogenesis. In Chapter 2, I show that the purported effector RARP-1 is not secreted to the host cytoplasm but instead acts in the periplasm to support various aspects of the rickettsial life cycle. In Chapter 3, I describe the development of a proteomic screen to identify a diverse set of novel secreted rickettsial factors, including an effector that interacts with Sec61. Finally, in Chapter 4, I discuss the implications of this work and future avenues of study.

References

1. Welch MD. 2015. Why should cell biologists study microbial pathogens? Mol Biol Cell 26:4295–4301.
2. Walker DH, Ismail N. 2008. Emerging and re-emerging rickettsioses: endothelial cell infection and early disease events. Nature Reviews Microbiology 6:375.
3. McGinn J, Lamason RL. 2021. The enigmatic biology of rickettsiae: recent advances, open questions and outlook. Pathog Dis 79:ftab019.

4. McClure EE, Oliva Chávez AS, Shaw DK, Carlyon JA, Ganta RR, Noh SM, Wood DO, Bavoil PM, Brayton KA, Martinez JJ, McBride JW, Valdivia1 RH, Munderloh UG, Pedra JHF. 2017. Engineering of obligate intracellular bacteria: progress, challenges and paradigms. Nat Rev Microbiol 15:544–558.

5. Hornok S, Kováts D, Csörgő T, Meli ML, Gönczi E, Hadnagy Z, Takács N, Farkas R, Hofmann-Lehmann R. 2014. Birds as potential reservoirs of tick-borne pathogens: first evidence of bacteraemia with Rickettsia helvetica. Parasit Vectors 7:128.

6. Sánchez-Montes S, Isaak-Delgado AB, Guzmán-Cornejo C, Rendón-Franco E, Muñoz-García CI, Bermúdez S, Morales-Diaz J, Cruz-Romero A, Romero-Salas D, Dzul-Rosado K, Lugo-Caballero C, Colunga-Salas P, Becker I. 2019. Rickettsia species in ticks that parasitize amphibians and reptiles: Novel report from Mexico and review of the worldwide record. Ticks and Tick-borne Diseases 10:987–994.

7. Helminiak L, Mishra S, Keun Kim H. Pathogenicity and virulence of Rickettsia. Virulence 13:1752–1771.

8. Sahni A, Fang R, Sahni S, Walker DH. 2019. Pathogenesis of Rickettsial Diseases: Pathogenic and Immune Mechanisms of an Endotheliotropic Infection. Annu Rev Pathol 14:127–152.

9. Stewart AG, Stewart AGA. 2021. An Update on the Laboratory Diagnosis of Rickettsia spp. Infection. Pathogens 10:1319.

10. Biggs HM. 2016. Diagnosis and Management of Tickborne Rickettsial Diseases: Rocky Mountain Spotted Fever and Other Spotted Fever Group Rickettsioses, Ehrlichioses, and Anaplasmosis — United States. MMWR Recomm Rep 65.

11. Bechah Y, Capo C, Mege J-L, Raoult D. 2008. Epidemic typhus. Lancet Infect Dis 8:417–426.

12. Parola P, Paddock CD, Socolovschi C, Labruna MB, Mediannikov O, Kernif T, Abdad MY, Stenos J, Bitam I, Fournier P-E, Raoult D. 2013. Update on Tick-Borne Rickettsioses around the World: a Geographic Approach. Clin Microbiol Rev 26:657–702.

13. Angelakis E, Bechah Y, Raoult D. 2016. The History of Epidemic Typhus. Microbiol Spectr 4.

14. Nguyen-Hieu T, Aboudharam G, Signoli M, Rigeade C, Drancourt M, Raoult D. 2010. Evidence of a Louse-Borne Outbreak Involving Typhus in Douai, 1710-1712 during the War of Spanish Succession. PLoS One 5:e15405.

15. Raoult D, Dutour O, Houhamdi L, Jankauskas R, Fournier P-E, Ardagna Y, Drancourt M, Signoli M, La VD, Macia Y, Aboudharam G. 2006. Evidence for Louse-Transmitted Diseases in Soldiers of Napoleon's Grand Army in Vilnius. J Infect Dis 193:112–120.

16. Salje J, Weitzel T, Newton PN, Varghese GM, Day N. 2021. Rickettsial infections: A blind spot in our view of neglected tropical diseases. PLOS Neglected Tropical Diseases 15:e0009353.

17. Heitman KN, Drexler NA, Cherry-Brown D, Peterson AE, Armstrong PA, Kersh GJ. 2019. National Surveillance Data Show Increase in Spotted Fever Rickettsiosis: United States, 2016–2017. Am J Public Health 109:719–721.

18. Gilbert L. 2021. The Impacts of Climate Change on Ticks and Tick-Borne Disease Risk. Annual Review of Entomology 66:373–388.

19. Andersson SGE, Zomorodipour A, Andersson JO, Sicheritz-Pontén T, Alsmark UCM, Podowski RM, Näslund AK, Eriksson A-S, Winkler HH, Kurland CG. 1998. The genome sequence of Rickettsia prowazekii and the origin of mitochondria. 6707. Nature 396:133–140.

20. Williams KP, Sobral BW, Dickerman AW. 2007. A Robust Species Tree for the Alphaproteobacteria. J Bacteriol 189:4578–4586.

21. Wang Z, Wu M. 2015. An integrated phylogenomic approach toward pinpointing the origin of mitochondria. 1. Sci Rep 5:7949.

22. Castelli M, Sabaneyeva E, Lanzoni O, Lebedeva N, Floriano AM, Gaiarsa S, Benken K, Modeo L, Bandi C, Potekhin A, Sassera D, Petroni G. 2019. Deianiraea, an extracellular bacterium associated with the ciliate Paramecium, suggests an alternative scenario for the evolution of Rickettsiales. ISME J 13:2280–2294.

23. Schön ME, Martijn J, Vosseberg J, Köstlbacher S, Ettema TJG. 2022. The evolutionary origin of host association in the Rickettsiales. 8. Nat Microbiol 7:1189–1199.

24. Gillespie JJ, Williams K, Shukla M, Snyder EE, Nordberg EK, Ceraul SM, Dharmanolla C, Rainey D, Soneja J, Shallom JM, Vishnubhat ND, Wattam R, Purkayastha A, Czar M, Crasta O, Setubal JC, Azad AF, Sobral BS. 2008. Rickettsia Phylogenomics: Unwinding the Intricacies of Obligate Intracellular Life. PLOS ONE 3:e2018.

25. El Karkouri K, Ghigo E, Raoult D, Fournier P-E. 2022. Genomic evolution and adaptation of arthropod-associated Rickettsia. 1. Sci Rep 12:3807.

26. Verhoeve VI, Fauntleroy TD, Risteen RG, Driscoll TP, Gillespie JJ. 2022. Cryptic Genes for Interbacterial Antagonism Distinguish Rickettsia Species Infecting Blacklegged Ticks From Other Rickettsia Pathogens. Front Cell Infect Microbiol 12:880813.

27. Perlman SJ, Hunter MS, Zchori-Fein E. 2006. The emerging diversity of Rickettsia. Proceedings of the Royal Society B: Biological Sciences https://doi.org/10.1098/rspb.2006.3541.

28. Caspi-Fluger A, Inbar M, Mozes-Daube N, Katzir N, Portnoy V, Belausov E, Hunter MS, Zchori-Fein E. 2012. Horizontal transmission of the insect symbiont Rickettsia is plant-mediated. Proc Biol Sci 279:1791–1796.

29. Kikuchi Y, Sameshima S, Kitade O, Kojima J, Fukatsu T. 2002. Novel Clade of Rickettsia spp. from Leeches. Appl Environ Microbiol 68:999–1004.

30. Dyková I, Veverková M, Fiala I, Macháčková B, Pecková H. 2003. Nuclearia pattersoni sp. n. (Filosea), a new species of amphizoic amoeba isolated from gills of roach (Rutilus rutilus), and its rickettsial endosymbiont. Folia Parasitol (Praha) 50:161–170.

31. Davis MJ, Ying Z, Brunner BR, Pantoja A, Ferwerda FH. 1998. Rickettsial relative associated with papaya bunchy top disease. Curr Microbiol 36:80–84.

32. Rachek LI, Tucker AM, Winkler HH, Wood DO. 1998. Transformation of Rickettsia prowazekii to Rifampin Resistance. J Bacteriol 180:2118–2124.

33. Clark TR, Lackey AM, Kleba B, Driskell LO, Lutter EI, Martens C, Wood DO, Hackstadt T. 2011. Transformation Frequency of a mariner-Based Transposon in Rickettsia rickettsii ▿. J Bacteriol 193:4993–4995.

34. Clark TR, Ellison DW, Kleba B, Hackstadt T. 2011. Complementation of Rickettsia rickettsii RelA/SpoT Restores a Nonlytic Plaque Phenotype. Infect Immun 79:1631–1637.

35. Lamason RL, Bastounis E, Kafai NM, Serrano R, del Álamo JC, Theriot JA, Welch MD. 2016. Rickettsia Sca4 Reduces Vinculin-Mediated Intercellular Tension to Promote Spread. Cell 167:670-683.e10.

36. Driskell LO, Yu X, Zhang L, Liu Y, Popov VL, Walker DH, Tucker AM, Wood DO. 2009. Directed Mutagenesis of the Rickettsia prowazekii pld Gene Encoding Phospholipase D. Infect Immun 77:3244–3248.

37. Noriea NF, Clark TR, Hackstadt T. 2015. Targeted Knockout of the Rickettsia rickettsii OmpA Surface Antigen Does Not Diminish Virulence in a Mammalian Model System. mBio 6:e00323-15.

38. Lamason RL, Kafai NM, Welch MD. 2018. A streamlined method for transposon mutagenesis of Rickettsia parkeri yields numerous mutations that impact infection. PLOS ONE 13:e0197012.

39. Kim HK, Premaratna R, Missiakas DM, Schneewind O. 2019. Rickettsia conorii O antigen is the target of bactericidal Weil–Felix antibodies. Proceedings of the National Academy of Sciences 116:19659–19664.

40. Chan YG-Y, Riley SP, Martinez JJ. 2010. Adherence to and Invasion of Host Cells by Spotted Fever Group Rickettsia Species. Front Microbiol 0.

41. Hillman RD, Baktash YM, Martinez JJ. 2013. OmpA-mediated rickettsial adherence to and invasion of human endothelial cells is dependent upon interaction with α2β1 integrin. Cell Microbiol 15:727–741.

42. Sahni A, Patel J, Narra HP, Schroeder CLC, Walker DH, Sahni SK. 2017. Fibroblast growth factor receptor-1 mediates internalization of pathogenic spotted fever rickettsiae into host endothelium. PLoS One 12:e0183181.

43. Martinez JJ, Seveau S, Veiga E, Matsuyama S, Cossart P. 2005. Ku70, a Component of DNA-Dependent Protein Kinase, Is a Mammalian Receptor for Rickettsia conorii. Cell 123:1013–1023.

44. Chan YGY, Cardwell MM, Hermanas TM, Uchiyama T, Martinez JJ. 2009. Rickettsial Outer-Membrane Protein B (rOmpB) Mediates Bacterial Invasion through Ku70 in an Actin, c-Cbl, Clathrin and Caveolin 2-Dependent Manner. Cell Microbiol 11:629–644.

45. Riley SP, Goh KC, Hermanas TM, Cardwell MM, Chan YGY, Martinez JJ. 2010. The Rickettsia conorii Autotransporter Protein Sca1 Promotes Adherence to Nonphagocytic Mammalian Cells. Infection and Immunity 78:1895–1904.

46. Cardwell MM, Martinez JJ. 2009. The Sca2 autotransporter protein from Rickettsia conorii is sufficient to mediate adherence to and invasion of cultured mammalian cells. Infect Immun 77:5272–5280.

47. Engström P, Burke TP, Mitchell G, Ingabire N, Mark KG, Golovkine G, Iavarone AT, Rape M, Cox JS, Welch MD. 2019. Evasion of autophagy mediated by Rickettsia surface protein OmpB is critical for virulence. 12. Nat Microbiol 4:2538–2551.

48. Laukaitis HJ, Cooper TT, Suwanbongkot C, Verhoeve VI, Kurtti TJ, Munderloh UG, Macaluso KR. 2022. Transposon mutagenesis of Rickettsia felis sca1 confers a distinct phenotype during flea infection. PLOS Pathogens 18:e1011045.

49. Reed SCO, Lamason RL, Risca VI, Abernathy E, Welch MD. 2014. Rickettsia Actin-Based Motility Occurs in Distinct Phases Mediated by Different Actin Nucleators. Current Biology 24:98–103.

50. Reed SCO, Serio AW, Welch MD. 2012. Rickettsia parkeri invasion of diverse host cells involves an Arp2/3 complex, WAVE complex and Rho-family GTPase-dependent pathway. Cell Microbiol 14:529–545.

51. Rennoll-Bankert KE, Rahman MS, Gillespie JJ, Guillotte ML, Kaur SJ, Lehman SS, Beier-Sexton M, Azad AF. 2015. Which Way In? The RalF Arf-GEF Orchestrates Rickettsia Host Cell Invasion. PLOS Pathogens 11:e1005115.

52. Rennoll-Bankert KE, Rahman MS, Guillotte ML, Lehman SS, Beier-Sexton M, Gillespie JJ, Azad AF. 2016. RalF-Mediated Activation of Arf6 Controls Rickettsia typhi Invasion by Co-Opting Phosphoinositol Metabolism. Infection and Immunity https://doi.org/10.1128/iai.00638-16.

53. Posor Y, Eichhorn-Grünig M, Haucke V. 2015. Phosphoinositides in endocytosis. Biochimica et Biophysica Acta (BBA) - Molecular and Cell Biology of Lipids 1851:794–804.

54. Voss OH, Gillespie JJ, Lehman SS, Rennoll SA, Beier-Sexton M, Rahman MS, Azad AF. 2020. Risk1, a Phosphatidylinositol 3-Kinase Effector, Promotes Rickettsia typhi Intracellular Survival. mBio https://doi.org/10.1128/mBio.00820-20.

55. Levin R, Grinstein S, Schlam D. 2015. Phosphoinositides in phagocytosis and macropinocytosis. Biochimica et Biophysica Acta (BBA) - Molecular and Cell Biology of Lipids 1851:805–823.

56. Teysseire N, Boudier JA, Raoult D. 1995. Rickettsia conorii entry into Vero cells. Infect Immun 63:366–374.

57. Whitworth T, Popov VL, Yu X-J, Walker DH, Bouyer DH. 2005. Expression of the Rickettsia prowazekii pld or tlyC Gene in Salmonella enterica Serovar Typhimurium Mediates Phagosomal Escape. Infect Immun 73:6668–6673.

58. Rahman MS, Gillespie JJ, Kaur SJ, Sears KT, Ceraul SM, Beier-Sexton M, Azad AF. 2013. Rickettsia typhi Possesses Phospholipase A2 Enzymes that Are Involved in Infection of Host Cells. PLOS Pathogens 9:e1003399.

59. Borgo GM, Burke TP, Tran CJ, Lo NTN, Engström P, Welch MD. 2022. A patatin-like phospholipase mediates Rickettsia parkeri escape from host membranes. 1. Nat Commun 13:3656.

60. Saftig P, Klumperman J. 2009. Lysosome biogenesis and lysosomal membrane proteins: trafficking meets function. 9. Nat Rev Mol Cell Biol 10:623–635.

61. Keller MD, Torres VJ, Cadwell K. 2020. Autophagy and microbial pathogenesis. 3. Cell Death Differ 27:872–886.

62. Engström P, Burke TP, Tran CJ, Iavarone AT, Welch MD. 2021. Lysine methylation shields an intracellular pathogen from ubiquitylation and autophagy. Science Advances https://doi.org/10.1126/sciadv.abg2517.

63. Policastro PF, Hackstadt T. 1994. Differential activity of Rickettsia rickettsii ompAand ompBpromoter regions in a heterologous reporter gene system. Microbiology 140:2941–2949.

64. Otten EG, Werner E, Casado AC, Boyle KB, Dharamdasani V, Pathe C, Santhanam B, Randow F. 2021. Ubiquitylation of lipopolysaccharide by RNF213 during bacterial infection. Nature 594:111–116.

65. Voss OH, Gaytan H, Ullah S, Sadik M, Moin I, Rahman MS, Azad AF. 2023. Autophagy facilitates intracellular survival of pathogenic rickettsiae in macrophages via evasion of autophagosomal maturation and reduction of microbicidal pro-inflammatory IL-1 cytokine responses. Microbiology Spectrum 0:e02791-23.

66. Bechelli J, Vergara L, Smalley C, Buzhdygan TP, Bender S, Zhang W, Liu Y, Popov VL, Wang J, Garg N, Hwang S, Walker DH, Fang R. 2018. Atg5 Supports Rickettsia australis Infection in Macrophages In Vitro and In Vivo. Infect Immun 87:e00651-18.

67. Huang J, Brumell JH. 2014. Bacteria–autophagy interplay: a battle for survival. Nat Rev Microbiol 12:101–114.

68. Burke TP, Engström P, Chavez RA, Fonbuena JA, Vance RE, Welch MD. 2020. Inflammasome-mediated antagonism of type I interferon enhances Rickettsia pathogenesis. Nat Microbiol 5:688–696.

69. Ngo CC, Man SM. 2017. Mechanisms and functions of guanylate-binding proteins and related interferon-inducible GTPases: Roles in intracellular lysis of pathogens. Cell Microbiol 19.

70. Chakravortty D, Hensel M. 2003. Inducible nitric oxide synthase and control of intracellular bacterial pathogens. Microbes Infect 5:621–627.

71. Feng HM, Walker DH. 2000. Mechanisms of intracellular killing of Rickettsia conorii in infected human endothelial cells, hepatocytes, and macrophages. Infect Immun 68:6729–6736.

72. Driscoll TP, Verhoeve VI, Guillotte ML, Lehman SS, Rennoll SA, Beier-Sexton M, Rahman MS, Azad AF, Gillespie JJ. 2017. Wholly Rickettsia! Reconstructed Metabolic Profile of the Quintessential Bacterial Parasite of Eukaryotic Cells. mBio 8:e00859-17.

73. Audia JP, Winkler HH. 2006. Study of the Five Rickettsia prowazekii Proteins Annotated as ATP/ADP Translocases (Tlc): Only Tlc1 Transports ATP/ADP, While Tlc4 and Tlc5 Transport Other Ribonucleotides. J Bacteriol 188:6261–6268.

74. Tucker AM, Winkler HH, Driskell LO, Wood DO. 2003. S-adenosylmethionine transport in Rickettsia prowazekii. J Bacteriol 185:3031–3035.

75. Omsland A, Cockrell DC, Howe D, Fischer ER, Virtaneva K, Sturdevant DE, Porcella SF, Heinzen RA. 2009. Host cell-free growth of the Q fever bacterium Coxiella burnetii. Proceedings of the National Academy of Sciences 106:4430–4434.

76. Ahyong V, Berdan CA, Burke TP, Nomura DK, Welch MD. 2019. A Metabolic Dependency for Host Isoprenoids in the Obligate Intracellular Pathogen *Rickettsia parkeri* Underlies a Sensitivity to the Statin Class of Host-Targeted Therapeutics. mSphere 4:e00536-19, /msphere/4/6/mSphere536-19.atom.

77. Sun H, Luu AP, Danielson M, Vo TT, Burke TP. 2023. Host glutathione is required for Rickettsia parkeri to properly septate, avoid ubiquitylation, and survive in macrophages. bioRxiv https://doi.org/10.1101/2023.10.02.560592.

78. Vannini C, Boscaro V, Ferrantini F, Benken KA, Mironov TI, Schweikert M, Görtz H-D, Fokin SI, Sabaneyeva EV, Petroni G. 2014. Flagellar Movement in Two Bacteria of the Family Rickettsiaceae: A Re-Evaluation of Motility in an Evolutionary Perspective. PLoS ONE 9.

79. Lamason RL, Welch MD. 2017. Actin-based motility and cell-to-cell spread of bacterial pathogens. Current Opinion in Microbiology 35:48–57.

80. Gouin E, Egile C, Dehoux P, Villiers V, Adams J, Gertler F, Li R, Cossart P. 2004. The RickA protein of Rickettsia conorii activates the Arp2/3 complex. 6973. Nature 427:457–461.

81. Jeng RL, Goley ED, D'Alessio JA, Chaga OY, Svitkina TM, Borisy GG, Heinzen RA, Welch MD. 2004. A Rickettsia WASP-like protein activates the Arp2/3 complex and mediates actin-based motility. Cellular Microbiology 6:761–769.

82. Kleba B, Clark TR, Lutter EI, Ellison DW, Hackstadt T. 2010. Disruption of the Rickettsia rickettsii Sca2 Autotransporter Inhibits Actin-Based Motility. Infect Immun 78:2240–2247.

83. Haglund CM, Choe JE, Skau CT, Kovar DR, Welch MD. 2010. Rickettsia Sca2 is a bacterial formin-like mediator of actin-based motility. Nat Cell Biol 12:1057–1063.

84. Serio AW, Jeng RL, Haglund CM, Reed SC, Welch MD. 2010. Defining a core set of actin cytoskeletal proteins critical for actin-based motility of Rickettsia. Cell Host Microbe 7:388–398.

85. Nock AM, Clark TR, Hackstadt T. 2022. Regulator of Actin-Based Motility (RoaM) Downregulates Actin Tail Formation by Rickettsia rickettsii and Is Negatively Selected in Mammalian Cell Culture. mBio https://doi.org/10.1128/mbio.00353-22.

86. Heinzen RA. 2003. Rickettsial actin-based motility: behavior and involvement of cytoskeletal regulators. Ann N Y Acad Sci 990:535–547.

87. Van Kirk LS, Hayes SF, Heinzen RA. 2000. Ultrastructure of Rickettsia rickettsii Actin Tails and Localization of Cytoskeletal Proteins. Infect Immun 68:4706–4713.

88. Silverman DJ, Wisseman CL. 1979. In Vitro Studies of Rickettsia-Host Cell Interactions: Ultrastructural Changes Induced by Rickettsia rickettsii Infection of Chicken Embryo Fibroblasts. INFECT IMMUN 26:14.

89. Silverman DJ, Wisseman CL, Waddell A. 1980. In Vitro Studies of Rickettsia-Host Cell Interactions: Ultrastructural Study of Rickettsia prowazekii-Infected Chicken Embryo Fibroblasts. Infect Immun 29:778–790.

90. Aistleitner K, Clark T, Dooley C, Hackstadt T. 2020. Selective fragmentation of the trans-Golgi apparatus by Rickettsia rickettsii. PLoS Pathog 16:e1008582.

91. Lehman SS, Noriea NF, Aistleitner K, Clark TR, Dooley CA, Nair V, Kaur SJ, Rahman MS, Gillespie JJ, Azad AF, Hackstadt T. 2018. The Rickettsial Ankyrin Repeat Protein 2 Is a Type IV Secreted Effector That Associates with the Endoplasmic Reticulum. mBio 9:e00975-18.

92. Acevedo-Sánchez Y, Woida PJ, Kraemer S, Lamason RL. 2023. An obligate intracellular bacterial pathogen forms a direct, interkingdom membrane contact site. bioRxiv https://doi.org/10.1101/2023.06.05.543771.

93. Phillips MJ, Voeltz GK. 2016. Structure and function of ER membrane contact sites with other organelles. 2. Nat Rev Mol Cell Biol 17:69–82.

94. Wu H, Carvalho P, Voeltz GK. 2018. Here, there, and everywhere: The importance of ER membrane contact sites. Science https://doi.org/10.1126/science.aan5835.

95. Labbé K, Saleh M. 2008. Cell death in the host response to infection. 9. Cell Death Differ 15:1339–1349.

96. Elmore S. 2007. Apoptosis: A Review of Programmed Cell Death. Toxicol Pathol 35:495–516.

97. Clifton DR, Goss RA, Sahni SK, Antwerp D van, Baggs RB, Marder VJ, Silverman DJ, Sporn LA. 1998. NF-κB-dependent inhibition of apoptosis is essential for host cell survival during Rickettsia rickettsii infection. PNAS 95:4646–4651.

98. Luo J-L, Kamata H, Karin M. 2005. IKK/NF-κB signaling: balancing life and death – a new approach to cancer therapy. J Clin Invest 115:2625–2632.

99. Park H, Lee JH, Gouin E, Cossart P, Izard T. 2011. The Rickettsia Surface Cell Antigen 4 Applies Mimicry to Bind to and Activate Vinculin. J Biol Chem 286:35096–35103.

100. Lecuit T, Yap AS. 2015. E-cadherin junctions as active mechanical integrators in tissue dynamics. Nature Cell Biology 17:533–539.

101. Serruto D, Rappuoli R, Scarselli M, Gros P, van Strijp JAG. 2010. Molecular mechanisms of complement evasion: learning from staphylococci and meningococci. 6. Nat Rev Microbiol 8:393–399.

102. Chan YG-Y, Riley SP, Chen E, Martinez JJ. 2011. Molecular basis of immunity to rickettsial infection conferred through outer membrane protein B. Infect Immun 79:2303–2313.

103. Riley SP, Patterson JL, Martinez JJ. 2012. The Rickettsial OmpB β-Peptide of Rickettsia conorii Is Sufficient To Facilitate Factor H-Mediated Serum Resistance. Infect Immun 80:2735–2743.

104. Riley SP, Patterson JL, Nava S, Martinez JJ. 2014. Pathogenic Rickettsia Species Acquire Vitronectin from Human Serum to Promote Resistance to Complement-mediated Killing. Cell Microbiol 16:849–861.

105. Garza DA, Riley SP, Martinez JJ. 2017. Expression of Rickettsia Adr2 protein in E. coli is sufficient to promote resistance to complement-mediated killing, but not adherence to mammalian cells. PLoS One 12:e0179544.

106. Eremeeva ME, Dasch GA. 2015. Challenges Posed by Tick-Borne Rickettsiae: Eco-Epidemiology and Public Health Implications. Front Public Health 3:132534.

107. Thepparit C, Bourchookarn A, Petchampai N, Barker SA, Macaluso KR. 2010. Interaction of Rickettsia felis with histone H2B facilitates the infection of a tick cell line. Microbiology (Reading) 156:2855–2863.

108. Petchampai N, Sunyakumthorn P, Guillotte ML, Verhoeve VI, Banajee KH, Kearney MT, Macaluso KR. 2014. Novel identification of Dermacentor variabilis Arp2/3 complex and its role in rickettsial infection of the arthropod vector. PLoS One 9:e93768.

109. Harris EK, Jirakanwisal K, Verhoeve VI, Fongsaran C, Suwanbongkot C, Welch MD, Macaluso KR. 2018. Role of Sca2 and RickA in the Dissemination of Rickettsia parkeri in Amblyomma maculatum. Infect Immun 86:e00123-18.

110. Martins LA, Palmisano G, Cortez M, Kawahara R, de Freitas Balanco JM, Fujita A, Alonso BI, Barros-Battesti DM, Braz GRC, Tirloni L, Esteves E, Daffre S, Fogaça AC. 2020. The intracellular bacterium Rickettsia rickettsii exerts an inhibitory effect on the apoptosis of tick cells. Parasites & Vectors 13:603.

111. Wang X-R, Burkhardt NY, Kurtti TJ, Oliver JD, Price LD, Cull B, Thorpe CJ, Thiel MS, Munderloh UG. Mitochondrion-Dependent Apoptosis Is Essential for Rickettsia parkeri Infection and Replication in Vector Cells. mSystems 6:e01209-20.

112. Gillespie JJ, Kaur SJ, Rahman MS, Rennoll-Bankert K, Sears KT, Beier-Sexton M, Azad AF. 2015. Secretome of obligate intracellular Rickettsia. FEMS Microbiol Rev 39:47–80.

113. du Plessis DJF, Nouwen N, Driessen AJM. 2011. The Sec translocase. Biochimica et Biophysica Acta (BBA) - Biomembranes 1808:851–865.

114. Beck K, Wu LF, Brunner J, Müller M. 2000. Discrimination between SRP- and SecA/SecB-dependent substrates involves selective recognition of nascent chains by SRP and trigger factor. EMBO J 19:134–143.

115. Ulbrandt ND, Newitt JA, Bernstein HD. 1997. The E. coli signal recognition particle is required for the insertion of a subset of inner membrane proteins. Cell 88:187–196.

116. Henderson IR, Navarro-Garcia F, Desvaux M, Fernandez RC, Ala'Aldeen D. 2004. Type V Protein Secretion Pathway: the Autotransporter Story. Microbiol Mol Biol Rev 68:692–744.

117. Zückert WR. 2014. Secretion of Bacterial Lipoproteins: Through the Cytoplasmic Membrane, the Periplasm and Beyond. Biochim Biophys Acta 1843:1509–1516.

118. Teufel F, Almagro Armenteros JJ, Johansen AR, Gíslason MH, Pihl SI, Tsirigos KD, Winther O, Brunak S, von Heijne G, Nielsen H. 2022. SignalP 6.0 predicts all five types of signal peptides using protein language models. 7. Nat Biotechnol 40:1023–1025.

119. Ammerman NC, Rahman MS, Azad AF. 2008. Characterization of Sec-Translocon-Dependent Extracytoplasmic Proteins of Rickettsia typhi. J Bacteriol 190:6234–6242.

120. Lee PA, Tullman-Ercek D, Georgiou G. 2006. The Bacterial Twin-Arginine Translocation Pathway. Annu Rev Microbiol 60:373–395.

121. Kaur SJ, Rahman MS, Ammerman NC, Ceraul SM, Gillespie JJ, Azad AF. 2012. TolC-Dependent Secretion of an Ankyrin Repeat-Containing Protein of Rickettsia typhi. J Bacteriol 194:4920–4932.

122. Delepelaire P. 2004. Type I secretion in gram-negative bacteria. Biochimica et Biophysica Acta (BBA) - Molecular Cell Research 1694:149–161.

123. Spitz O, Erenburg IN, Kanonenberg K, Peherstorfer S, Lenders MHH, Reiners J, Ma M, Luisi BF, Smits SHJ, Schmitt L. 2022. Identity Determinants of the Translocation Signal for a Type 1 Secretion System. Front Physiol 12:804646.

124. Clapham DE. 2007. Calcium Signaling. Cell 131:1047–1058.

125. Yamanaka H, Nomura T, Fujii Y, Okamoto K. 1998. Need for TolC, anEscherichia coliouter membrane protein, in the secretion of heat-stable enterotoxin I across the outer membrane. Microbial Pathogenesis 25:111–120.

126. Yamanaka H, Kobayashi H, Takahashi E, Okamoto K. 2008. MacAB Is Involved in the Secretion of Escherichia coli Heat-Stable Enterotoxin II. J Bacteriol 190:7693–7698.

127. Gillespie JJ, Phan IQH, Driscoll TP, Guillotte ML, Lehman SS, Rennoll-Bankert KE, Subramanian S, Beier-Sexton M, Myler PJ, Rahman MS, Azad AF. 2016. The Rickettsia type IV secretion system: unrealized complexity mired by gene family expansion. Pathog Dis 74:ftw058.

128. Trokter M, Waksman G. 2018. Translocation through the Conjugative Type IV Secretion System Requires Unfolding of Its Protein Substrate. J Bacteriol 200:e00615-17.

129. Amyot WM, deJesus D, Isberg RR. 2013. Poison Domains Block Transit of Translocated Substrates via the Legionella pneumophila Icm/Dot System. Infect Immun 81:3239–3252.

130. Lettl C, Haas R, Fischer W. 2021. Kinetics of CagA type IV secretion by Helicobacter pylori and the requirement for substrate unfolding. Molecular Microbiology 116:794–807.

131. Gillespie JJ, Phan IQH, Scheib H, Subramanian S, Edwards TE, Lehman SS, Piitulainen H, Sayeedur Rahman M, Rennoll-Bankert KE, Staker BL, Taira S, Stacy R, Myler PJ, Azad AF, Pulliainen AT. 2015. Structural Insight into How Bacteria Prevent Interference between Multiple Divergent Type IV Secretion Systems. mBio 6:e01867-15.

132. Sears KT, Ceraul SM, Gillespie JJ, Allen ED, Popov VL, Ammerman NC, Rahman MS, Azad AF. 2012. Surface proteome analysis and characterization of surface cell antigen (Sca) or autotransporter family of Rickettsia typhi. PLoS Pathog 8:e1002856.

133. Alvarez-Martinez CE, Christie PJ. 2009. Biological Diversity of Prokaryotic Type IV Secretion Systems. Microbiol Mol Biol Rev 73:775–808.

134. Vergunst AC, van Lier MCM, den Dulk-Ras A, Grosse Stüve TA, Ouwehand A, Hooykaas PJJ. 2005. Positive charge is an important feature of the C-terminal transport signal of the VirB/D4-translocated proteins of Agrobacterium. Proceedings of the National Academy of Sciences 102:832–837.

135. Huang L, Boyd D, Amyot WM, Hempstead AD, Luo Z-Q, O'Connor TJ, Chen C, Machner M, Montminy T, Isberg RR. 2011. The E Block motif is associated with Legionella pneumophila translocated substrates. Cell Microbiol 13:227–245.

136. Nagai H, Cambronne ED, Kagan JC, Amor JC, Kahn RA, Roy CR. 2005. A C-terminal translocation signal required for Dot/Icm-dependent delivery of the Legionella RalF protein to host cells. Proc Natl Acad Sci U S A 102:826–831.

137. Schulein R, Guye P, Rhomberg TA, Schmid MC, Schröder G, Vergunst AC, Carena I, Dehio C. 2005. A bipartite signal mediates the transfer of type IV secretion substrates of Bartonella henselae into human cells. Proc Natl Acad Sci U S A 102:856–861.

138. Cambronne ED, Roy CR. 2007. The Legionella pneumophila IcmSW complex interacts with multiple Dot/Icm effectors to facilitate type IV translocation. PLoS Pathog 3:e188.

139. McDermott JE, Corrigan A, Peterson E, Oehmen C, Niemann G, Cambronne ED, Sharp D, Adkins JN, Samudrala R, Heffron F. 2011. Computational Prediction of Type III and IV Secreted Effectors in Gram-Negative Bacteria. Infection and Immunity 79:23–32.

140. Noroy C, Lefrançois T, Meyer DF. 2019. Searching algorithm for Type IV effector proteins (S4TE) 2.0: Improved tools for Type IV effector prediction, analysis and comparison in proteobacteria. PLOS Computational Biology 15:e1006847.

141. Esna Ashari Z, Brayton KA, Broschat SL. 2019. Prediction of T4SS Effector Proteins for Anaplasma phagocytophilum Using OPT4e, A New Software Tool. Front Microbiol 10:1391.

142. Gillespie JJ, Joardar V, Williams KP, Driscoll T, Hostetler JB, Nordberg E, Shukla M, Walenz B, Hill CA, Nene VM, Azad AF, Sobral BW, Caler E. 2012. A Rickettsia Genome Overrun by Mobile Genetic Elements Provides Insight into the Acquisition of Genes Characteristic of an Obligate Intracellular Lifestyle. J Bacteriol 194:376–394.

143. Gillespie JJ, Driscoll TP, Verhoeve VI, Utsuki T, Husseneder C, Chouljenko VN, Azad AF, Macaluso KR. 2014. Genomic Diversification in Strains of Rickettsia felis Isolated from Different Arthropods. Genome Biol Evol 7:35–56.

144. Ogata H, La Scola B, Audic S, Renesto P, Blanc G, Robert C, Fournier P-E, Claverie J-M, Raoult D. 2006. Genome Sequence of Rickettsia bellii Illuminates the Role of Amoebae in Gene Exchanges between Intracellular Pathogens. PLoS Genet 2:e76.

145. Nock AM, Aistleitner K, Clark TR, Sturdevant D, Ricklefs S, Virtaneva K, Zhang Y, Gulzar N, Redekar N, Roy A, Hackstadt T. 2023. Identification of an autotransporter peptidase of Rickettsia rickettsii responsible for maturation of surface exposed autotransporters. PLOS Pathogens 19:e1011527.

146. Hackstadt T, Messer R, Cieplak W, Peacock MG. 1992. Evidence for proteolytic cleavage of the 120-kilodalton outer membrane protein of rickettsiae: identification of an avirulent mutant deficient in processing. Infection and Immunity 60:159.

147. Luo Z-Q, Isberg RR. 2004. Multiple substrates of the Legionella pneumophila Dot/Icm system identified by interbacterial protein transfer. Proceedings of the National Academy of Sciences 101:841–846.

148. Galka F, Wai SN, Kusch H, Engelmann S, Hecker M, Schmeck B, Hippenstiel S, Uhlin BE, Steinert M. 2008. Proteomic Characterization of the Whole Secretome of Legionella pneumophila and Functional Analysis of Outer Membrane Vesicles. Infect Immun 76:1825–1836.

149. Radulovic S, Troyer JM, Beier MS, Lau AOT, Azad AF. 1999. Identification and Molecular Analysis of the Gene Encoding Rickettsia typhi Hemolysin. Infect Immun 67:6104–6108.

150. Charpentier X, Oswald E. 2004. Identification of the Secretion and Translocation Domain of the Enteropathogenic and Enterohemorrhagic Escherichia coli Effector Cif, Using TEM-1 β-Lactamase as a New Fluorescence-Based Reporter. J Bacteriol 186:5486–5495.

151. Torruellas Garcia J, Ferracci F, Jackson MW, Joseph SS, Pattis I, Plano LRW, Fischer W, Plano GV. 2006. Measurement of Effector Protein Injection by Type III and Type IV Secretion Systems by Using a 13-Residue Phosphorylatable Glycogen Synthase Kinase Tag. Infect Immun 74:5645–5657.

152. Renesto P, Dehoux P, Gouin E, Touqui L, Cossart P, Raoult D. 2003. Identification and characterization of a phospholipase D-superfamily gene in rickettsiae. J Infect Dis 188:1276–1283.

153. Burstein D, Amaro F, Zusman T, Lifshitz Z, Cohen O, Gilbert JA, Pupko T, Shuman HA, Segal G. 2016. Genomic analysis of 38 Legionella species identifies large and diverse effector repertoires. 2. Nat Genet 48:167–175.

154. Geddes K, Worley M, Niemann G, Heffron F. 2005. Identification of New Secreted Effectors in Salmonella enterica Serovar Typhimurium. Infection and Immunity 73:6260–6271.

155. Fielden LF, Moffatt JH, Kang Y, Baker MJ, Khoo CA, Roy CR, Stojanovski D, Newton HJ. 2017. A Farnesylated Coxiella burnetii Effector Forms a Multimeric Complex at the Mitochondrial Outer Membrane during Infection. Infect Immun 85:e01046-16.

156. Steiert B, Icardi CM, Faris R, McCaslin PN, Smith P, Klingelhutz AJ, Yau PM, Weber MM. 2023. The Chlamydia trachomatis type III-secreted effector protein CteG induces centrosome amplification through interactions with centrin-2. Proceedings of the National Academy of Sciences 120:e2303487120.

157. Mou X, Souter S, Du J, Reeves AZ, Lesser CF. 2018. Synthetic bottom-up approach reveals the complex interplay of Shigella effectors in regulation of epithelial cell death. Proc Natl Acad Sci U S A 115:6452–6457.

158. Pillay TD, Hettiarachchi SU, Gan J, Diaz-Del-Olmo I, Yu X-J, Muench JH, Thurston TLM, Pearson JS. 2023. Speaking the host language: how Salmonella effector proteins manipulate the host. Microbiology 169:001342.

159. Lutter EI, Martens C, Hackstadt T. 2012. Evolution and Conservation of Predicted Inclusion Membrane Proteins in Chlamydiae. Comp Funct Genomics 2012:362104.

160. Lifshitz Z, Burstein D, Schwartz K, Shuman HA, Pupko T, Segal G. 2014. Identification of Novel Coxiella burnetii Icm/Dot Effectors and Genetic Analysis of Their Involvement in Modulating a Mitogen-Activated Protein Kinase Pathway. Infect Immun 82:3740–3752.

161. Gemmer M, Förster F. 2020. A clearer picture of the ER translocon complex. J Cell Sci 133.

162. McGilvray PT, Anghel SA, Sundaram A, Zhong F, Trnka MJ, Fuller JR, Hu H, Burlingame AL, Keenan RJ. An ER translocon for multi-pass membrane protein biogenesis. eLife 9:e56889.

163. Sundaram A, Yamsek M, Zhong F, Hooda Y, Hegde RS, Keenan RJ. 2022. Substrate-driven assembly of a translocon for multipass membrane proteins. Nature 611:167–172.

164. Shurtleff MJ, Itzhak DN, Hussmann JA, Oakdale NTS, Costa EA, Jonikas M, Weibezahn J, Popova KD, Jan CH, Sinitcyn P, Vembar SS, Hernandez H, Cox J, Burlingame AL, Brodsky JL, Frost A, Borner GH, Weissman JS. 2018. The ER membrane protein complex interacts cotranslationally to enable biogenesis of multipass membrane proteins. eLife. eLife Sciences Publications Limited. https://elifesciences.org/articles/37018. Retrieved 1 December 2023.

165. Chitwood PJ, Juszkiewicz S, Guna A, Shao S, Hegde RS. 2018. EMC Is Required to Initiate Accurate Membrane Protein Topogenesis. Cell 175:1507-1519.e16.

166. O'Keefe S, Zong G, Duah KB, Andrews LE, Shi WQ, High S. 2021. An alternative pathway for membrane protein biogenesis at the endoplasmic reticulum. 1. Commun Biol 4:1–15.

167. Jaskolowski M, Jomaa A, Gamerdinger M, Shrestha S, Leibundgut M, Deuerling E, Ban N. 2023. Molecular basis of the TRAP complex function in ER protein biogenesis. 6. Nat Struct Mol Biol 30:770–777.

168. Voigt S, Jungnickel B, Hartmann E, Rapoport TA. 1996. Signal sequence-dependent function of the TRAM protein during early phases of protein transport across the endoplasmic reticulum membrane. J Cell Biol 134:25–35.

169. Shao S, Hegde RS. 2011. A calmodulin-dependent translocation pathway for small secretory proteins. Cell 147:1576–1588.

170. Lakkaraju AKK, Thankappan R, Mary C, Garrison JL, Taunton J, Strub K. 2012. Efficient secretion of small proteins in mammalian cells relies on Sec62-dependent posttranslational translocation. Mol Biol Cell 23:2712–2722.

171. Jadhav B, McKenna M, Johnson N, High S, Sinning I, Pool MR. 2015. Mammalian SRP receptor switches the Sec61 translocase from Sec62 to SRP-dependent translocation. 1. Nat Commun 6:10133.

172. Lang S, Benedix J, Fedeles SV, Schorr S, Schirra C, Schäuble N, Jalal C, Greiner M, Haßdenteufel S, Tatzelt J, Kreutzer B, Edelmann L, Krause E, Rettig J, Somlo S, Zimmermann R, Dudek J. 2012. Different effects of Sec61α, Sec62 and Sec63 depletion on transport of polypeptides into the endoplasmic reticulum of mammalian cells. J Cell Sci 125:1958–1969.

173. Erdmann F, Schäuble N, Lang S, Jung M, Honigmann A, Ahmad M, Dudek J, Benedix J, Harsman A, Kopp A, Helms V, Cavalié A, Wagner R, Zimmermann R. 2011. Interaction of calmodulin with Sec61α limits Ca2+ leakage from the endoplasmic reticulum. EMBO J 30:17–31.

174. Schäuble N, Lang S, Jung M, Cappel S, Schorr S, Ulucan Ö, Linxweiler J, Dudek J, Blum R, Helms V, Paton AW, Paton JC, Cavalié A, Zimmermann R. 2012. BiP-mediated closing of the Sec61 channel limits Ca2+ leakage from the ER. The EMBO Journal 31:3282–3296.

175. Sundaram A, Plumb R, Appathurai S, Mariappan M. 2017. The Sec61 translocon limits IRE1α signaling during the unfolded protein response. eLife. eLife Sciences Publications Limited. https://elifesciences.org/articles/27187. Retrieved 1 December 2023.

176. Li X, Sun S, Appathurai S, Sundaram A, Plumb R, Mariappan M. 2020. A Molecular Mechanism for Turning Off IRE1α Signaling during Endoplasmic Reticulum Stress. Cell Reports 33:108563.

177. Luesch H, Paavilainen VO. 2020. Natural products as modulators of eukaryotic protein secretion. Nat Prod Rep 37:717–736.

178. Itskanov S, Wang L, Junne T, Sherriff R, Xiao L, Blanchard N, Shi WQ, Forsyth C, Hoepfner D, Spiess M, Park E. 2023. A common mechanism of Sec61 translocon inhibition by small molecules. 9. Nat Chem Biol 19:1063–1071.

179. Baron L, Paatero AO, Morel J-D, Impens F, Guenin-Macé L, Saint-Auret S, Blanchard N, Dillmann R, Niang F, Pellegrini S, Taunton J, Paavilainen VO, Demangel C. 2016. Mycolactone subverts immunity by selectively blocking the Sec61 translocon. J Exp Med 213:2885–2896.

180. Hsieh LT-H, Hall BS, Newcombe J, Mendum TA, Umrania Y, Deery MJ, Shi WQ, Salguero FJ, Simmonds RE. 2023. Mycolactone causes catastrophic Sec61-dependent loss of the endothelial glycocalyx and basement membrane: a new indirect mechanism driving tissue necrosis in Mycobacterium ulcerans infection. eLife 12.

CHAPTER 2: THE ANKYRIN REPEAT PROTEIN RARP-1 IS A PERIPLASMIC FACTOR THAT SUPPORTS *RICKETTSIA PARKERI* GROWTH AND HOST CELL INVASION

This chapter contains a modified version of work in press at the Journal of Bacteriology as:

Allen G. Sanderlin, Ruth E. Hanna, Rebecca L. Lamason. The Ankyrin Repeat Protein RARP-1 Is a Periplasmic Factor That Supports *Rickettsia parkeri* Growth and Host Cell Invasion. *J Bacteriol* 204: e0018222 (2022). DOI: 10.1128/jb.00182-22.

AGS: Conceptualization, Methodology, Investigation, Formal Analysis, Validation, Visualization, Writing – Original Draft, Writing – Review & Editing. REH: Validation, Writing – Review & Editing. RLL: Conceptualization, Methodology, Investigation, Writing – Original Draft, Writing – Review & Editing, Supervision, Funding Acquisition.

Abstract

Rickettsia spp. are obligate intracellular bacterial pathogens that have evolved a variety of strategies to exploit their host cell niche. However, the bacterial factors that contribute to this intracellular lifestyle are poorly understood. Here, we show that the conserved ankyrin repeat protein RARP-1 supports *Rickettsia parkeri* infection. Specifically, RARP-1 promotes efficient host cell entry and growth within the host cytoplasm, but it is not necessary for cell-to-cell spread or evasion of host autophagy. We further demonstrate that RARP-1 is not secreted into the host cytoplasm by *R. parkeri*. Instead, RARP-1 resides in the periplasm, and we identify several binding partners that are predicted to work in concert with RARP-1 during infection. Altogether, our data reveal that RARP-1 plays a critical role in the rickettsial life cycle.

Introduction

Intracellular bacterial pathogens face considerable challenges and opportunities when invading and occupying their host cell niche. The host cell membrane physically occludes entry and the endolysosomal pathway imperils invading microbes. Moreover, host cell defenses like autophagy create a hostile environment for internalized bacteria. If a bacterium successfully navigates these obstacles, however, it can conceal itself from humoral immunity, commandeer host metabolites, and exploit host cell biology to support infection. Not surprisingly, the host cell niche has provided fertile ground for the evolution of diverse lifestyles across many well-studied bacterial pathogens such as *Shigella*, *Listeria*, *Salmonella*, and *Legionella* (1, 2). The prospect of uncovering unique infection strategies invites a thorough investigation of these adaptations in more enigmatic pathogens.

Members of the genus *Rickettsia* include emerging global health threats that can cause mild to severe diseases such as typhus and Rocky Mountain spotted fever (3). These Gram-negative bacterial pathogens are transmitted from arthropod vectors to vertebrate hosts where they primarily target the vascular endothelium. As obligate intracellular pathogens, *Rickettsia* spp. define the extreme end of adaptation to intracellular life and are completely dependent on their hosts for survival (4). Consequently, they have evolved a complex life cycle to invade, grow, and disseminate across host tissues.

As the first step of their life cycle, *Rickettsia* spp. adhere to and invade host cells by inducing phagocytosis (5–7). Once inside, these bacteria rapidly escape the phagocytic vacuole to access the host cytoplasm (8, 9). To establish a hospitable niche for proliferation, *Rickettsia* spp. scavenge host nutrients, modulate apoptosis, and thwart antimicrobial autophagy (10–13). Successful colonization of the host cytoplasm allows *Rickettsia* spp. to spread to neighboring cells. Members of the spotted fever group (SFG) *Rickettsia* hijack the host actin cytoskeleton, forming tails that propel the bacteria around the cytoplasm, and then protrude through cell-cell junctions to repeat the infection cycle (14, 15).

Recent work using the model SFG member *Rickettsia parkeri* has highlighted a short list of surface-exposed proteins and secreted effectors that manipulate host cell processes during infection (4). For example, the surface protein Sca2 nucleates actin at the bacterial pole and promotes motility by mimicking host formins (14). Sca4, a secreted effector, interacts with host vinculin to reduce intercellular tension and facilitate protrusion engulfment (15). Additionally, methylation of outer membrane proteins like OmpB protects *R. parkeri* from ubiquitylation and autophagy (13, 16). Despite these advances, our knowledge of the factors that govern the multi-step rickettsial life cycle is still limited. Indeed, *Rickettsia* spp. genomes are replete with

hypothetical proteins that are conserved even among less virulent members of the genus (17), but a paucity of genetic tools has stunted investigation of these proteins. Such factors could support infection directly, by targeting host processes, or indirectly, by controlling the bacterial mediators at the host-pathogen interface. Thus, it is critical to reveal how these uncharacterized proteins contribute to infection.

In a recent transposon mutagenesis screen in *R. parkeri* (18), we identified over 100 mutants that exhibited defects in infection. Although several hits from this screen have been functionally characterized (13–16), many play unknown roles during infection. One such unexplored hit is the *Rickettsia* ankyrin repeat protein 1 (RARP-1), which is conserved across the genus and predicted to be secreted into the host cytoplasm (19). To better understand the factors that influence the rickettsial life cycle, we investigated the function of RARP-1 during *R. parkeri* infection. We demonstrated that RARP-1 promotes both efficient host cell invasion and growth in the host cytoplasm, but it is otherwise dispensable for cell-to-cell spread and avoidance of host autophagy. Although prior work indicated that RARP-1 is secreted into the host cytoplasm (19), we found instead that it localizes to the *R. parkeri* periplasm. Furthermore, we showed that RARP-1 interacts with a variety of factors that are predicted to support bacterial fitness. Our results suggest that RARP-1 is a *Rickettsia*-specific tool that promotes the obligate intracellular life cycle.

Results

Transposon mutagenesis of rarp-1 impairs R. parkeri infection

In a previous *mariner*-based transposon mutagenesis screen (18), we identified a number of *R. parkeri* mutants that displayed abnormal plaque sizes after infection of Vero host cell

monolayers. We hypothesized that the plaque phenotypes for these mutants were due to defects in growth, cell-to-cell spread, or other steps of the rickettsial life cycle. Two such small plaque (Sp) mutants contained a transposon (Tn) insertion within the *rarp-1* gene, giving a predicted truncation of RARP-1 at residues 305 (Sp116) and 480 (Sp64) (Figure 2.1A). RARP-1 is a 573 amino acid protein conserved across the *Rickettsia* genus, but the lack of loss-of-function mutants has thus far prevented characterization of RARP-1 function. Due to the upstream position of its Tn insertion within the *rarp-1* CDS, we focused on Sp116 (herein referred to as *rarp-1*::Tn) for all subsequent studies and confirmed that it formed smaller plaques than GFP-expressing wild-type bacteria (WT, Figure 2.1B). We generated polyclonal antibodies against a RARP-1 peptide upstream of the Tn insertion site to assess RARP-1 expression in the mutant. As expected, the *rarp-1*::Tn mutant did not express the full-length protein by immunoblotting (Figure 2.1C). Furthermore, we were unable to detect an obvious band consistent with the expected 30 kDa product resulting from Tn insertion. Altogether, these results suggest that the loss of RARP-1 expression in the *rarp-1*::Tn mutant leads to a small plaque phenotype.

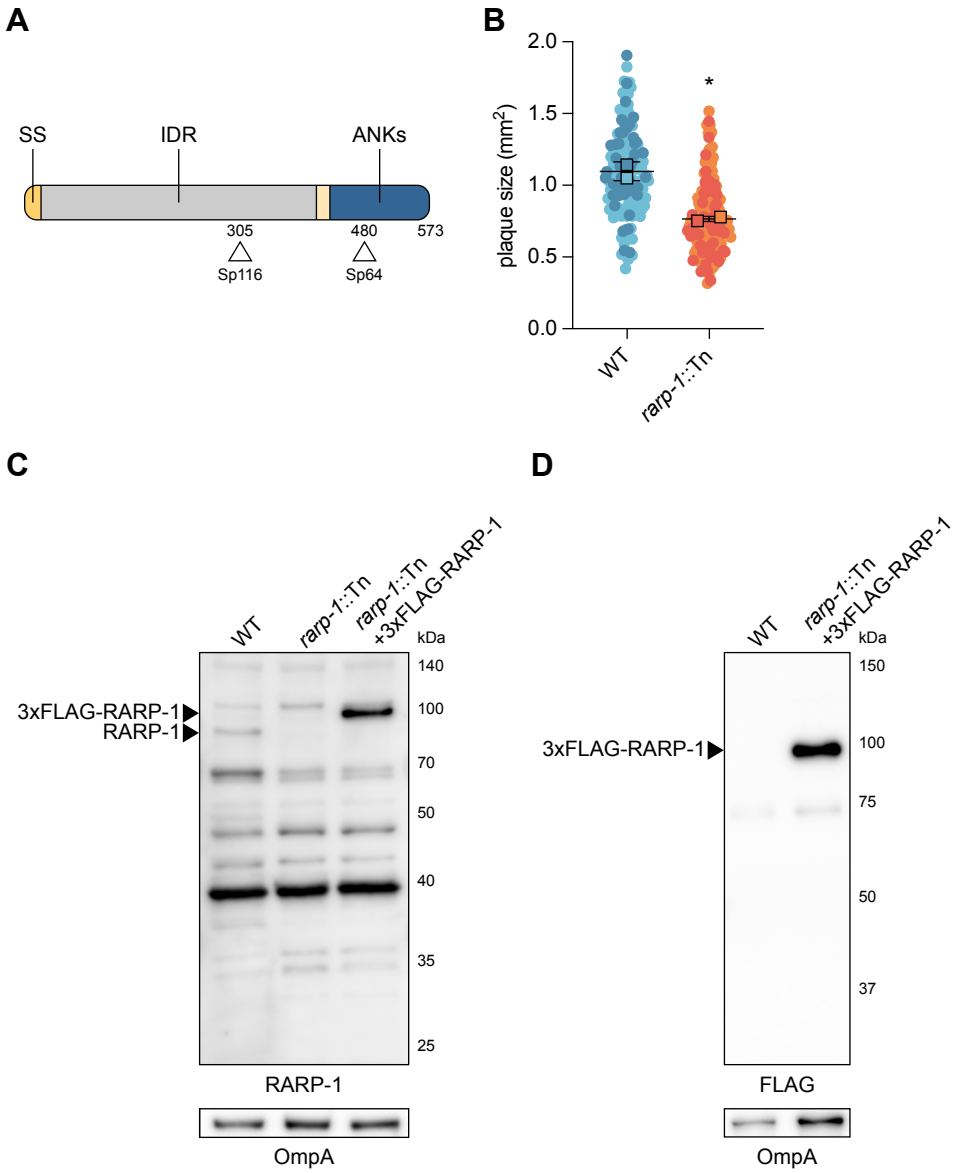

Figure 2.1 – Transposon mutagenesis of *rarp-1* impairs *R. parkeri* infection. (A) *R. parkeri* RARP-1 contains an N-terminal Sec secretion signal (SS, yellow), a central intrinsically disordered region (IDR, grey), and C-terminal ankyrin repeats (ANKs, dark blue). Tn insertions at residues 305 (Sp116) and 480 (Sp64) are indicated (arrowheads). (B) Plaque areas in infected Vero cell monolayers. Means from two independent experiments (squares) are superimposed over the raw data (circles) and were used to calculate the mean ± SD and p-value (unpaired two-tailed *t* test, *p < 0.05 relative to WT). Data are shaded by replicate experiment. (C) Western blot for RARP-1 using purified *R. parkeri* strains. 3xFLAG-tagged and endogenous RARP-1 are indicated (arrowheads). OmpA, loading control. (D) Western blot for FLAG using purified *R. parkeri* strains. 3xFLAG-tagged RARP-1 is indicated (arrowhead). OmpA, loading control.

RARP-1 supports bacterial growth and is dispensable for cell-to-cell spread

The small plaques formed by the *rarp-1*::Tn mutant could be the result of defects in one or more steps of the rickettsial life cycle, and determining when RARP-1 acts during infection

would support characterization of its function. We first performed infectious focus assays in A549 host cell monolayers to assess the growth and cell-to-cell spread of the *rarp-1*::Tn mutant on a shorter timescale than is required for plaque formation (28 h versus 5 d post-infection). A549 cells support all known aspects of the *R. parkeri* life cycle, and the use of gentamicin prevents asynchronous invasion events (15). Consistent with the small plaque phenotype, the *rarp-1*::Tn mutant generated smaller foci than WT bacteria (Figure 2.2A). To confirm that this phenotype was due specifically to the disruption of *rarp-1*, we complemented the *rarp-1*::Tn mutant with a plasmid expressing 3xFLAG-tagged RARP-1 (*rarp-1*::Tn + 3xFLAG-RARP-1). Since *rarp-1* is predicted to be part of an operon (19), we selected a 247 bp region immediately upstream of the first gene in the operon (encoding the outer membrane channel TolC) as a putative promoter to drive *rarp-1* expression. This construct was sufficient for expression of epitope-tagged RARP-1 in the *rarp-1*::Tn mutant (Figure 2.1C,D). Importantly, the complemented strain exhibited infectious focus sizes comparable to WT (Figure 2.2A), indicating that the putative promoter and epitope-tagged RARP-1 are functionally relevant. Thus, RARP-1 specifically supports the size of *R. parkeri* infectious foci.

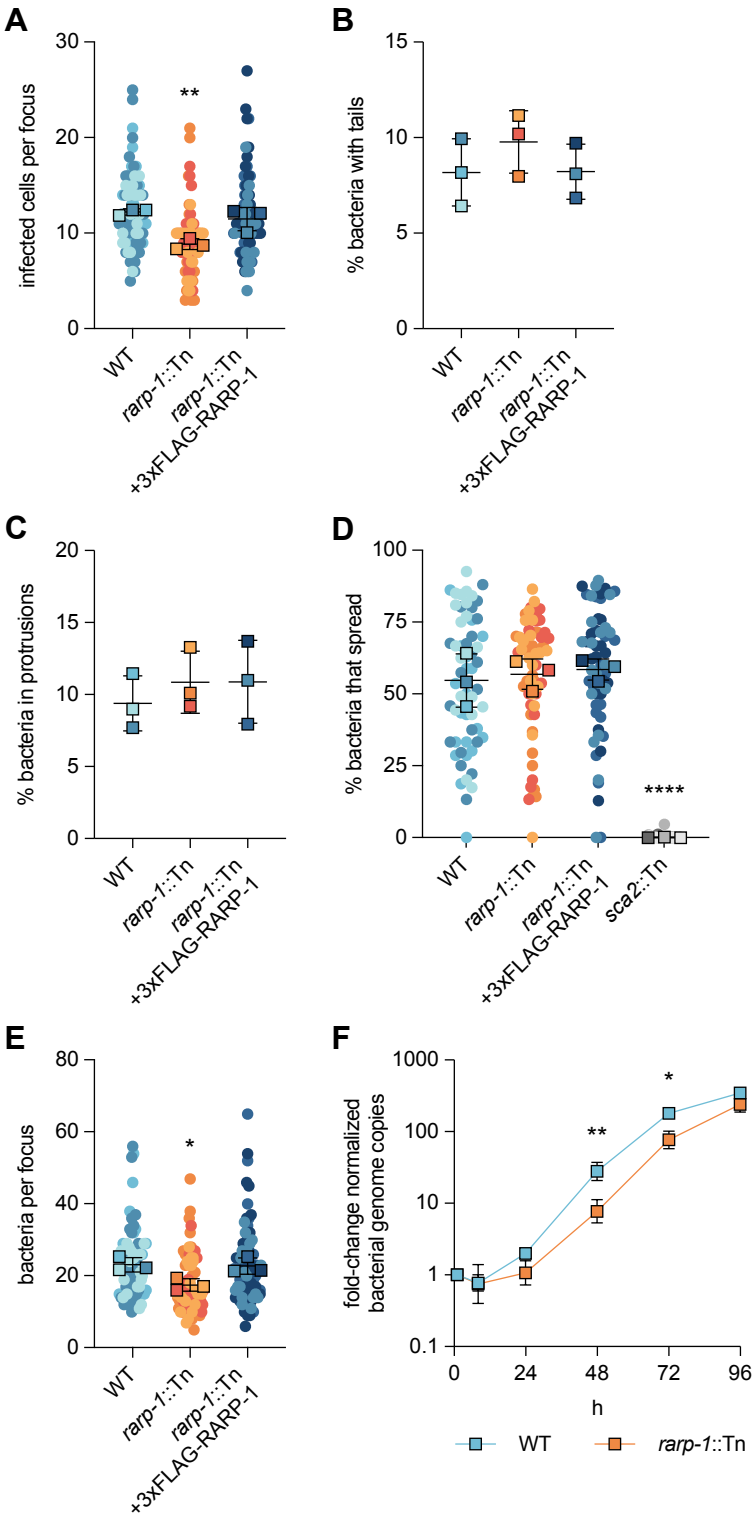

Figure 2.2 – RARP-1 supports bacterial growth and is dispensable for cell-to-cell spread. (A) Infected cells per focus during infection of A549 cells. The means from three independent experiments (squares) are superimposed over the raw data (circles) and were used to calculate the mean ± SD and p-value (one-way ANOVA with post-hoc Dunnett's test, **p < 0.01 relative to WT). Data are shaded by replicate experiment. (B) Percentage of bacteria with actin tails during infection of A549 cells. (C) Percentage of bacteria within a protrusion during infection of A549 cells. In (B) and (C), the percentages were determined from three independent experiments (≥ 380 bacteria were

counted for each infection) and were used to calculate the mean ± SD and p-value (one-way ANOVA with post-hoc Dunnett's test, n.s. relative to WT). Data are shaded by replicate experiment. (D) Percentage of bacteria per focus that spread from infected donor cells to uninfected recipient cells by mixed-cell assay in A549 cells. The means from three independent experiments (squares) are superimposed over the raw data (circles) and were used to calculate the mean ± SD and p-value (one-way ANOVA with post-hoc Dunnett's test, ****$p < 0.0001$ relative to WT). The *sca2*::Tn mutant was used as a positive control. Data are shaded by replicate experiment. (E) Bacteria per focus during infection of A549 cells. The means from three independent experiments (squares) are superimposed over the raw data (circles) and were used to calculate the mean ± SD and p-value (one-way ANOVA with post-hoc Dunnett's test, *$p < 0.05$). These data correspond to the same set of infectious focus assays displayed in (A). Data are shaded by replicate experiment. (F) Growth curves as measured by *R. parkeri* (17 kDa surface antigen) genome equivalents per Vero host cell (*GAPDH*) genome equivalent normalized to 1 h post-infection. The mean ± SD for triplicate samples from a representative experiment were compared at each timepoint after $\log_2$ transformation (unpaired two-tailed *t* test, *$p < 0.05$ and **$p < 0.01$ relative to WT).

A reduction in infectious focus size could be caused by defects in cell-to-cell spread. For example, Tn mutagenesis of *sca2* and *sca4* specifically disrupts spread by limiting actin tail formation and protrusion resolution, respectively, leading to smaller infectious foci (14, 15). Loss of RARP-1 did not alter the frequency of actin tails or protrusions (Figure 2.2B,C), suggesting that spread may not be regulated by RARP-1. As an orthogonal approach, we also evaluated the efficiency of spread by performing a mixed-cell infectious focus assay (15). In this assay, donor host cells stably expressing a cytoplasmic marker are infected, mixed with unlabeled recipient host cells, and then infection of the mixed monolayer is allowed to progress. Bacteria that spread to unlabeled recipient cells can thus be distinguished from bacteria that remain in the labeled donor cell for each focus. As expected, a *sca2*::Tn mutant failed to spread from infected donor cells (Figure 2.2D). In contrast, the *rarp-1*::Tn mutant exhibited similar efficiency of spread from donors to recipients as compared to WT bacteria. Altogether, these results indicate that RARP-1 is dispensable for cell-to-cell spread.

Alternatively, a reduction in infectious focus size could be caused by defects in bacterial growth. When performing the infectious focus assays, we noted that the number of *rarp-1*::Tn mutant bacteria within the infectious foci was reduced compared to WT (Figure 2.2E). This was in contrast to Tn mutants of *sca2* and *sca4*, which do not exhibit reduced bacterial loads despite

forming smaller foci (14, 15). Restoring RARP-1 expression in the complemented strain rescued the bacterial load defect (Figure 2.2E), suggesting that RARP-1 regulates bacterial growth. To determine if the *rarp-1*:Tn mutant displayed altered growth behavior over the course of infection, we used qPCR to monitor bacterial genome equivalents during infection of Vero host cell monolayers. In agreement with the bacterial load defect observed in the infectious focus assay, the *rarp-1*::Tn mutant exhibited a growth defect compared to WT (Figure 2.2F), with a doubling time of 8.4 h versus 6.3 h approximated from exponential phase growth. Furthermore, the viability of *rarp-1*::Tn mutant bacteria during infection was identical to WT (Figure 2.3); thus, the observed growth defects for the *rarp-1*::Tn mutant are not due to the generation of non-viable progeny. Together, our data support a role for RARP-1 during bacterial growth in multiple cell types.

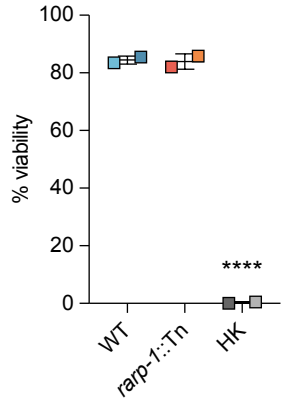

Figure 2.3 – RARP-1 is dispensable for bacterial viability. Bacteria were released from infected A549 cells after 48 h and viability was assessed by differential staining. Percentages were determined from two independent experiments (≥ 160 bacteria were counted for each infection) and were used to calculate the mean ± SD and p-value (one-way ANOVA with post-hoc Dunnett's test, ****$p < 0.0001$ relative to WT). Heat-killed (HK) bacteria served as a positive control. Data are shaded by replicate experiment.

RARP-1 is dispensable for evasion of autophagy

Given the *rarp-1*::Tn mutant growth defect, we hypothesized that RARP-1 might promote bacterial growth by preventing clearance from the host cell. *R. parkeri* avoids

recognition and destruction by the host cell autophagy machinery using the abundant outer membrane protein OmpB (13). Bacteria lacking OmpB are readily polyubiquitinated by the host cell and associate with LC3-positive autophagic membranes. We tested whether the *rarp-1*::Tn mutant likewise associates with LC3 during infection of A549 cells. In contrast to an *ompB*::Tn mutant, the *rarp-1*::Tn mutant failed to mobilize host LC3 (Figure 2.4A). Thus, loss of RARP-1 expression does not render this mutant more susceptible to autophagic clearance, indicating that RARP-1 supports growth through a different mechanism.

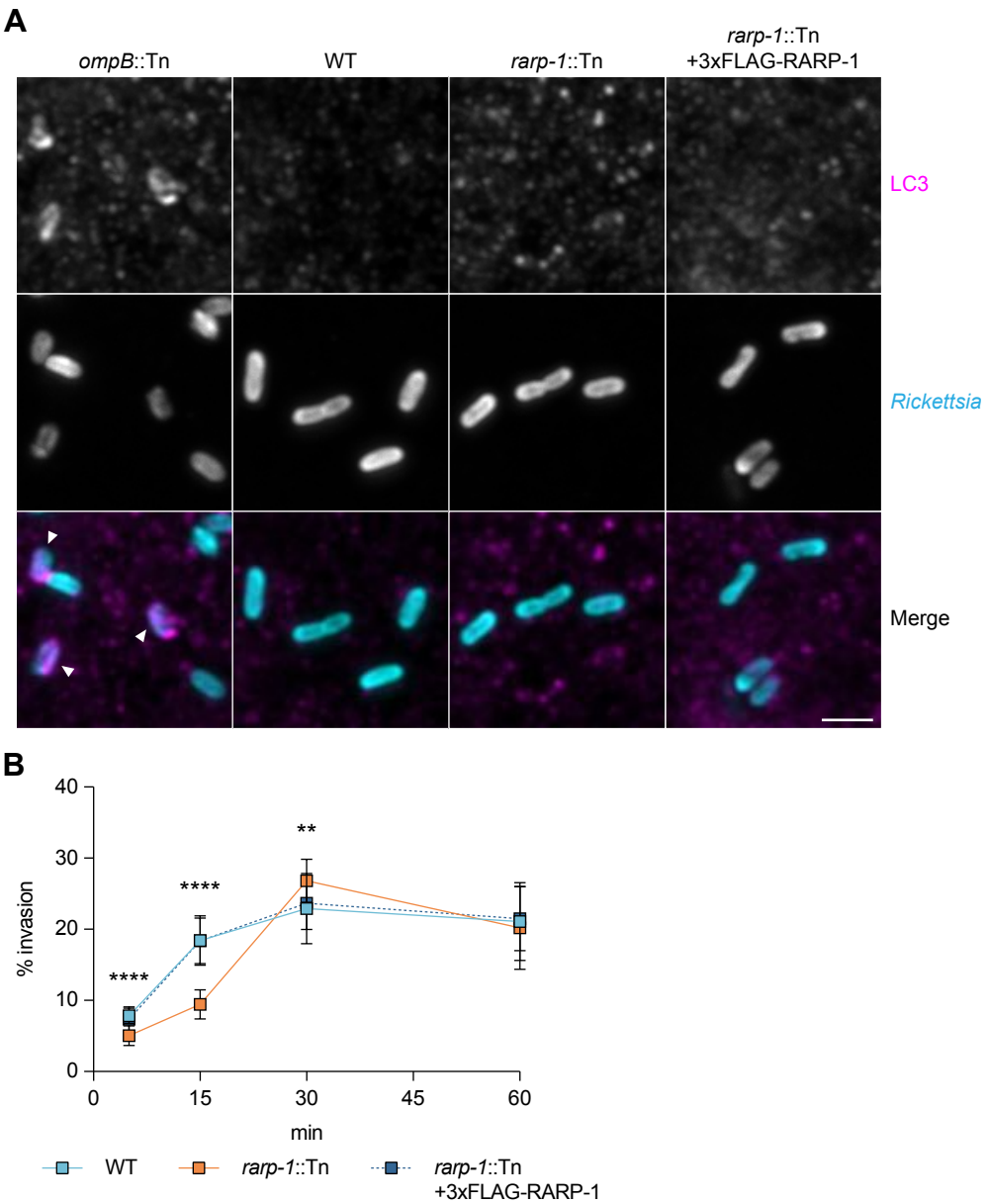

Figure 2.4 – RARP-1 is dispensable for evasion of host cell autophagy and supports host cell invasion. (A) Recruitment of LC3 during infection of A549 cells. Samples were stained for LC3 (magenta) and bacteria (cyan). The *ompB*::Tn mutant was used as a positive control, and bacteria associated with LC3-positive membranes are indicated (arrowheads). Scale bar, 2 µm. (B) Efficiency of invasion into A549 cells. The means ± SD from a representative experiment (n = 20 fields of view each with ≥ 45 bacteria) were compared at each timepoint (one-way ANOVA with post-hoc Dunnett's test, **p < 0.01 and ****p < 0.0001 relative to WT).

RARP-1 supports host cell invasion

We next wanted to determine if RARP-1 plays other roles in the infection cycle upstream of growth inside the host cytoplasm. We tested whether the *rarp-1*::Tn mutant exhibited defects

during invasion of A549 host cells using differential immunofluorescent staining (6). In this assay, bacteria are stained both before and after host cell permeabilization to distinguish external and internal bacteria, respectively. Invasion of the *rarp-1*::Tn mutant was delayed compared to WT but otherwise recovered within 30 min post-infection (Figure 2.4B). We observed similar invasion kinetics for WT bacteria and the complemented strain, indicating that the delayed invasion of the *rarp-1*::Tn mutant is due to loss of RARP-1 expression. Thus, RARP-1 supports efficient host cell invasion. We therefore turned our investigation to the localization and binding partners of RARP-1 so that we could reveal how this factor contributes to infection.

RARP-1 is not secreted into the host cytoplasm by R. parkeri

RARP-1 contains an N-terminal Sec secretion signal and several C-terminal ankyrin repeats. Ankyrin repeats are often involved in protein-protein interactions (20), and various intracellular pathogens secrete ankyrin repeat-containing proteins to target an array of host cell processes (21, 22). Previous work with the typhus group *Rickettsia* species *R. typhi* suggested that RARP-1 is delivered into host cells through a non-canonical mechanism mediated by the Sec translocon and TolC (19). We originally hypothesized that *R. parkeri* also secretes RARP-1 to target host cell functions and ultimately promote bacterial growth and invasion. To monitor secretion of RARP-1 during infection of A549 cells, we used selective lysis to separate supernatants containing the infected host cytoplasm from pellets containing intact bacteria (Figure 2.5A). A protein that is secreted during infection should be detected in both the supernatant and pellet fractions by immunoblotting, as was observed for the secreted effector Sca4. The absence of the bacterial RNA polymerase subunit RpoA in the supernatant fraction confirmed that our lysis conditions did not cause bacterial lysis and release of non-secreted

bacterial proteins. Unexpectedly, we detected 3xFLAG-RARP-1 in the bacterial pellet but not in the supernatant fraction of cells infected with the *rarp-1*::Tn + 3xFLAG-RARP-1 complemented strain.

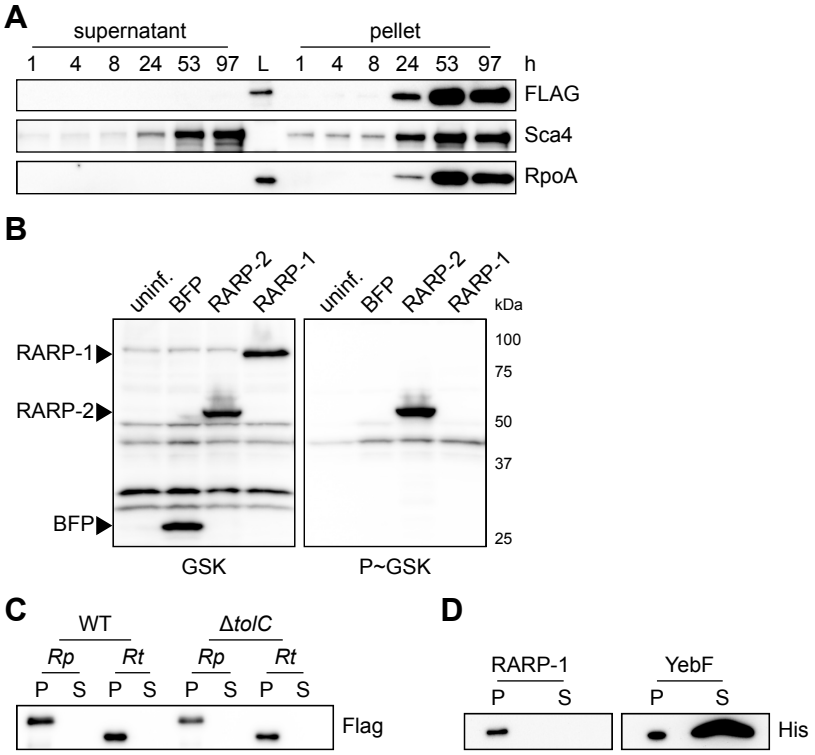

Figure 2.5 – RARP-1 is not secreted. (A) Western blots for FLAG (top) and Sca4 (middle) during infection of A549 cells with *rarp-1*::Tn + 3xFLAG-RARP-1 bacteria. Infected host cells were selectively lysed at various timepoints to separate supernatants containing the infected host cytoplasm from pellets containing intact bacteria. RpoA (bottom) served as a control for bacterial lysis or contamination of the infected cytoplasmic fraction. L, ladder. (B) Western blot for GSK-tagged constructs during infection of Vero cells. Whole cell infected lysates were probed with antibodies against the GSK tag (left) or its phosphorylated form (P~GSK, right) to detect exposure to the host cytoplasm. BFP (non-secreted) and RARP-2 (secreted) were used as controls. Uninf, uninfected whole cell lysate. (C) Western blot for FLAG using N-terminal FLAG-tagged *R. parkeri* (*Rp*) or *R. typhi* (*Rt*) RARP-1 expressed by WT or Δ*tolC E. coli*. (D) Western blot for His using C-terminal Myc-6xHis-tagged *R. typhi* RARP-1 or C-terminal 6xHis-tagged *E. coli* YebF expressed by WT *E. coli*. For (C) and (D), cultures were pelleted (P) and the culture supernatant (S) was filtered and precipitated to concentrate proteins released into the medium.

Similar results were observed for a 3xFLAG-RARP-1 construct containing an additional Ty1 epitope tag inserted proximal to the C-terminus (Figure 2.6A), suggesting that the lack of detection was not due to proteolytic processing of the RARP-1 protein. As with the 3xFLAG-RARP-1 construct, this dual-tagged variant rescued the *rarp-1*::Tn mutant infectious focus

defects (Figure 2.6B,C), demonstrating the functional relevance of the tagged RARP-1 construct. Moreover, endogenous RARP-1 protein was detectable in the WT bacterial pellet but not in the supernatant fraction with our polyclonal antibody (Figure 2.6D), confirming that the epitope-tagged constructs recapitulate the behavior of the endogenous protein. Together, these results suggest that RARP-1 is not secreted by *R. parkeri* into the host cytoplasm.

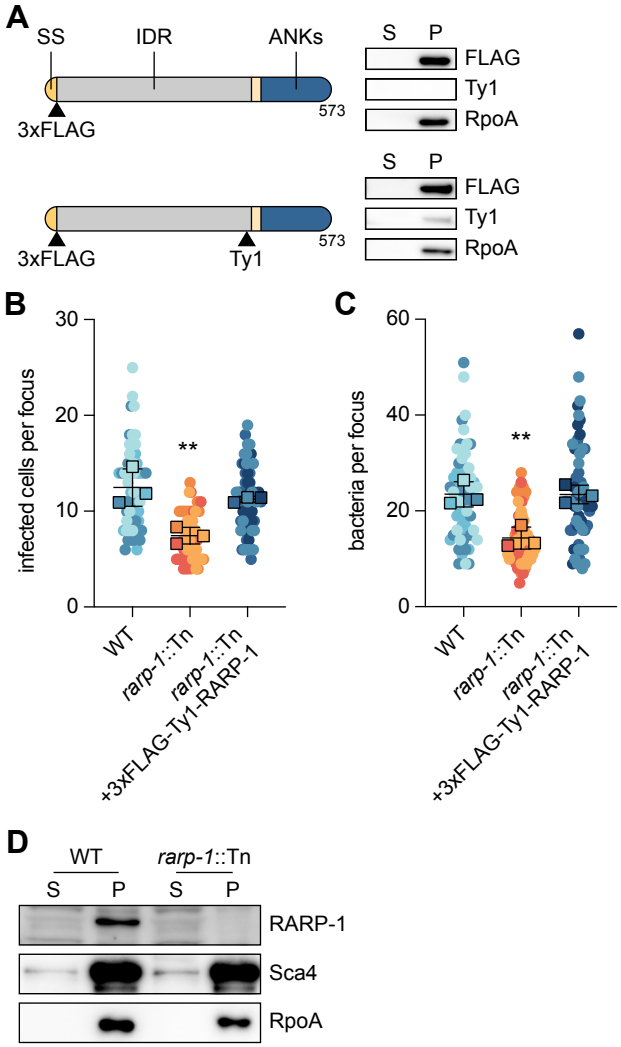

Figure 2.6 – Tagged RARP-1 constructs and endogenous RARP-1 are not secreted. (A) *R. parkeri* RARP-1 with insertion sites for 3xFLAG and Ty1 epitope tags indicated (arrowheads). Western blots for FLAG (top) and Ty1 (middle) after infection of A549 cells with *rarp-1*::Tn + 3xFLAG-RARP-1 (single-tagged) or *rarp-1*::Tn + 3xFLAG-Ty1-RARP-1 (dual-tagged) bacteria. (B) Infected cells per focus during infection of A549 cells. (C) Bacteria per focus during infection of A549 cells. In (B) and (C), the means from three independent experiments (squares) are superimposed over the raw data (circles) and were used to calculate the mean ± SD and p-value (one-way ANOVA with post-hoc Dunnett's test, **p < 0.01 relative to WT). Data are shaded by replicate experiment. (D)

Western blots for RARP-1 (top) and Sca4 (middle) after infection of A549 cells with WT or *rarp-1*::Tn bacteria. Note the specific RARP-1 band in the pellet sample for WT bacteria only, in contrast to the identical non-specific bands in the supernatant samples for WT and *rarp-1*::Tn bacteria. In (A) and (D), infected host cells were selectively lysed after 48 h to separate supernatants (S) containing the infected host cytoplasm from pellets (P) containing intact bacteria. RpoA (bottom) served as a control for bacterial lysis or contamination of the infected cytoplasmic fraction.

As an alternative strategy to evaluate RARP-1 secretion, we introduced glycogen synthase kinase (GSK)-tagged constructs into *R. parkeri*. This system has been used to assess secretion of effector proteins by *Rickettsia* spp. and other bacteria, and it does not rely on the selective lysis of infected samples (23, 24). GSK-tagged proteins become phosphorylated by host kinases upon entering the host cytoplasm, and secretion of the tagged protein can be validated by phospho-specific antibodies (25). Although GSK-tagged RARP-2, a known secreted effector (23), was phosphorylated, GSK-tagged RARP-1 and a non-secreted control (BFP) were not phosphorylated during infection (Figure 2.5B). These results provide further evidence that RARP-1 is not secreted into the host cytoplasm by *R. parkeri*.

Heterologously expressed RARP-1 is not secreted by E. coli

We were surprised by the results above since previous work suggested that RARP-1 is delivered into host cells by *R. typhi*. Heterologous expression in *Escherichia coli* provided evidence that *R. typhi* RARP-1 is secreted in a Sec- and TolC-dependent manner (19). Following the methodology described by that work, we assessed secretion of *R. parkeri* and *R. typhi* RARP-1 by WT and Δ*tolC E. coli*. In this assay, *E. coli* cultures expressing RARP-1 are pelleted and the culture supernatant is then filtered and precipitated to concentrate proteins released into the extracellular milieu. Although *R. parkeri* RARP-1 was clearly detectable in the bacterial pellets of both strains, it was not observed in the supernatants for either strain (Figure 2.5C). Likewise, we were unable to detect secretion of *R. typhi* RARP-1 by either strain, in contrast to the

previously described secretion pattern for this protein. To confirm that our use of an N-terminal 3xFLAG tag did not disrupt secretion by *E. coli*, we generated an *R. typhi* RARP-1 construct with a C-terminal Myc-6xHis tag, as described in the previous work. Again, we were unable to detect secretion of *R. typhi* RARP-1 (Figure 2.5D). To validate our ability to detect secreted proteins in the culture supernatant, we assessed secretion of 6xHis-tagged YebF, a protein known to be exported into the medium by *E. coli* (26). As expected, YebF was observed in both the bacterial pellet and culture supernatant. The lack of RARP-1 secretion by *E. coli* is consistent with our immunoblotting results for infection with *R. parkeri*, suggesting that RARP-1 is not a secreted effector.

RARP-1 resides within R. parkeri

Given that RARP-1 is not secreted by *R. parkeri*, we next investigated where it localized during infection using differential immunofluorescent staining (15). In this assay, infected A549 host cells are first selectively permeabilized such that only the host cell contents and bacterial surface are accessible for staining. Then, the bacteria are permeabilized with lysozyme and detergent to permit immunostaining of proteins inside the bacteria. By staining with a FLAG tag-specific antibody either with or without this second permeabilization step, we can distinguish the localization of tagged proteins inside or outside the bacteria, respectively. We predicted that epitope-tagged RARP-1 expressed by the *rarp-1*::Tn + 3xFLAG-RARP-1 complemented strain would be absent from the host cytoplasm but present inside permeabilized bacteria. In agreement with our immunoblotting results above, we did not detect specific FLAG staining in the host cytoplasm after infection with the complemented strain, similar to results with the *rarp-1*::Tn mutant (Figure 2.7A). We also did not detect the protein on the bacterial surface. Instead,

3xFLAG-RARP-1 was only detectable after permeabilizing bacteria with lysozyme and detergent. Under these conditions, the 3xFLAG-RARP-1 signal surrounded the bacteria with variable localization patterns and often formed bipolar puncta (Figure 2.7B). Line scan analysis of permeabilized bacteria confirmed that 3xFLAG-RARP-1 localized adjacent to the bacterial cytoplasm (Figure 2.7C). These localization patterns suggest that RARP-1 is not secreted into the host cytoplasm but instead localizes within *R. parkeri*. The presence of an N-terminal Sec secretion signal and the lack of predicted transmembrane domains suggest that RARP-1 localizes to the *R. parkeri* periplasmic space or is otherwise associated with the inner or outer membrane leaflets facing the periplasm.

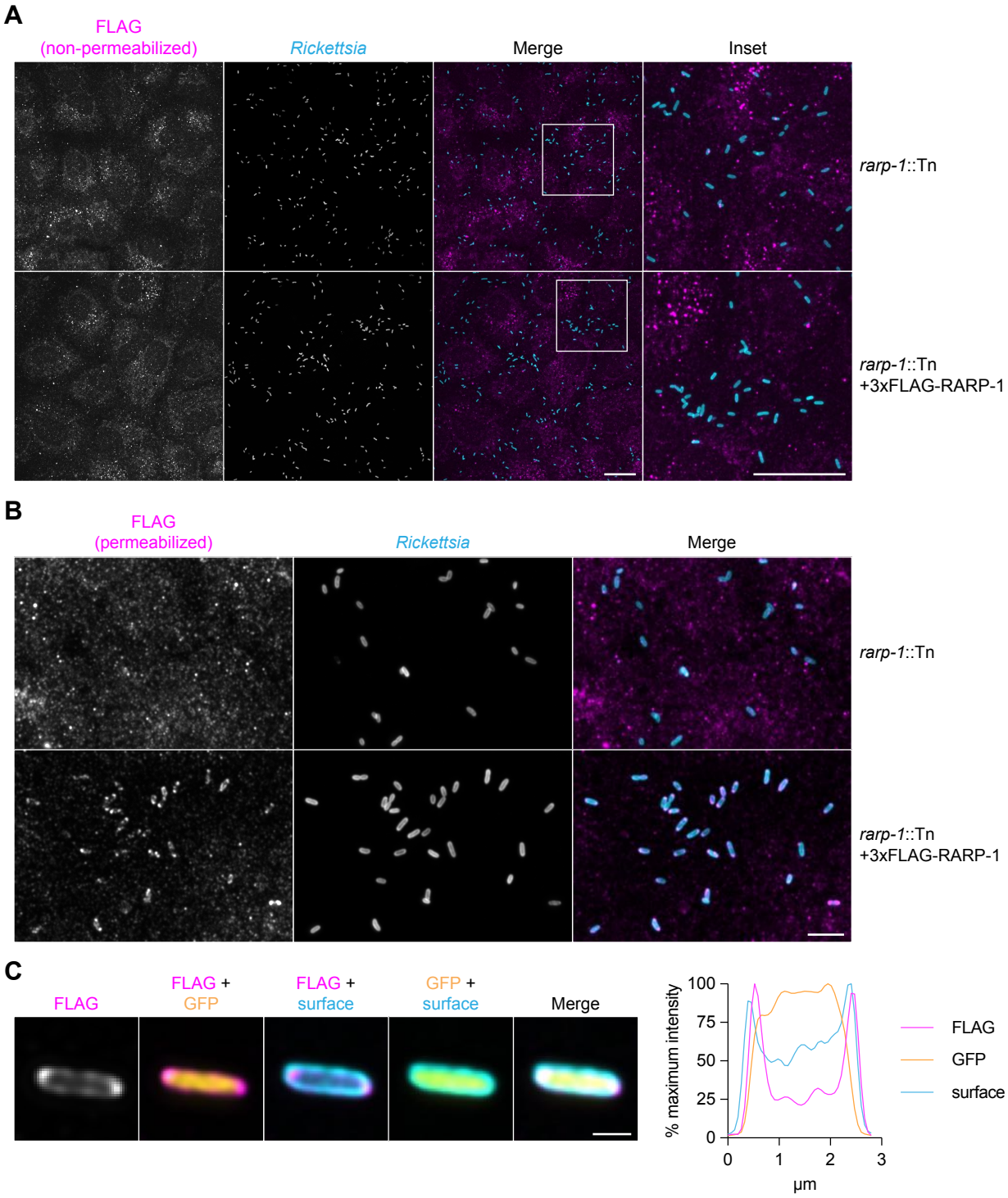

Figure 2.7 – RARP-1 resides within *R. parkeri*. (A) Images of *rarp-1*::Tn (top) and *rarp-1*::Tn + 3xFLAG-RARP-1 (bottom) bacteria during infection of A549 cells. Samples were stained for FLAG (magenta) and the bacterial surface (cyan) without permeabilization of bacteria. Scale bars, 20 µm. (B) Images of *rarp-1*::Tn (top) and *rarp-1*::Tn + 3xFLAG-RARP-1 (bottom) bacteria during infection of A549 cells. The bacterial surface (cyan) was stained prior to permeabilization by lysozyme and detergent and subsequent staining for FLAG (magenta). Scale bar, 5 µm. (C) Subcellular localization of 3xFLAG-RARP-1 in a representative *rarp-1*::Tn + 3xFLAG-RARP-1 bacterium during infection of A549 cells. The bacterial surface (cyan) was stained prior to permeabilization by lysozyme and

detergent and subsequent staining for FLAG (magenta). GFP (yellow) demarcates the bacterial cytoplasm. Scale bar, 1 μm. A pole-to-pole 0.26 μm width line scan (right) was generated for FLAG, GFP, and the bacterial surface.

RARP-1 interacts with other bacterial factors that access the periplasm

Based on the 3xFLAG-RARP-1 localization pattern, we hypothesized that RARP-1 might interact with other factors in the *R. parkeri* periplasm to support growth and host cell invasion. To test this hypothesis, we isolated *rarp-1*::Tn + 3xFLAG-Ty1-RARP-1 bacteria and treated them with lysozyme-containing lysis buffer to release non-secreted proteins for pulldown. As a control, we also prepared lysates from WT bacteria that do not express tagged RARP-1. We then immunoprecipitated the lysates with a FLAG tag-specific antibody, performed an acid elution to release bound proteins, and analyzed the eluates by mass spectrometry to identify putative RARP-1 binding partners (Figure 2.8A,B). Proteins that were present in the tagged lysate pulldown but absent from the untagged lysate pulldown were called as hits (Figure 2.9).

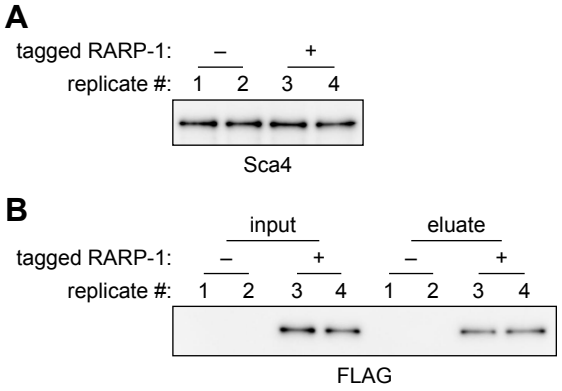

Figure 2.8 – Inputs and eluates from co-immunoprecipitation of lysozyme-permeabilized bacteria. (A) Western blot for Sca4 (loading control) in input lysates. (B) Western blot for FLAG in input lysates and FLAG immunoprecipitation eluates. In (A) and (B), bacteria expressing tagged (+) or untagged (–) RARP-1 were purified and then permeabilized by lysozyme prior to immunoprecipitation. Two replicate samples were harvested from each strain.

Gene ID	Description
MC1_RS01995	RvhB10; T4SS outer membrane core complex
MC1_RS00605	Sca2; autotransporter; surface actin nucleation
MC1_RS00420	hypothetical lipoprotein
MC1_RS06520	hypothetical porin
MC1_RS02895	hypothetical lipoprotein
MC1_RS00535	hypothetical porin
MC1_RS00570	OmpW family protein; porin
MC1_RS01970	RvhB9a; T4SS outer membrane core complex
MC1_RS01990	RvhB9b; T4SS outer membrane core complex
MC1_RS06075	Pal; peptidoglycan-associated lipoprotein
MC1_RS05020	50S ribosomal protein L17
MC1_RS06525	hypothetical porin
MC1_RS02795	PcaH; protocatechuate-3,4-dioxgenase
MC1_RS00865	HflC; protease modulator
MC1_RS06550	17 kDa lipoprotein surface antigen

Figure 2.9 – Co-immunoprecipitation of lysozyme-permeabilized bacteria reveals that RARP-1 interacts with other bacterial factors that access the periplasm. Putative RARP-1 binding partners are ordered by decreasing spectral count. MC1_RS05020 is the only hit not predicted to access the periplasm.

Of the hits identified, only Sca2 has been functionally characterized in *R. parkeri* (14). Although Sca2 promotes late-stage actin-based motility, the *rarp-1*::Tn mutant formed actin tails at frequencies comparable to WT (Figure 2.2B), indicating that the loss of RARP-1 does not dramatically impair Sca2 function. However, it is possible that RARP-1 functions in a more subtle way to influence Sca2 activity. To test this hypothesis, we used immunoblotting to assess Sca2 expression in the *rarp-1*::Tn mutant (Figure 2.10A). The abundance of full-length Sca2 and its processed products was comparable between the *rarp-1*::Tn mutant and the complemented strain, suggesting that RARP-1 does not grossly impact Sca2 levels. Likewise, we observed similar patterns of Sca2 localization between strains (Figure 2.10B), suggesting that RARP-1 does not play a role in the polar positioning of Sca2. Taken together, these results suggest that RARP-1 does not regulate the activity of its putative binding partner Sca2.

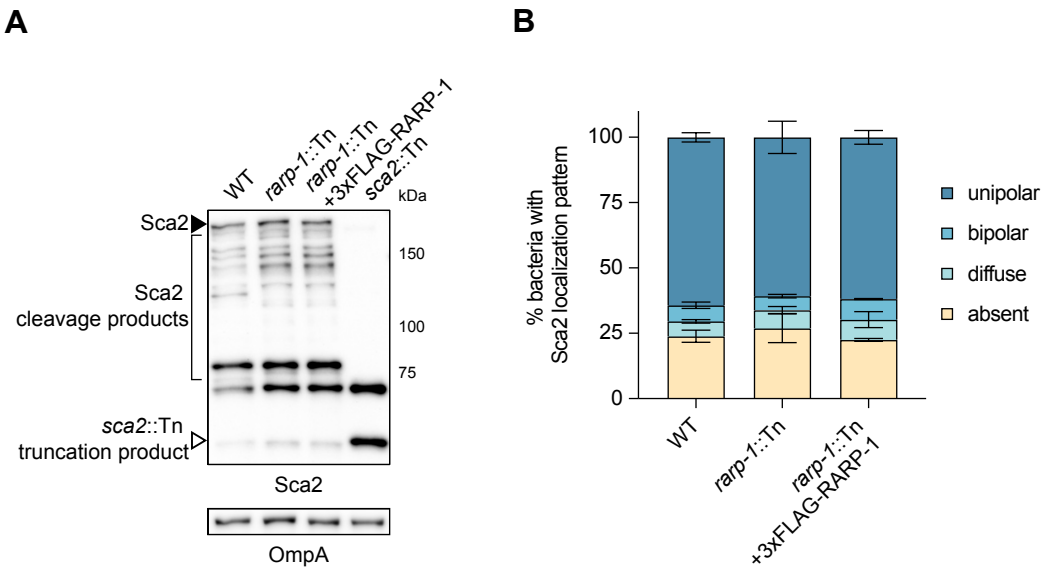

Figure 2.10 – RARP-1 does not regulate the abundance or localization of Sca2. (A) Western blot for Sca2 from purified *R. parkeri* strains. Full-length Sca2 (arrowhead), Sca2 cleavage products (bracket), and the truncation product in the *sca2*::Tn mutant (open arrowhead) are indicated. (B) Percentage of bacteria with the indicated Sca2 localization pattern during infection of A549 cells. Percentages were determined from two independent experiments (≥ 350 bacteria were counted for each infection) and were used to calculate the mean ± SD and p-value (one-way ANOVA with post-hoc Dunnett's test, n.s. relative to WT).

Additional hits identified in our analysis include the type IV secretion system outer membrane components RvhB9 and RvhB10 as well as several hypothetical lipoproteins and porins (Figure 2.9). At this time, none of these proteins have been functionally characterized in *R. parkeri*. Consistent with RARP-1 localization to the periplasm, however, nearly all of these hits are predicted to reside in the periplasm or otherwise access and transit the periplasm *en route* to the bacterial surface. Thus, it remains possible that RARP-1 acts with one or more of these binding partners to support growth and host cell invasion.

Discussion

After host cell invasion, obligate intracellular bacteria must scavenge host nutrients, proliferate, and avoid destruction by their hosts (2). Disruption of one or all of these activities will diminish intracellular bacterial loads and ultimately reduce pathogenicity. While many

studies have revealed important regulators of invasion, nutrient acquisition, and bacterial growth for other species, little is known about the factors that support rickettsial physiology during infection, and only recently have we begun to uncover the protective strategies *Rickettsia* spp. employ to ward off host cell defenses (13, 16). Consequently, we sought to better understand the genetic determinants of rickettsial infection using our functional genetic approaches in *R. parkeri*. We found that RARP-1 likely resides in the periplasm where it interacts with proteins predicted or known to drive bacterial fitness or interactions with the host. Furthermore, our results suggest that RARP-1 supports the *R. parkeri* life cycle by promoting bacterial growth as well as efficient host cell invasion.

Several studies have identified rickettsial surface proteins and candidate secreted effectors that facilitate invasion. For example, the outer membrane proteins OmpA and OmpB respectively interact with α2β1 integrin and Ku70 at the host cell surface to support receptor-mediated invasion (5, 7), while the effectors RalF and Risk1 modulate host membrane phosphoinositides during entry (27, 28). Loss of RARP-1 expression led to a transient invasion delay, indicating that RARP-1 also plays a role in host cell entry. A similar invasion delay was reported for an *ompB*::Tn mutant (13), suggesting that *Rickettsia* spp. use several redundant strategies to enter their hosts. Although RARP-1 itself is not exported from the bacterium, one or more of the RARP-1 interaction partners may contribute to efficient internalization as discussed above. Loss of RARP-1 expression would therefore have pleiotropic effects on infection by hindering both invasion and growth. Alternatively, it is possible that the *rarp-1*::Tn mutant invasion delay is the result of defective growth in the preceding infection cycles when the bacteria were harvested. Indeed, invasion competency of the intracellular bacterial pathogen

Brucella abortus is linked to cell cycle progression (29). Perhaps rickettsial invasion efficiency relies on robust growth, without which the invasion program is impaired.

Loss of RARP-1 expression also reduced bacterial loads, persisting long after the initial invasion delay was overcome. This defect suggests that RARP-1 plays a role in bacterial growth through the regulation of bacterial physiology or avoidance of host defenses. Normally, *R. parkeri* shields itself from autophagy receptors by methylating outer membrane proteins such as OmpB (13). Loss of OmpB or the methyltransferases PKMT1 and PKMT2 promotes autophagy of *R. parkeri* and reduction of intracellular bacterial burdens (16). Since the *rarp-1*::Tn mutant did not display enhanced recruitment of the autophagy marker LC3, we concluded that the loss of RARP-1 does not render this mutant more susceptible to autophagy. Nevertheless, we cannot rule out that growth of the *rarp-1*::Tn mutant is restricted by other host defense strategies employed by the cell lines used in this study.

Prior work reported that RARP-1 was robustly secreted into the host cytoplasm by *R. typhi*, and experiments in *E. coli* suggested that RARP-1 relied on a non-canonical Sec- and TolC-dependent pathway for export (19). We were unable to detect secretion of endogenous or epitope-tagged RARP-1 into the host cytoplasm by *R. parkeri*, even though the tagged constructs functionally complemented the *rarp-1*::Tn mutant phenotype. Similarly, we were unable to detect phosphorylation of GSK-tagged RARP-1 in infected cell lysates as an orthogonal secretion assay. Notably, this lack of secretion was observed during infection of multiple host cell types and for both WT and *rarp-1*::Tn backgrounds. We also could not detect secretion of RARP-1 by *E. coli*, despite testing both *R. parkeri* and *R. typhi* homologs under the same conditions previously published (19). Nevertheless, it is formally possible that our use of a different *E. coli* K-12 strain (BW25513 rather than C600) prevented release of RARP-1 due to

incompatibility with the endogenous secretion system. Since *R. typhi* is a BSL-3 pathogen, we are not able to assess secretion of *R. typhi* RARP-1 by *R. parkeri*, and a loss-of-function *rarp-1* mutant does not exist in *R. typhi*. Altogether, our data suggest that RARP-1 is not secreted into the host cytoplasm by *R. parkeri*; instead, it is likely targeted to the periplasm by its Sec secretion signal where it stays to support bacterial growth and invasion.

RARP-1 is not predicted to possess enzymatic activity, but it does contain a large central intrinsically disordered region (IDR). The structural plasticity of IDRs affords them diverse biological functions, such as chaperone recruitment, passage through narrow protein channels, and binding of multiple protein partners (30–33). RARP-1 also possesses several C-terminal ankyrin repeats (ANKs), and many intracellular bacterial pathogens secrete ANK-containing effectors to target host cell functions (21, 22). Nevertheless, ANKs have been shown to support the activity of bacterial proteins that are not secreted into the extracellular milieu. For example, AnkB localizes to the periplasm of *Pseudomonas aeruginosa* where it protects against oxidative stress (34), and Bd3460 of *Bdellovibrio bacteriovorus* complexes with endopeptidases in the periplasm to prevent degradation of its own cell wall (35). Although ANKs are best known for mediating protein-protein interactions, recent work has demonstrated that ANKs can also bind sugars and lipids (36, 37). Future mutational and biochemical analyses may reveal if the RARP-1 IDR and ANKs are necessary for interactions with its putative binding partners or if these domains otherwise support RARP-1 activity.

Our data suggest that RARP-1 interacts with several classes of proteins to support growth and invasion. Since many of these binding partners have not been functionally characterized, we focused our attention on the interaction between RARP-1 and Sca2. Sca2 is required for late-stage actin-based motility in mammalian and tick cells (14, 38), and it is necessary for virulence

in animal models of SFG rickettsial infection (39). Tn mutagenesis of *rarp-1* did not reduce actin tail frequency or Sca2 localization to the cell poles, suggesting that RARP-1 does not govern Sca2 function. Nevertheless, it is possible that Sca2 supports the localization or function of RARP-1 in the periplasm as it acts on other factors to regulate invasion and growth.

We also detected interactions between RARP-1 and components of the Rickettsiales *vir* homolog type IV secretion system (*rvh* T4SS). In the canonical *vir* T4SS of *Agrobacterium tumefaciens*, VirB9 and VirB10, together with VirB7, form a core complex positioned in the periplasm and outer membrane (40). It is unknown to what extent the *rvh* subunits play similar roles as their *vir* counterparts and how RARP-1 might be involved. Furthermore, few *rvh* T4SS effectors are known and none of them have been shown to modulate growth (23, 27, 28). Recent work has suggested that the putative *rvh* T4SS effector Risk1 promotes host cell invasion by *R. typhi* (28); whether Risk1 plays a similar role in *R. parkeri* or if its secretion is impacted in the *rarp-1*::Tn mutant is unknown. As new effectors are characterized, it will be important to determine if their secretion depends on the interaction between RARP-1 and the *rvh* T4SS.

Interestingly, many of the RARP-1 binding partners we identified include predicted porins and lipoproteins of unknown function. Porins are major components of the outer membrane and regulate the transport of hydrophilic compounds such as nutrients, toxins, and antibiotics (41). Homologs of MC1_RS00535 and MC1_RS00570 have been identified on the surface of the related SFG member *R. rickettsii* (42), but the substrates for these and other rickettsial porins have yet to be characterized. Lipoproteins are lipid-modified proteins that anchor to the membrane and support many aspects of bacterial physiology, including nutrient uptake, protein folding, signal transduction, and cell division (43). Based on remote homology predictions (via HHpred (44)), the lipoproteins identified in this study appear to be unique to the

Rickettsia genus and remain largely uncharacterized. Indeed, although Tn mutagenesis of the 17 kDa lipoprotein surface antigen reduces *R. parkeri* plaque size, its function is unknown (18, 45). In future studies, it will be important to investigate how disruption of one or more of these factors contributes to the invasion and growth defects we observed for the *rarp-1*::Tn mutant.

The remaining RARP-1 interaction partners include homologs of proteins with known roles in bacterial physiology. These include factors that regulate cell division (Pal (46)), metabolism (PcaH (47)), and protein stability (HflC (48)), but none of these functions has been experimentally validated in *Rickettsia* spp. Although we did not observe any obvious morphological defects for the *rarp-1*::Tn mutant, the interaction between RARP-1 and a Pal homolog could influence rickettsial growth in a more subtle manner. It is also possible that disruption of metabolism or membrane protein quality control underlies the *rarp-1*::Tn mutant invasion and growth defects.

Our work uncovers an important role for RARP-1 in supporting the *R. parkeri* life cycle. Through its targeting to the periplasm, we propose that RARP-1 regulates invasion and growth by acting in concert with one or more of the factors revealed in our study. Further work is needed to characterize these interactions since many of the RARP-1 binding partners we identified have unknown functions in the *Rickettsia* genus. Expansion of the rickettsial toolkit could facilitate these efforts as well as help determine if there is temporal or spatial control of RARP-1 activity during the *R. parkeri* life cycle. Moreover, structure-function analyses of RARP-1 will provide valuable insight into its mechanism of action in particular and the function of ANK- and IDR-containing proteins in general. Homologs of RARP-1 are notably absent outside the genus, despite conservation of the protein across *Rickettsia* spp. (19). We therefore speculate that RARP-1 represents a core and unique adaptation to the demands of the host cell niche, and future

studies may extend its relevance to infection of arthropod vectors. The success of *Rickettsia* spp. hinges on their ability to access and thrive within the complex environment of the host cytoplasm. Continued investigation into the factors that support these fundamental processes will not only improve our understanding of rickettsial biology, but will also highlight the diverse strategies underpinning obligate intracellular bacterial life.

Methods

Cell culture

A549 human lung epithelial and Vero monkey kidney epithelial cell lines were obtained from the University of California, Berkeley Cell Culture Facility (Berkeley, CA). A549 cells were maintained in DMEM (Gibco #11965118) containing 10% FBS. Vero cells were maintained in DMEM containing 5% FBS. A549 cells stably expressing cytoplasmic TagRFP-T (A549-TRT) were generated by retroviral transduction as previously described (15). Cell lines were confirmed to be mycoplasma-negative by MycoAlert PLUS Assay (Lonza #LT07-710) performed by the Koch Institute High Throughput Sciences Facility (Cambridge, MA).

Plasmid construction

pRAM18dSGA-3xFLAG-RARP-1 was generated from pRAM18dSGA[MCS] (kindly provided by Dr. Ulrike Munderloh) and contains the 247 bp immediately upstream of the *tolC* start codon (MC1_RS01570), the first 23 aa (amino acids) of *R. parkeri* RARP-1 (MC1_RS01585) containing the Sec SS, a HVDYKDHDGDYKDHDIDYKDDDDKHV sequence (3xFLAG epitope tag underlined), the remaining 550 aa of RARP-1, and the *R. parkeri ompA* terminator (MC1_RS06480). pRL0079 is identical to pRAM18dSGA-3xFLAG-RARP-1

but contains GSGGEVHTNQDPLDGGT (Ty1 epitope tag underlined) between residues 396 and 397.

pRL0284 was generated from pRAM18dSGA[MCS] and contains the *R. parkeri ompA* promoter, an N-terminal MSGRPRTTSFAESGS sequence (GSK epitope tag underlined), TagBFP from pRAM18dRA-2xTagBFP (15), and the *ompA* terminator. pRL0285 is identical to pRL0284 but contains *R. parkeri* RARP-2 (MC1_RS04780) in place of TagBFP. Similarly, pRL0286 contains *R. parkeri* RARP-1 in place of TagBFP, but GSMSGRPRTTSFAESGS was inserted after the Sec SS (as in pRAM18dSGA-3xFLAG-RARP-1) instead of at the N-terminus.

pRL0287 was generated from pEXT20 (kindly provided by Dr. Michael Laub) and contains the *R. parkeri* RARP-1 insert with intervening 3xFLAG epitope tag from pRAM18dSGA-3xFLAG-RARP-1. pRL0288 is identical to pRL0287, except the 23 aa Sec SS of *R. typhi* RARP-1 (RT0218) and the remaining 563 aa of *R. typhi* RARP-1 were used. In contrast, pRL0289 contains the full 586 aa of *R. typhi* RARP-1 with a C-terminal KGEFEAYVEQKLISEEDLNSAVDHHHHHH sequence (Myc and 6xHis epitope tags underlined) as previously described (19). For pRL0290, a C-terminal VDHHHHHH sequence (6xHis epitope tag underlined) was added to *E. coli* YebF (NCBI b1847).

Generation of R. parkeri strains

Parental *R. parkeri* str. Portsmouth (kindly provided by Dr. Chris Paddock) and all derived strains were propagated by infection and mechanical disruption of Vero cells grown in DMEM containing 2% FBS at 33 °C as previously described (15, 18). Bacteria were clonally isolated and expanded from plaques formed after overlaying infected Vero cell monolayers with agarose as previously described (18). When appropriate, bacteria were further purified by

centrifugation through a 30% MD-76R gradient (Mallinckrodt Inc. #1317-07) as previously described (15). Bacterial stocks were stored as aliquots at -80 °C to minimize variability due to freeze-thaws. Titers were determined for bacterial stocks by plaque assay (15), and plaque sizes were measured with ImageJ after 5 d infection.

Bacteria were transformed with plasmids by small-scale electroporation as previously described (18), except infections were scaled down to a T25 cm^2 flask and bacteria were electroporated with 1 μg dialyzed plasmid DNA. When appropriate, rifampicin (200 ng/mL) or spectinomycin (50 μg/mL) was included to select for transformants. GFP-expressing WT bacteria were generated as previously described (15); this control strain behaves similarly to the parental WT strain in a variety of assays, such as actin tail assays (14) and mixed-cell assays (9). The *rarp-1*::Tn and *sca2*::Tn mutants were generated as previously described (18), and the genomic locations of the Tn insertion sites were determined by semi-random nested PCR and Sanger sequencing. The expanded strains were verified by PCR amplification of the Tn insertion site using primers flanking the region. The *ompB*^{STOP}::Tn mutant (referred to as *ompB*::Tn in this work; kindly provided by Dr. Matthew Welch) was generated as previously described (13).

Infectious focus assays

Confluent A549 cells grown on 12 mm coverslips in 24-well plates were infected at an MOI of 0.005-0.025, centrifuged at 200 x g for 5 min at RT, and incubated at 33 °C for 1 h. Infected cells were washed three times with PBS before adding complete media with 10 μg/mL gentamicin. Infections progressed for 28 h at 33°C until fixation with 4% PFA in PBS for 10 min at RT. Fixed samples were incubated with 0.1 M glycine in PBS for 10 min at RT to quench residual PFA. Samples were then washed three times with PBS, permeabilized with 0.5% Triton

X-100 in PBS for 5 min at RT, and washed another three times with PBS. Samples were then incubated with blocking buffer (2% BSA in PBS) for 30 min at RT. Primary and secondary antibodies were diluted in blocking buffer and incubated for 1 h each at RT with three 5 min PBS washes after each incubation step. The following antibodies and stains were used: mouse anti-β-catenin (Cell Signaling Technology #2677) to detect host membrane, rabbit anti-*Rickettsia* I7205 (kindly provided by Dr. Ted Hackstadt), goat anti-mouse conjugated to Alexa Fluor 568 (Invitrogen #A-11004), goat anti-rabbit conjugated to Alexa Fluor 488 (Invitrogen #A-11008), and Hoechst (Invitrogen #H3570) to detect host nuclei. Coverslips were mounted using ProLong Gold Antifade Mountant (Invitrogen #P36934). Images were acquired using a 60X UPlanSApo (1.30 NA) objective on an Olympus IXplore Spin microscope system. Image analysis was performed with ImageJ. For each strain, 20-35 foci were imaged and the number of infected cells and bacteria per focus was calculated.

Actin tail and protrusion assays

Confluent A549 cells were infected and processed as above, but an MOI of 0.3-0.6 was used and phalloidin conjugated to Alexa Fluor 647 (Invitrogen #A22287) was included to detect actin. For each strain, ≥ 380 bacteria were imaged using a 100X UPlanSApo (1.35 NA) objective and the percentage of bacteria with tails (> 1 bacterial length) and the percentage of bacteria within protrusions were calculated.

Mixed cell assays

A549-TRT donor cells were plated in 96-well plates and unlabeled A549 recipient cells were plated in 6-well plates and grown to confluency. Donors were infected at an MOI of 9-10,

centrifuged at 200 x g for 5 min at RT, and incubated at 33 °C for 1 h. Infected donors and uninfected recipients were washed with PBS, lifted with citric saline (135 mM KCl, 15 mM sodium citrate) at 37 °C to preserve cell surface receptors, recovered in complete media, washed twice with complete media to remove residual citric saline, and resuspended in complete media with 10 μg/mL gentamicin (6 x 10^5 cells/mL donors and 8 x 10^5 cells/mL recipients). Cells were then mixed at a 1:125 ratio (5.3 μL donors and 500 μL recipients) and plated on 12 mm coverslips in 24-well plates. Infections progressed for 31 h at 33 °C until fixation with 4% PFA in PBS for 1 h at RT. Fixed samples were processed as above, except the following antibodies and stains were used: mouse anti-*Rickettsia* 14-13 (kindly provided by Dr. Ted Hackstadt), goat anti-mouse conjugated to Alexa Fluor 647 (Invitrogen #A-21235), and phalloidin-iFluor 405 Reagent (Abcam #ab176752). For each strain, 20 foci were imaged using a 60X objective and the percentage of bacteria per focus that had spread to recipient cells was calculated.

Growth curves

Confluent Vero cells grown in 24-well plates were infected in triplicate at an MOI of 0.025, centrifuged at 200 x g for 5 min at RT, and incubated at 33 °C for 1 h. Infected cells were washed three times with serum-free DMEM before adding complete media and allowing infections to progress at 33 °C. To harvest samples at the indicated time point, infected cells were scraped into the media and centrifuged at 20,000 x g for 5 min. The resulting pellets were resuspended in 600 μL Nuclei Lysis Solution (Promega #A7941), boiled for 10 min to release genomic DNA, and processed with a Wizard Genomic DNA Purification Kit (Promega #A1125) according to manufacturer instructions. After air-drying, the DNA pellets were resuspended in 100 μL H_2O, incubated at 65 °C for 1 h, and allowed to completely rehydrate overnight at RT.

For qPCR, runs were carried out on a LightCycler 480 (Roche) at the MIT BioMicro Center (Cambridge, MA). Primers to the *R. parkeri* 17 kDa surface antigen gene (MC1_RS06550; 5'-TTCGGTAAGGGCAAAGGACA-3' and 5'-GCACCGATTTGTCCACCAAG-3') and to *Chlorocebus sabaeus GAPDH* (5'-AATGGGACTGAAGCTCCTGC-3' and 5'-ATCACCACCCCTCTACCTCC-3') were used to determine bacterial and host genome equivalents, respectively, relative to a standard curve prepared from a pooled mixture of the 96 h time point WT infection samples. Results from each biological replicate were normalized to the 1 h time point and fold-change was calculated. Doubling times were computed from the 24-48 h exponential growth phase for each strain.

Viability assays

Confluent A549 cells grown in 24-well plates were infected at an MOI of 0.2-0.8, centrifuged at 200 x g for 5 min at RT, and incubated at 33 °C for 48 h. Bacteria were released by incubating infected cells with ice-cold H_2O for 2.5 min, immediately recovered in ice-cold 250 mM sucrose, and stained for 15 min at RT using a LIVE/DEAD BacLight Bacterial Viability Kit (Thermo Scientific #L7012) according to manufacturer instructions. *R. parkeri* were heat-killed by incubating at 65 °C for 20 min prior to staining. For each condition, ≥ 160 bacteria were imaged using a 60X objective and the percentage of viable bacteria was calculated.

LC3 recruitment assays

Confluent A549 cells grown on 12 mm coverslips in 24-well plates were infected at an MOI of 1.8-3.6, centrifuged at 200 x g for 5 min at RT, and incubated at 33 °C for 2 h until fixation with 4% PFA in PBS for 10 min. Fixed samples were processed as above, except cells

were permeabilized with 100% methanol for 5 min at RT instead of Triton X-100 and the following antibodies and stains were used: rabbit anti-LC3B (ABclonal #A7198), mouse anti-*Rickettsia* 14-13, goat anti-rabbit conjugated to Alexa Fluor 568 (Invitrogen #A-11011), goat anti-mouse conjugated to Alexa Fluor 488 (Invitrogen #A-11001), and Hoechst. Representative images were acquired using a 100X objective.

Invasion assays

Confluent A549 cells grown on 12 mm coverslips in 24-well plates were placed on ice and the media was replaced with 500 µL ice-cold complete media. The cells were then infected at an MOI of 0.7-1.2, centrifuged at 200 x g for 5 min at 4 °C, 500 µL 37 °C complete media was added, and the plates were immediately moved to 37 °C until fixation with 4% PFA in PBS for 10 min. Fixed samples were incubated with 0.1 M glycine in PBS for 10 min at RT to quench residual PFA. Samples were then washed three times with PBS and incubated with blocking buffer for 30 min at RT. To stain external bacteria, primary and secondary antibodies were diluted in blocking buffer and incubated for 30 min each at RT with three 5 min PBS washes after each incubation step. The following antibodies and stains were used: mouse anti-*Rickettsia* 14-13 and goat anti-mouse conjugated to Alexa Fluor 647. The samples were then fixed with 4% PFA in PBS for 5 min at RT, washed three times with PBS, and quenched with 0.1 M glycine in PBS for 10 min at RT. Samples were then washed three times with PBS, permeabilized with 0.5% Triton X-100 in PBS for 5 min at RT, and washed another three times with PBS. To stain both external and internal bacteria, primary and secondary antibodies were diluted in blocking buffer and incubated for 30 min each at RT with three 5 min PBS washes after each incubation step. The following antibodies and stains were used: mouse anti-*Rickettsia* 14-13 and goat anti-

mouse conjugated to Alexa Fluor 488. For each strain, 20 fields of view each containing ≥ 45 bacteria were imaged using a 60X objective. To facilitate analysis, internal and external bacteria were quantified using ilastik (49); the pixel classifier was trained to distinguish bacteria from background, and then the object classifier was trained to distinguish between internal (single-stained) and external (double-stained) bacteria.

RARP-1 antibody production

The RARP-1 peptide antigen (SNEMHEAQVASNEHND, corresponding to residues 159-174) was selected and synthesized by New England Peptide (Gardner, MA). The peptide antigen was conjugated to KLH and used for immunization by Pocono Rabbit Farm and Laboratory (Canadensis, PA) according to their 70 day rabbit polyclonal antibody protocol.

R. parkeri RARP-1 secretion assays

Confluent A549 cells grown in 24-well plates were infected at an MOI of 0.5-1.0, centrifuged at 200 x g for 5 min at RT, and incubated at 33 °C until the indicated harvest time point. Infected cells were washed three times with PBS, lifted with trypsin-EDTA, and centrifuged at 2,400 x g for 5 min at RT. The resulting pellets were resuspended in selective lysis buffer (50 mM HEPES pH 7.9, 150 mM NaCl, 1 mM EDTA, 10% glycerol, 1% IGEPAL) containing protease inhibitors (Sigma-Aldrich #P1860), incubated on ice for 15 min, and centrifuged at 11,300 x g for 10 min at 4 °C. The resulting pellets were washed with PBS and boiled in loading buffer (50 mM Tris-HCl pH 6.8, 2% SDS, 10% glycerol, 0.1% bromophenol blue, 5% β-mercaptoethanol). The resulting supernatants were passed through a 0.22 μm cellulose acetate filter (Thermo Scientific #F2517-1) by centrifugation at 6,700 x g for 10 min at

4 °C, combined with loading buffer (to a final volume equal to the final pellet volume), and boiled. Lysates were analyzed by western blot using rabbit anti-FLAG (Cell Signaling Technology #2368), rabbit anti-Sca4 (15), mouse anti-Ty1 (kindly provided by Dr. Sebastian Lourido), rabbit RARP-1 peptide antisera, and mouse anti-RpoA (BioLegend #663104).

R. parkeri GSK secretion assays

Confluent Vero cells grown in 24-well plates were infected with the indicated strains, centrifuged at 200 x g for 5 min at RT, and incubated at 33 °C with spectinomycin for 72 h (when infected cells were approximately 90% rounded) before harvesting. Infected cells were washed with ice-cold serum-free DMEM, directly lysed in loading buffer, and boiled. Lysates were analyzed by western blot using rabbit anti-GSK-3β-Tag (Cell Signaling Technology #9325) and rabbit anti-phospho-GSK-3β (Cell Signaling Technology #9336).

E. coli secretion assays

E. coli K-12 BW25113 (WT) and JW5503-1 (Δ*tolC*) from the Keio Knockout Collection (50) were obtained from Horizon Discovery. SDS sensitivity and the KanR cassette insertion site were confirmed for the Δ*tolC* strain. Secretion assay samples were collected and processed as previously described (19). Bacterial pellets and precipitated proteins were boiled in loading buffer. Bacterial pellet lysates (equivalent to 0.025 OD_{600}-mL of cultured cells) and precipitated culture supernatants (equivalent to 2 mL of culture supernatant prior to precipitation) were analyzed by western blot using rabbit anti-FLAG and HRP-conjugated mouse anti-His (ABclonal #AE028).

RARP-1 localization assays

Confluent A549 cells grown in 24-well plates were infected at an MOI of 0.3-0.6, centrifuged at 200 x g for 5 min at RT, and incubated at 33 °C for 27 h until fixation with 4% PFA in PBS for 1 h. Fixed samples were incubated with 0.1 M glycine in PBS for 10 min at RT to quench residual PFA. Samples were then washed three times with PBS, permeabilized with 0.5% Triton X-100 in PBS for 5 min at RT, and washed another three times with PBS. Samples were then incubated with goat serum blocking buffer (2% BSA and 10% normal goat serum in PBS) for 30 min at RT. To stain host cell contents and bacterial surface proteins, primary and secondary antibodies were diluted in goat serum blocking buffer and incubated for 3 h at 37 °C and 1 h at RT, respectively, with three 5 min PBS washes after each incubation step. To stain non-permeabilized bacteria, rabbit anti-FLAG, mouse anti-*Rickettsia* 14-13, goat anti-rabbit conjugated to Alexa Fluor 647 (Invitrogen #A-21245), and goat anti-mouse conjugated to Alexa Fluor 488 were used, and coverslips were mounted after washing. To stain permeabilized bacteria, only mouse anti-*Rickettsia* 14-13 and goat anti-mouse conjugated to Alexa Fluor 488 were used in the first round of staining, and coverslips were instead fixed with 4% PFA in PBS for 5 min at RT after washing. These samples were then incubated with 0.1 M glycine in PBS for 10 min at RT to quench residual PFA and washed three times with PBS. To expose proteins inside the bacteria for staining, these samples were incubated with lysozyme reaction buffer (0.8X PBS, 50 mM glucose, 5 mM EDTA, 0.1% Triton X-100, 5 mg/mL lysozyme (Sigma #L6876)) for 20 min at 37 °C and then washed three times with PBS. Rabbit anti-FLAG and goat anti-rabbit conjugated to Alexa Fluor 647 were diluted in goat serum blocking buffer and incubated for 3 h at 37 °C and 1 h at RT, respectively, with three 5 min PBS washes after each incubation step. Coverslips were mounted after the second round of staining. For subcellular

localization images, goat anti-mouse conjugated to Alexa Fluor 488 was replaced with Alexa Fluor 405 (Invitrogen #A-31553) to permit imaging of bacterial GFP. Representative images were acquired using a 100X objective, deconvolved by performing five iterations of the cellSens (Olympus) advanced maximum likelihood estimation algorithm, and a 0.26 μm width pole-to-pole line scan was performed with ImageJ.

Sca2 localization assays

Confluent A549 cells grown in 24-well plates were infected at an MOI of 0.3-0.6, centrifuged at 200 x g for 5 min at RT, and incubated at 33 °C for 28 h until fixation with 4% PFA in PBS for 10 min. Fixed samples were processed as in the infectious focus assays, except the following antibodies and stains were used: rabbit anti-Sca2 (kindly provided by Dr. Matthew Welch), mouse anti-*Rickettsia* 14-13, goat anti-rabbit conjugated to Alexa Fluor 568, goat anti-mouse conjugated to Alexa Fluor 488, phalloidin conjugated to Alexa Fluor 647, and Hoechst. For each strain, ≥ 350 bacteria were imaged using a 100X objective and the Sca2 localization pattern was determined (following the classification scheme from (14)).

Immunoblotting of RARP-1 and Sca2 from purified bacteria

Purified bacteria were boiled in loading buffer and analyzed by western blot using rabbit RARP-1 peptide antisera, rabbit anti-FLAG, rabbit anti-Sca2, and mouse anti-OmpA 13-3 (kindly provided by Dr. Ted Hackstadt). The apparent MW of RARP-1 is greater than its predicted MW (60 kDa). This aberrant migration by SDS-PAGE is typical of proteins with IDRs (51).

Co-immunoprecipitation assays

Two replicate samples each of WT and *rarp-1*::Tn + 3xFLAG-Ty1-RARP-1 bacteria were processed in parallel for FLAG co-immunoprecipitation. For each sample, bacteria purified from a fully infected T175 cm^2 flask were centrifuged at 16,200 x g for 2 min at RT, resuspended in 1 mL immunoprecipitation lysis buffer (50 mM Tris-HCl pH 7.4, 150 mM NaCl, 1 mM EDTA, 1% Triton X-100) containing 50 U/µL Ready-Lyse Lysozyme (Lucigen #R1804M) and protease inhibitors, incubated for 25 min at RT, and centrifuged at 11,300 x g for 15 min at 4 °C. The resulting supernatants were pre-cleared twice by incubation with 28 µL 50% mouse IgG agarose slurry (Sigma #A0919) for 30 min at 4 °C. The pre-cleared input lysates were then incubated with 28 µL 50% anti-FLAG M2 magnetic bead slurry (Sigma #M8823) overnight at 4 °C. The bound complexes were washed four times with 500 µL ice-cold immunoprecipitation wash buffer (50 mM Tris-HCl pH 7.4, 150 mM NaCl) containing protease inhibitors, eluted by incubation with 65.2 µL 0.1 M glycine (pH 2.8) for 20 min at RT, and neutralized with 9.8 µL 1 M Tris-HCl (pH 8.5). The neutralized eluates were then combined with loading buffer and submitted to the Whitehead Institute Proteomics Core Facility (Cambridge, MA) for sample workup and mass spectrometry analysis. Bacterial inputs were evaluated by immunoblotting for Sca4 and FLAG.

Mass spectrometry

Samples were run 1 cm into an SDS-PAGE gel, excised, and then reduced, alkylated, and digested with trypsin overnight at 37 °C. The resulting peptides were extracted, concentrated, and injected onto a nanoACQUITY UPLC (Waters) equipped with a self-packed Aeris 3.6 µm C18 analytical column (20 cm x 75 µm; Phenomenex). Peptides were eluted using standard

reverse-phase gradients. The effluent from the column was analyzed using an Orbitrap Elite mass spectrometer (nanospray configuration; Thermo Scientific) operated in a data-dependent manner. Peptides were identified using SEQUEST (Thermo Scientific) and the results were compiled in Scaffold (Proteome Software). RefSeq entries for *R. parkeri* str. Portsmouth (taxonomy ID 1105108) and *Homo sapiens* (taxonomy ID 9606) were downloaded from NCBI and concatenated with a database of common contaminants. Peptide identifications were accepted at a threshold of 95%. Protein identifications were accepted with a threshold of 99% and two unique peptides. Rickettsial proteins that were present in both replicates of the tagged (*rarp-1*::Tn + 3xFLAG-Ty1-RARP-1) lysate pulldown but absent from both replicates of the untagged (WT) lysate pulldown were called as hits.

Statistical analyses

Statistical analysis was performed using Prism 9 (GraphPad Software). Graphical representations, statistical parameters, and significance are reported in the figure legends. Data were considered to be statistically significant when $p < 0.05$, as determined by an unpaired Student's *t* test or one-way ANOVA with post-hoc Dunnett's test.

Data Availability

Mass spectral data and the protein sequence database used for searches have been deposited in the public proteomics repository MassIVE (https://massive.ucsd.edu, MSV000088867).

Acknowledgements

We are grateful to Michael Laub, Jon McGinn, and Brandon Sit for critical review of the manuscript. We thank Ted Hackstadt, Michael Laub, Sebastian Lourido, Ulrike Munderloh, Chris Paddock, and Matthew Welch for reagents and Sebastian Lourido, Elizabeth Boydston, Natasha Kafai, and Adam Nock for technical help. We also thank Whitehead Institute Proteomics Core Facility members Eric Spooner and Edward Dudek for experimental support. This work was supported by NIH/NIGMS T32GM007287 and T32GM136540 (AGS, REH), NIH/NIGMS R00GM115765 (RLL), and NIH/NIAID R01AI155489 (RLL).

References

1. Kumar Y, Valdivia RH. 2009. Leading a sheltered life: Intracellular pathogens and maintenance of vacuolar compartments. Cell Host Microbe 5:593–601.

2. Ray K, Marteyn B, Sansonetti PJ, Tang CM. 2009. Life on the inside: the intracellular lifestyle of cytosolic bacteria. Nature Reviews Microbiology 7:333–340.

3. Walker DH, Ismail N. 2008. Emerging and re-emerging rickettsioses: endothelial cell infection and early disease events. Nature Reviews Microbiology 6:375.

4. McGinn J, Lamason RL. 2021. The enigmatic biology of rickettsiae: recent advances, open questions and outlook. Pathog Dis 79:ftab019.

5. Chan YGY, Cardwell MM, Hermanas TM, Uchiyama T, Martinez JJ. 2009. Rickettsial Outer-Membrane Protein B (rOmpB) Mediates Bacterial Invasion through Ku70 in an Actin, c-Cbl, Clathrin and Caveolin 2-Dependent Manner. Cell Microbiol 11:629–644.

6. Reed SCO, Serio AW, Welch MD. 2012. Rickettsia parkeri invasion of diverse host cells involves an Arp2/3 complex, WAVE complex and Rho-family GTPase-dependent pathway. Cell Microbiol 14:529–545.

7. Hillman RD, Baktash YM, Martinez JJ. 2013. OmpA-mediated rickettsial adherence to and invasion of human endothelial cells is dependent upon interaction with α2β1 integrin. Cell Microbiol 15:727–741.

8. Teysseire N, Boudier JA, Raoult D. 1995. Rickettsia conorii entry into Vero cells. Infect Immun 63:366–374.

9. Borgo GM, Burke TP, Tran CJ, Lo NTN, Engström P, Welch MD. 2022. A patatin-like phospholipase mediates Rickettsia parkeri escape from host membranes. 1. Nat Commun 13:3656.

10. Driscoll TP, Verhoeve VI, Guillotte ML, Lehman SS, Rennoll SA, Beier-Sexton M, Rahman MS, Azad AF, Gillespie JJ. 2017. Wholly Rickettsia! Reconstructed Metabolic Profile of the Quintessential Bacterial Parasite of Eukaryotic Cells. mBio 8:e00859-17.

11. Ahyong V, Berdan CA, Burke TP, Nomura DK, Welch MD. 2019. A Metabolic Dependency for Host Isoprenoids in the Obligate Intracellular Pathogen *Rickettsia parkeri* Underlies a Sensitivity to the Statin Class of Host-Targeted Therapeutics. mSphere 4:e00536-19, /msphere/4/6/mSphere536-19.atom.

12. Clifton DR, Goss RA, Sahni SK, Antwerp D van, Baggs RB, Marder VJ, Silverman DJ, Sporn LA. 1998. NF-κB-dependent inhibition of apoptosis is essential for host cell survival during Rickettsia rickettsii infection. PNAS 95:4646–4651.

13. Engström P, Burke TP, Mitchell G, Ingabire N, Mark KG, Golovkine G, Iavarone AT, Rape M, Cox JS, Welch MD. 2019. Evasion of autophagy mediated by Rickettsia surface protein OmpB is critical for virulence. 12. Nat Microbiol 4:2538–2551.

14. Reed SCO, Lamason RL, Risca VI, Abernathy E, Welch MD. 2014. Rickettsia Actin-Based Motility Occurs in Distinct Phases Mediated by Different Actin Nucleators. Current Biology 24:98–103.

15. Lamason RL, Bastounis E, Kafai NM, Serrano R, del Álamo JC, Theriot JA, Welch MD. 2016. Rickettsia Sca4 Reduces Vinculin-Mediated Intercellular Tension to Promote Spread. Cell 167:670-683.e10.

16. Engström P, Burke TP, Tran CJ, Iavarone AT, Welch MD. 2021. Lysine methylation shields an intracellular pathogen from ubiquitylation and autophagy. Science Advances https://doi.org/10.1126/sciadv.abg2517.

17. Gillespie JJ, Williams K, Shukla M, Snyder EE, Nordberg EK, Ceraul SM, Dharmanolla C, Rainey D, Soneja J, Shallom JM, Vishnubhat ND, Wattam R, Purkayastha A, Czar M, Crasta O, Setubal JC, Azad AF, Sobral BS. 2008. Rickettsia Phylogenomics: Unwinding the Intricacies of Obligate Intracellular Life. PLOS ONE 3:e2018.

18. Lamason RL, Kafai NM, Welch MD. 2018. A streamlined method for transposon mutagenesis of Rickettsia parkeri yields numerous mutations that impact infection. PLOS ONE 13:e0197012.

19. Kaur SJ, Rahman MS, Ammerman NC, Ceraul SM, Gillespie JJ, Azad AF. 2012. TolC-Dependent Secretion of an Ankyrin Repeat-Containing Protein of Rickettsia typhi. J Bacteriol 194:4920–4932.

20. Mosavi LK, Cammett TJ, Desrosiers DC, Peng Z. 2004. The ankyrin repeat as molecular architecture for protein recognition. Protein Sci 13:1435–1448.

21. Al-Khodor S, Price CT, Kalia A, Kwaik YA. 2010. Ankyrin-repeat containing proteins of microbes: a conserved structure with functional diversity. Trends Microbiol 18:132–139.

22. Aistleitner K, Clark T, Dooley C, Hackstadt T. 2020. Selective fragmentation of the trans-Golgi apparatus by Rickettsia rickettsii. PLoS Pathog 16:e1008582.

23. Lehman SS, Noriea NF, Aistleitner K, Clark TR, Dooley CA, Nair V, Kaur SJ, Rahman MS, Gillespie JJ, Azad AF, Hackstadt T. 2018. The Rickettsial Ankyrin Repeat Protein 2 Is a Type IV Secreted Effector That Associates with the Endoplasmic Reticulum. mBio 9:e00975-18.

24. Bauler LD, Hackstadt T. 2014. Expression and Targeting of Secreted Proteins from Chlamydia trachomatis. Journal of Bacteriology https://doi.org/10.1128/JB.01290-13.

25. Torruellas Garcia J, Ferracci F, Jackson MW, Joseph SS, Pattis I, Plano LRW, Fischer W, Plano GV. 2006. Measurement of Effector Protein Injection by Type III and Type IV Secretion Systems by Using a 13-Residue Phosphorylatable Glycogen Synthase Kinase Tag. Infect Immun 74:5645–5657.

26. Zhang G, Brokx S, Weiner JH. 2006. Extracellular accumulation of recombinant proteins fused to the carrier protein YebF in Escherichia coli. Nat Biotechnol 24:100–104.

27. Rennoll-Bankert KE, Rahman MS, Gillespie JJ, Guillotte ML, Kaur SJ, Lehman SS, Beier-Sexton M, Azad AF. 2015. Which Way In? The RalF Arf-GEF Orchestrates Rickettsia Host Cell Invasion. PLOS Pathogens 11:e1005115.

28. Voss OH, Gillespie JJ, Lehman SS, Rennoll SA, Beier-Sexton M, Rahman MS, Azad AF. 2020. Risk1, a Phosphatidylinositol 3-Kinase Effector, Promotes *Rickettsia typhi* Intracellular Survival. mBio 11:e00820-20, /mbio/11/3/mBio.00820-20.atom.

29. Deghelt M, Mullier C, Sternon J-F, Francis N, Laloux G, Dotreppe D, Van der Henst C, Jacobs-Wagner C, Letesson J-J, De Bolle X. 2014. G1-arrested newborn cells are the predominant infectious form of the pathogen Brucella abortus. Nature Communications 5.

30. Dyson HJ, Wright PE. 2005. Intrinsically unstructured proteins and their functions. Nat Rev Mol Cell Biol 6:197–208.

31. Rodgers L, Gamez A, Riek R, Ghosh P. 2008. The Type III Secretion Chaperone SycE Promotes a Localized Disorder-to-Order Transition in the Natively Unfolded Effector YopE *. Journal of Biological Chemistry 283:20857–20863.

32. Housden NG, Hopper JTS, Lukoyanova N, Rodriguez-Larrea D, Wojdyla JA, Klein A, Kaminska R, Bayley H, Saibil HR, Robinson CV, Kleanthous C. 2013. Intrinsically Disordered Protein Threads through the Bacterial Outer Membrane Porin OmpF. Science 340:10.1126/science.1237864.

33. Holmes JA, Follett SE, Wang H, Meadows CP, Varga K, Bowman GR. 2016. Caulobacter PopZ forms an intrinsically disordered hub in organizing bacterial cell poles. PNAS 113:12490–12495.

34. Howell ML, Alsabbagh E, Ma J-F, Ochsner UA, Klotz MG, Beveridge TJ, Blumenthal KM, Niederhoffer EC, Morris RE, Needham D, Dean GE, Wani MA, Hassett DJ. 2000. AnkB, a Periplasmic Ankyrin-Like Protein in Pseudomonas aeruginosa, Is Required for Optimal Catalase B (KatB) Activity and Resistance to Hydrogen Peroxide. J Bacteriol 182:4545–4556.

35. Lambert C, Cadby IT, Till R, Bui NK, Lerner TR, Hughes WS, Lee DJ, Alderwick LJ, Vollmer W, Sockett RE, Lovering AL. 2015. Ankyrin-mediated self-protection during cell invasion by the bacterial predator Bdellovibrio bacteriovorus. Nat Commun 6:8884.

36. Woodford CR, Thoden JB, Holden HM. 2015. A New Role for the Ankyrin Repeat Revealed by the Study of the N-formyltransferase from Providencia alcalifaciens. Biochemistry 54:631–638.

37. Kim DH, Park M-J, Gwon GH, Silkov A, Xu Z-Y, Yang EC, Song S, Song K, Kim Y, Yoon HS, Honig B, Cho W, Cho Y, Hwang I. 2014. Chloroplast targeting factor AKR2 evolved from an ankyrin repeat domain coincidentally binds two chloroplast lipids. Dev Cell 30:598–609.

38. Harris EK, Jirakanwisal K, Verhoeve VI, Fongsaran C, Suwanbongkot C, Welch MD, Macaluso KR. 2018. Role of Sca2 and RickA in the Dissemination of Rickettsia parkeri in Amblyomma maculatum. Infect Immun 86:e00123-18.

39. Kleba B, Clark TR, Lutter EI, Ellison DW, Hackstadt T. 2010. Disruption of the Rickettsia rickettsii Sca2 Autotransporter Inhibits Actin-Based Motility. Infect Immun 78:2240–2247.

40. Costa TRD, Harb L, Khara P, Zeng L, Hu B, Christie PJ. 2021. Type IV secretion systems: Advances in structure, function, and activation. Mol Microbiol 115:436–452.

41. Vergalli J, Bodrenko IV, Masi M, Moynié L, Acosta-Gutiérrez S, Naismith JH, Davin-Regli A, Ceccarelli M, van den Berg B, Winterhalter M, Pagès J-M. 2020. Porins and small-molecule translocation across the outer membrane of Gram-negative bacteria. Nat Rev Microbiol 18:164–176.

42. Gong W, Xiong X, Qi Y, Jiao J, Duan C, Wen B. 2014. Identification of Novel Surface-Exposed Proteins of Rickettsia rickettsii by Affinity Purification and Proteomics. PLOS ONE 9:e100253.

43. Kovacs-Simon A, Titball RW, Michell SL. 2011. Lipoproteins of Bacterial Pathogens. Infect Immun 79:548–561.

44. Gabler F, Nam S-Z, Till S, Mirdita M, Steinegger M, Söding J, Lupas AN, Alva V. 2020. Protein Sequence Analysis Using the MPI Bioinformatics Toolkit. Current Protocols in Bioinformatics 72:e108.

45. Anderson BE. 1990. The 17-Kilodalton Protein Antigens of Spotted Fever and Typhus Group Rickettsiae. Annals of the New York Academy of Sciences 590:326–333.

46. Yakhnina AA, Bernhardt TG. 2020. The Tol-Pal system is required for peptidoglycan-cleaving enzymes to complete bacterial cell division. PNAS 117:6777–6783.

47. Harwood CS, Parales RE. 1996. THE β-KETOADIPATE PATHWAY AND THE BIOLOGY OF SELF-IDENTITY. Annu Rev Microbiol 50:553–590.

48. Bittner L-M, Arends J, Narberhaus F. 2017. When, how and why? Regulated proteolysis by the essential FtsH protease in Escherichia coli. Biological Chemistry 398:625–635.

49. Berg S, Kutra D, Kroeger T, Straehle CN, Kausler BX, Haubold C, Schiegg M, Ales J, Beier T, Rudy M, Eren K, Cervantes JI, Xu B, Beuttenmueller F, Wolny A, Zhang C, Koethe U, Hamprecht FA, Kreshuk A. 2019. ilastik: interactive machine learning for (bio)image analysis. Nat Methods 16:1226–1232.

50. Baba T, Ara T, Hasegawa M, Takai Y, Okumura Y, Baba M, Datsenko KA, Tomita M, Wanner BL, Mori H. 2006. Construction of Escherichia coli K-12 in-frame, single-gene knockout mutants: the Keio collection. Mol Syst Biol 2:2006.0008.

51. Tompa P. 2002. Intrinsically unstructured proteins. Trends in Biochemical Sciences 27:527–533.

CHAPTER 3: CELL-SELECTIVE PROTEOMICS REVEAL NOVEL EFFECTORS SECRETED BY AN OBLIGATE INTRACELLULAR BACTERIAL PATHOGEN

This chapter contains a modified version of work currently under review at Nature Communications. A pre-print is available on bioRxiv as:

Allen G. Sanderlin, Hannah K. Margolis, Abigail F. Meyer, Rebecca L. Lamason. Cell-selective proteomics reveal novel effectors secreted by an obligate intracellular bacterial pathogen. *bioRxiv* (2023). DOI: 10.1101/2023.11.17.567466.

AGS: Conceptualization, Methodology, Investigation, Formal Analysis, Validation, Visualization, Writing - Original Draft, Writing - Review & Editing. HKM: Investigation, Validation, Writing - Review & Editing. AFM: Validation. RLL: Conceptualization, Writing - Original Draft, Writing - Review & Editing, Supervision, Funding Acquisition.

Abstract

Pathogenic bacteria secrete protein effectors to hijack host machinery and remodel their infectious niche. *Rickettsia* spp. are obligate intracellular bacteria that can cause life-threatening disease, but their absolute dependence on the host cell environment has impeded discovery of rickettsial effectors and their host targets. We implemented bioorthogonal non-canonical amino acid tagging (BONCAT) during *R. parkeri* infection to selectively label, isolate, and identify secreted effectors. As the first use of BONCAT in an obligate intracellular bacterium, our screen more than doubles the number of experimentally validated effectors for *R. parkeri*. The novel secreted rickettsial factors (Srfs) we identified include *Rickettsia*-specific proteins of unknown function that localize to the host cytoplasm, mitochondria, and ER. We further show that one such effector, SrfD, interacts with the host Sec61 translocon. Altogether, our work uncovers a diverse set of previously uncharacterized rickettsial effectors and lays the foundation for a deeper exploration of the host-pathogen interface.

Introduction

Rickettsia spp. are Gram-negative bacteria that live exclusively inside of eukaryotic host cells. Members of this genus include arthropod-borne pathogens that cause typhus and spotted fever diseases in humans and pose a significant global health risk (1, 2). By virtue of their intimate connection with the intracellular niche, these bacteria are poised to exploit host cell biology. *Rickettsia* spp., like other intracellular pathogens, secrete protein effectors to subvert diverse host cell processes, but their obligate intracellular lifestyle has precluded a detailed investigation of the host-pathogen interface (3). Identifying such effectors and their host cell

targets is an essential first step towards a mechanistic understanding of rickettsial biology and pathogenesis.

Recent studies have characterized a handful of secreted rickettsial effectors that interact with the host cell during infection. For example, the effector Sca4 inhibits host vinculin and promotes rickettsial cell-to-cell spread (4). RARP-2, a predicted protease, disrupts the *trans*-Golgi network during infection (5, 6). Moreover, the phospholipase Pat1 mediates escape from membrane-bound vacuoles (7), whereas Risk1 and RalF directly and indirectly manipulate host membrane phosphoinositides (8–10). In spite of this progress, very few secreted rickettsial effectors have been experimentally validated, leaving much of the effector arsenal a mystery.

An expanding suite of biochemical, genetic, and *in silico* methods has facilitated the identification of secreted effectors in a variety of bacterial pathogens. For example, effectors have been identified from bacteria grown in broth by fractionation and proteomic analysis (11–13). Reporter fusion libraries have enabled large-scale screens for secreted proteins (14, 15), and heterologous expression by surrogate hosts has provided support for putative effectors of genetically intractable bacteria (16–18). Computational tools, used in parallel with the above strategies, have highlighted core features of verified effectors to identify new candidate effectors (19, 20).

However, reappropriating these methods for the discovery of rickettsial effectors remains a challenge. Axenic culture of *Rickettsia* spp. is not yet possible, and scalable reporter screens are limited by inefficient transformation (21). The short list of experimentally validated rickettsial effectors has hindered *in silico* identification of new candidates, especially if they lack the sequence features found in the larger effector repertoires of well-studied bacteria (22).

Heterologous expression bypasses these obstacles, but the secretion of a candidate effector *ex situ* does not prove its secretion during rickettsial infection. Thus, alternative approaches are necessary to identify new secreted effectors.

Labeling strategies that enable the isolation of secreted effectors from the host cell milieu may circumvent these issues. For example, bioorthogonal non-canonical amino acid tagging (BONCAT) permits metabolic labeling of newly synthesized proteins with amino acid analogues (23). Labeling is restricted to cells expressing a mutant methionyl-tRNA synthetase (MetRS*) which, unlike the wild-type synthetase (WT MetRS), can accommodate the azide-functionalized methionine analogue azidonorleucine (Anl) (24). Anl-labeled proteins are then chemoselectively tagged with alkyne-functionalized probes by click chemistry for visualization or pull-down followed by mass spectrometry. This approach has been adapted to a variety of bacterial pathogens, including *Salmonella typhimurium* (25), *Yersinia enterocolitica* (26), *Mycobacterium tuberculosis* (27), and *Burkholderia thailandensis* (28), enabling selective labeling and isolation of bacterial proteins during infection.

We therefore implemented cell-selective BONCAT during infection with the obligate intracellular bacterium *Rickettsia parkeri*. Using this approach, we detected both known and novel secreted effectors, including proteins of unknown function found only in the *Rickettsia* genus. In addition to confirming their secretion, we demonstrate diverse localization patterns for these new effectors. Moreover, we show that the novel secreted effector SrfD localizes to the ER where it interacts with the host Sec61 complex. Our findings expand the toolkit for exploring rickettsial biology, which will provide much-needed insight into how these pathogens engage with the host cell niche.

Results

BONCAT permits selective labeling of rickettsial proteins

We sought to identify new effectors secreted during rickettsial infection. We needed an approach that would overcome the limitations associated with the rickettsial lifestyle and enable detection of low abundance effectors in the host cytoplasmic milieu (29). Inspired by the use of cell-selective BONCAT with facultative intracellular bacteria, we adapted this technique to the obligate intracellular bacterial pathogen, *R. parkeri*, to label rickettsial proteins for subsequent identification (Figure 3.1A). We first generated *R. parkeri* harboring a plasmid encoding MetRS*. To determine if MetRS* expression adversely impacted rickettsial infection, we performed infectious focus assays in A549 host cell monolayers. We found that infectious foci formed by the MetRS* strain were indistinguishable in both size and bacterial load from those formed by the WT strain (Figure 3.1B,C), indicating that MetRS* expression does not impede cell-to-cell spread or bacterial growth, respectively.

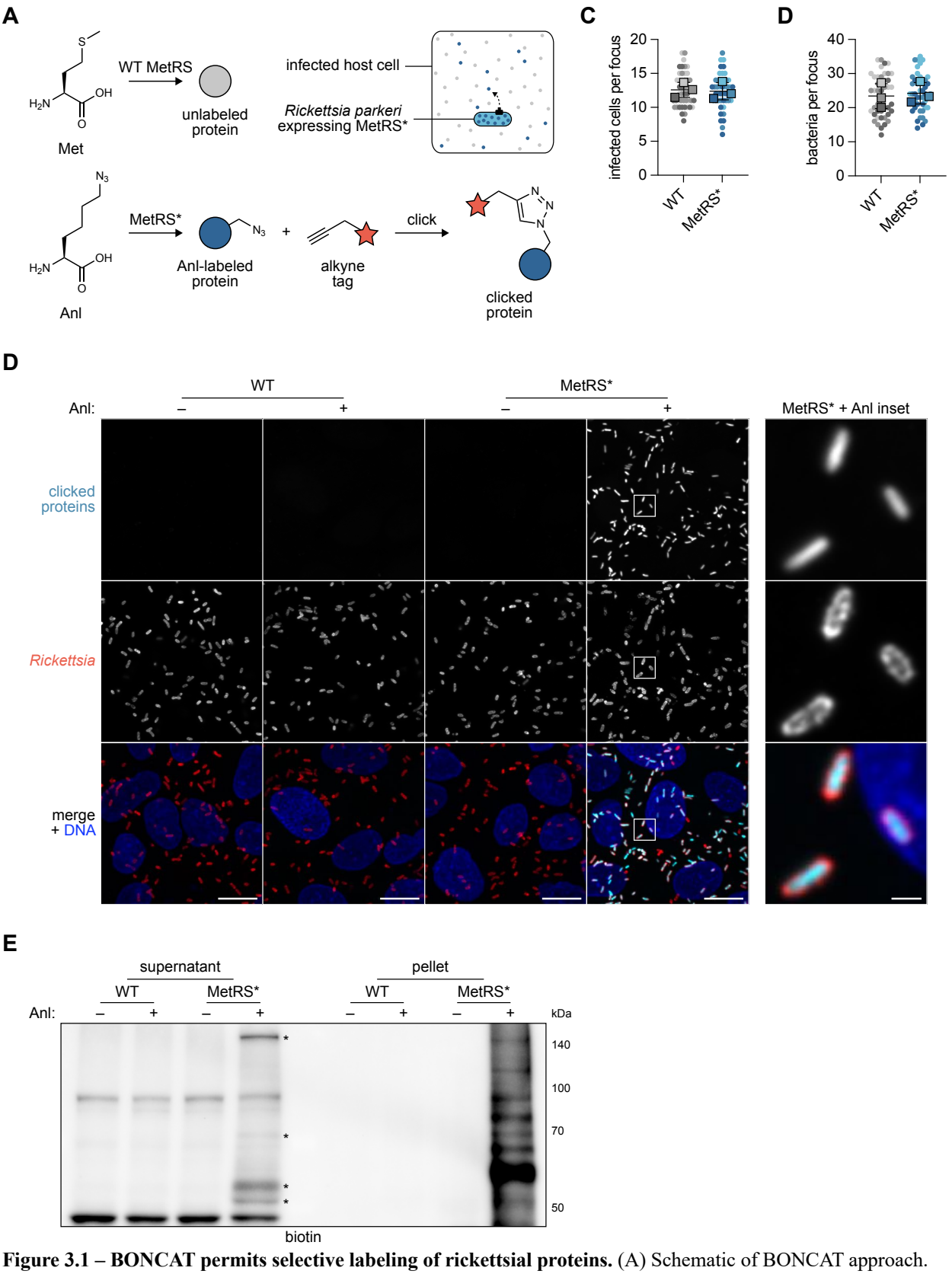

Figure 3.1 – BONCAT permits selective labeling of rickettsial proteins. (A) Schematic of BONCAT approach. *Rickettsia parkeri* expressing a mutant methionyl-tRNA synthetase (MetRS*) incorporates the Met analogue azidonorleucine (Anl) into nascent proteins, some of which are secreted into the host cell during infection. Anl-

labeled proteins (blue circle), but not unlabeled proteins (gray circle), are tagged (red star) by click chemistry. (B) Infected cells and (C) bacteria per focus during infection of A549 cells by WT or MetRS* *R. parkeri*. The means from $n = 3$ independent experiments (squares) are superimposed over the raw data (circles) and were used to calculate the means ± SD and p-values (unpaired two-tailed *t* test, n.s. relative to WT). Data are shaded by replicate experiment. (D) Images of WT and MetRS* *R. parkeri* treated with (+) or without (–) Anl during infection of A549 cells (Hoechst, blue). Bacteria were permeabilized and stained (red), and Anl-labeled proteins were detected by tagging with an alkyne-functionalized fluorescent dye (cyan). Scale bar, 10 μm (inset, 1 μm). (E) Western blot for biotin in lysates harvested from A549 cells infected with WT or MetRS* *R. parkeri* with (+) or without (–) Anl treatment. Infected host cells were selectively lysed to separate supernatants containing the infected host cytoplasm from pellets containing intact bacteria. Anl-labeled proteins were detected by tagging with alkyne-functionalized biotin. Asterisks indicate putative secreted effector bands.

Having confirmed that *R. parkeri* tolerates MetRS* expression, we next tested the functionality of MetRS* to label rickettsial proteins. We infected A549 cells for two days and then treated infected cells with Anl for 3 h prior to fixation. To visualize incorporation of Anl by fluorescence microscopy, we tagged labeled proteins with an alkyne-functionalized fluorophore. As expected, labeling was restricted to MetRS* bacteria following treatment with Anl (Figure 3.1D). To evaluate labeling of secreted and non-secreted proteins during infection, we used a previously established selective lysis protocol to separate the infected host cytoplasm from intact bacteria after 3 h of Anl labeling (30). We then tagged labeled proteins from each fraction with alkyne-functionalized biotin and detected them by Western blotting. Consistent with our microscopy results, only the MetRS* strain exhibited appreciable labeling following treatment with Anl (Figure 3.1E). Within this sample, the pellet fraction yielded a smear of bands, as expected for proteome-wide incorporation of Anl. Furthermore, the supernatant fraction contained several unique bands. Altogether, these findings demonstrate that BONCAT can be used to selectively label proteins produced by obligate intracellular bacteria during infection.

BONCAT identifies known and novel secreted effectors

We hypothesized that the unique bands present in the supernatant fraction during infection with MetRS* bacteria represented secreted rickettsial effectors. To identify these

effectors, we infected cells for two days, labeled with Anl during the last 5 h of infection, tagged cytoplasmic fractions with alkyne-functionalized biotin as before, and isolated biotinylated proteins using streptavidin resin. We then analyzed these pull-downs by mass spectrometry to identify rickettsial proteins (Figure 3.2).

Gene ID	Name	Description
MC1_RS04780	RARP-2	protease
MC1_RS04700	Pat1	phospholipase
MC1_RS00985	Risk1	PI3K
MC1_RS00120	Sca1	autotransporter
MC1_RS06480	OmpA	autotransporter
MC1_RS02555	SrfA	amidase
MC1_RS01090	SrfB	hypothetical protein
MC1_RS04185	SrfC	hypothetical protein
MC1_RS04150	SrfD	hypothetical protein
MC1_RS05980	SrfE	hypothetical protein
MC1_RS02820	SrfF	hypothetical protein
MC1_RS02530	SrfG	hypothetical protein

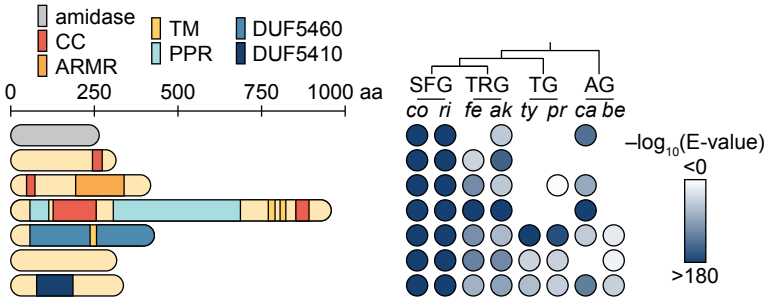

Figure 3.2 – BONCAT identifies novel secreted rickettsial factors (Srfs) that are structurally diverse and variably conserved. *R. parkeri* protein hits identified from infected host cytoplasmic lysates using BONCAT include known secreted effectors (light blue), autotransporter proteins (dark blue), and the novel secreted effectors SrfA–G (beige). Hit calling is described in the Methods. Protein lengths, putative domains, and structural motifs are indicated for SrfA–G. CC, coiled coil; ARMR, armadillo-like repeats; TM, transmembrane helix; PPR, pentapeptide repeats; DUF, Pfam domain of unknown function. BLAST E-values were computed to evaluate similarity between *R. parkeri* SrfA–G and homologs in representative members of the *Rickettsia* genus. Species lacking a detected Srf homolog were left blank. SFG, spotted fever group; TRG, transitional group; TG, typhus group; AG, ancestral group; *co*, *R. conorii*; *ri*, *R. rickettsii*; *fe*, *R. felis*; *ak*, *R. akari*; *ty*, *R. typhi*; *pr*, *R. prowazekii*; *ca*, *R. canadensis*; *be*, *R. bellii*.

This analysis yielded twelve hits, several of which had been previously studied. Importantly, these included proteins previously characterized as secreted effectors, providing validation of our approach. We identified the patatin-like phospholipase A_2 enzyme Pat1 (31), the ankyrin repeat protein RARP-2 (5), and the phosphatidylinositol 3-kinase Risk1 (8), all known secreted effectors. The autotransporter proteins Sca1 and OmpA were also identified in the supernatant fraction despite their localization to the bacterial outer membrane (32). However, both Sca1 and OmpA are post-translationally processed (33–35), and the tryptic peptides from our experiments mapped exclusively to their surface-exposed passenger domains (Figure 3.3),

suggesting that we detected cleavage-dependent release of surface proteins into the host cytoplasm.

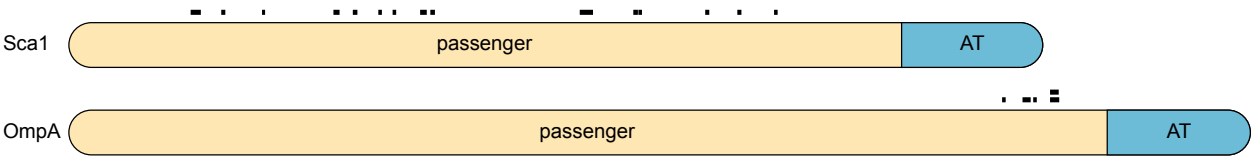

Figure 3.3 – Tryptic peptides mapping to autotransporter proteins Sca1 and OmpA. Positions of unique peptides (black boxes) and passenger and autotransporter (AT) domains are indicated.

The remaining proteins identified in our screen include seven putative secreted rickettsial factors (SrfA–G) that are variably conserved within the genus (Figure 3.2). SrfA is a predicted *N*-acetylmuramoyl-L-alanine amidase, and the *R. conorii* homolog RC0497 exhibits peptidoglycan hydrolase activity (36). In contrast, SrfB–G are hypothetical proteins with limited or no sequence homology outside the *Rickettsia* genus. For further insight into these hypothetical proteins, we used a variety of remote homology prediction tools to identify putative domains (37–40). SrfC is predicted to contain an α-superhelical armadillo repeat-like motif, whereas SrfD harbors β-solenoid-forming pentapeptide repeats. In addition to these repeat motifs, which may facilitate protein-protein interactions (41, 42), secondary structure prediction further identified coiled coils and transmembrane helices in several Srfs (39). Finally, SrfE and SrfG contain the *Rickettsia*-specific domains of unknown function DUF5460 and DUF5410, respectively.

The *srf* loci are scattered across the *R. parkeri* genome (Figure 3.4), in contrast to the effector gene clusters (pathogenicity islands) observed in more well-studied pathogens (43). The Srfs are also not encoded proximal to components of either the type IV (T4SS: *rvhBD*) or type I (T1SS: *tolC*, *aprDE*) secretion systems, which may mediate Srf export to the host cell (44). Moreover, *in silico* T4SS effector search tools do not clearly predict SrfA–G as likely effectors (22, 45). Similarly, SrfA–G lack the glycine-rich repeat motifs common in T1SS effectors (46).

The limitations of such bioinformatic methods for Srf identification underscore the utility of our proteomics-based approach to uncover putative rickettsial effectors.

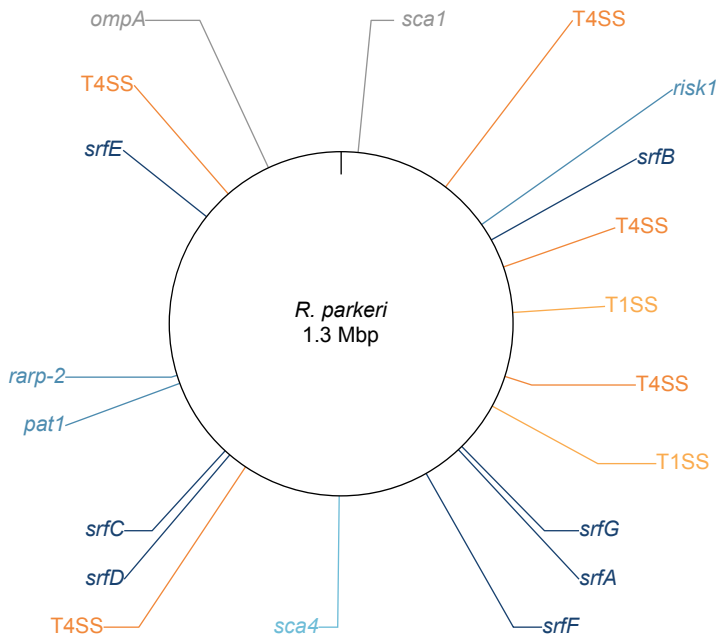

Figure 3.4 – Genomic positions of *srf* loci. *R. parkeri* genome map displaying loci encoding SrfA–G; autotransporter proteins Sca1 and OmpA; known secreted effectors RARP-2, Pat1, Risk1, and Sca4; and components of the type IV (T4SS: RvhBD) and putative type I (T1SS: TolC, AprDE) secretion systems.

Srfs are secreted by R. parkeri into the host cell during infection

We next sought to validate secretion of SrfA–G by *R. parkeri* using an orthogonal approach. We generated *R. parkeri* strains expressing Srfs with glycogen synthase kinase (GSK) tags and infected Vero host cells. Upon secretion into the host cytoplasm, GSK-tagged proteins are phosphorylated by host kinases (47). This strategy does not require selective lysis, and secreted proteins can be detected by immunoblotting with phospho-specific antibodies (30). As expected, a non-secreted control (GSK-tagged BFP) was not phosphorylated whereas a secreted effector control (GSK-tagged RARP-2) was phosphorylated (Figure 3.5A). We extended this analysis to our GSK-tagged Srf strains and confirmed secretion for SrfA, SrfC, SrfD, SrfF, and SrfG. Despite expression from a common promoter (*ompA*), expression of these GSK-tagged

constructs varied considerably, with SrfA having the most robust expression. Additionally, expression of GSK-tagged SrfB and SrfE was not detectable and we were therefore unable to verify their secretion (Figure 3.6). Nevertheless, the results from this assay demonstrate that the BONCAT screen revealed *bona fide* secreted effectors.

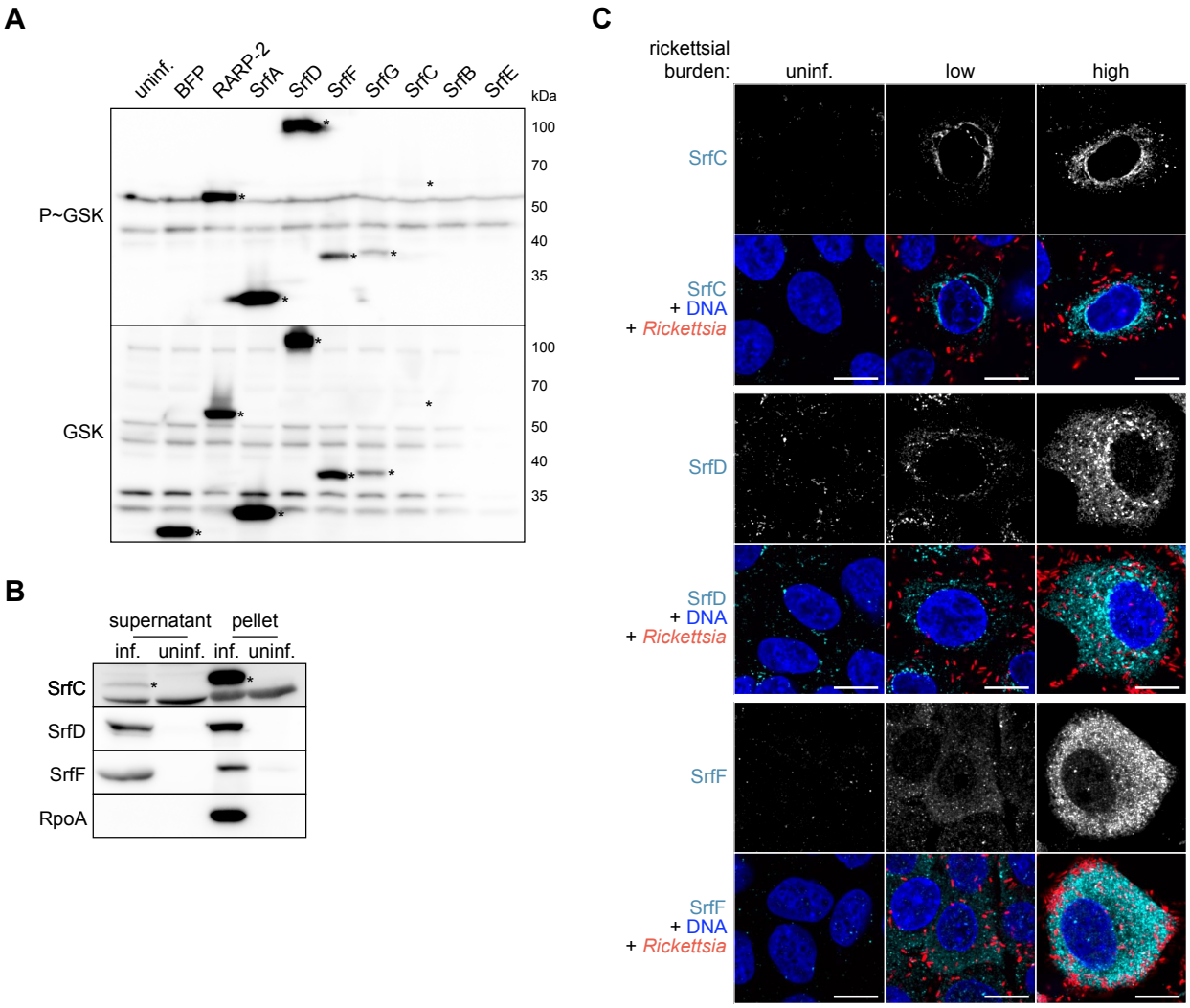

Figure 3.5 – Srfs are secreted by *R. parkeri* into the host cell during infection. (A) Western blots for GSK-tagged constructs expressed by *R. parkeri* during infection of Vero cells. Whole-cell infected lysates were probed with antibodies against the GSK tag (bottom) or its phosphorylated form (P~GSK, top) to detect exposure to the host cytoplasm. BFP (non-secreted) and RARP-2 (secreted) were used as controls. SrfA–G are ordered by observed expression level. Asterisks indicate GSK-tagged protein bands. SrfB and SrfE (expected 37 and 50 kDa, respectively) were not detected. (B) Western blots for endogenous, untagged Srfs during *R. parkeri* infection of A549 cells. Infected host cells were selectively lysed to separate supernatants containing the infected host cytoplasm from pellets containing intact bacteria. Asterisks indicate SrfC bands (apparent 55 kDa, but expected 48 kDa). SrfD and SrfF ran at the expected sizes (107 and 36 kDa, respectively). RpoA, lysis control. (C) Images of Srfs (cyan)

secreted by GFP-expressing *R. parkeri* (red) during infection of A549 cells (Hoechst, blue). Srfs were detected at both low and high rickettsial burdens. Scale bar, 10 μm. Uninfected host cells (uninf.) were included as controls for (A–C).

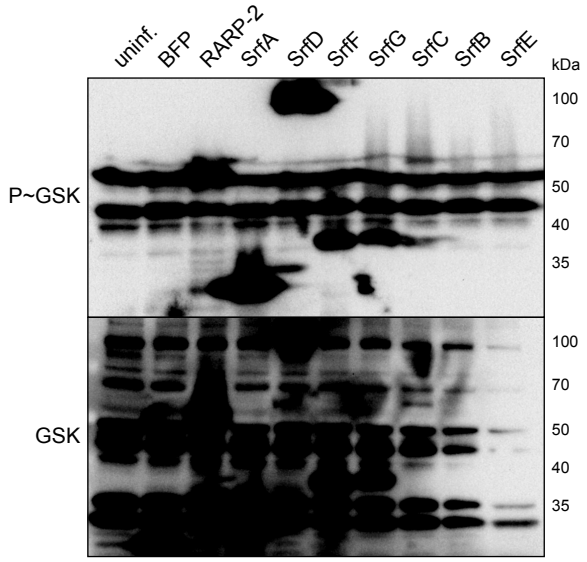

Figure 3.6 – GSK-tagged SrfB and SrfE are not obviously expressed by *R. parkeri*.
Western blots from Figure 3.5A with enhanced contrast. SrfB and SrfE (expected 37 and 50 kDa, respectively) were not detected.

To confirm secretion of the endogenous, untagged effectors, we raised antibodies against SrfC, SrfD, and SrfF. We then used selective lysis to check for secretion during infection of A549 host cells by WT *R. parkeri*. As shown previously (30), the bacterial RNA polymerase subunit RpoA was only detected in the pellet fraction and served as a control for our lysis strategy (Figure 3.5B). In contrast, we detected endogenous SrfC, SrfD, and SrfF in both the pellet and supernatant fractions, providing further validation that these effectors are secreted into the host cytoplasm.

We next performed immunofluorescence microscopy to determine where secreted SrfC, SrfD, and SrfF localize during infection of A549 host cells (Figure 3.5C). We observed rare instances of perinuclear staining for SrfC during infection, which was typically undetectable even at higher bacterial burdens. For SrfD, we detected perinuclear speckles and faint diffuse

staining that became more apparent with increased bacterial burden, possibly as a result of greater effector abundance. We noted cytoplasmic staining for SrfF during infection, the intensity of which similarly increased at higher bacterial burdens.

Srfs exhibit diverse subcellular localization patterns

Motivated by the varied staining patterns for SrfC, SrfD, and SrfF during infection, we expanded our localization analysis to include the remaining Srfs. Secreted effectors target various subcellular compartments, and we reasoned that exogenous expression of these effectors in uninfected cells would offer a more tractable way to study their localization by microscopy (16, 48). We transiently expressed 3xFLAG-tagged SrfA–G in HeLa cells and used immunofluorescence microscopy to assess their localization (Figure 3.7A). We observed diffuse staining of SrfA in the cytoplasm and nucleus. SrfB was detected along narrow structures of various sizes reminiscent of mitochondria. Colocalization between SrfB and mitochondrial apoptosis-inducing factor (AIF) confirmed this hypothesis (Figure 3.7B), and we noted no obvious impact on mitochondrial morphology in SrfB-positive cells. SrfC and SrfD both exhibited a reticulate perinuclear localization pattern suggestive of localization to the ER, which was not as apparent for their endogenous, secreted counterparts detected during infection. Expression of SrfC or SrfD alongside ER-targeted mNeonGreen confirmed colocalization with ER tubules (Figure 3.7C), and no obvious changes in ER morphology were noted for these cells. SrfE exhibited punctate staining throughout the cytoplasm. Finally, we observed diffuse staining of SrfF and SrfG in the cytoplasm; for SrfF, this localization recapitulated the pattern we saw for the endogenous protein secreted during infection. Altogether, the diversity of these localization patterns suggests that the Srfs target distinct host cell compartments during infection.

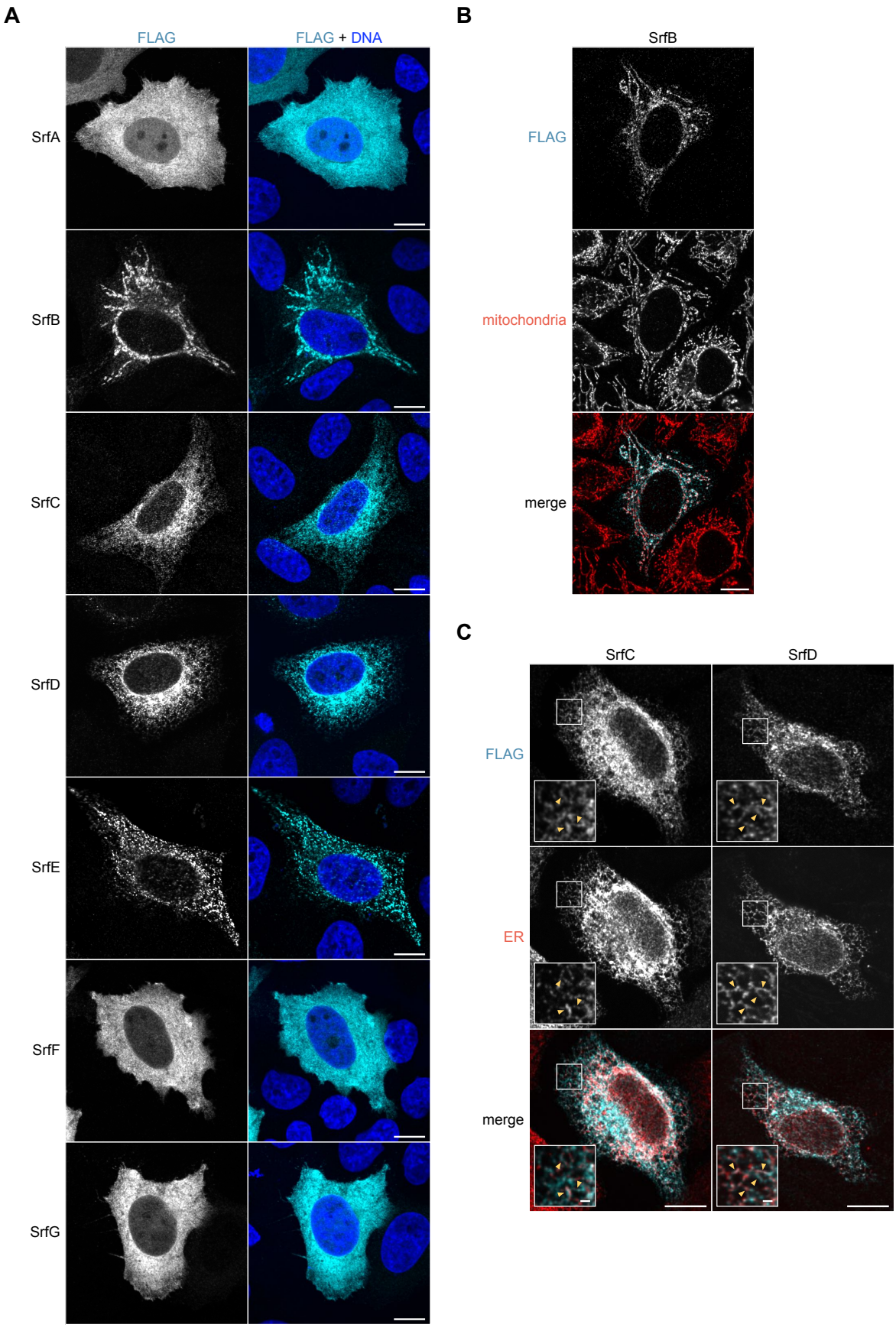
A
FLAG
FLAG + DNA
SrfA
SrfB
SrfC
SrfD
SrfE
SrfF
SrfG
B
SrfB
FLAG
mitochondria
merge
C
SrfC
SrfD
FLAG
ER
merge

Figure 3.7 – Srfs exhibit diverse subcellular localization patterns. (A) Images of 3xFLAG-tagged SrfA–G (cyan) expressed by transiently transfected HeLa cells (Hoechst, blue). Scale bar, 10 μm. (B) Images of 3xFLAG-tagged SrfB (cyan) in transiently transfected HeLa cells (mitochondrial AIF, red). Scale bar, 10 μm. (C) Images of 3xFLAG-tagged SrfC or SrfD (cyan) and ER-targeted mNeonGreen (red) expressed by transiently co-transfected HeLa cells. Scale bar, 10 μm (inset, 1 μm). Arrowheads highlight Srf colocalization with ER tubules.

SrfD interacts with host Sec61

Upon secretion, effectors can modulate host processes by interacting with target host proteins. Due to its robust secretion during infection, localization to the ER, and interesting structural motifs, we decided to focus on SrfD for further investigation. To identify potential SrfD binding partners during infection, we immunoprecipitated endogenous SrfD from WT *R. parkeri*-infected host cytoplasmic lysates and performed mass spectrometry on the resulting protein complexes. As a control, we also processed lysates from uninfected host cells. In addition to SrfD itself, we found that the α and β subunits of the host Sec61 complex were highly enriched in the infected lysate pull-downs (Figure 3.8A), suggesting that SrfD interacts with Sec61 at the ER. The IgG receptor protein TRIM21 was also enriched (49), but it was not considered further as it had been observed as a common infection-specific contaminant in our hands. To verify the SrfD-Sec61 interaction, we performed the reverse pull-down and confirmed that SrfD is immunoprecipitated with Sec61β during infection (Figure 3.8B). To determine if the SrfD-Sec61 interaction could be recapitulated in the absence of infection, we transiently expressed 3xFLAG-SrfD in HEK293T cells and repeated our Sec61β immunoprecipitation assays. We found that 3xFLAG-SrfD immunoprecipitated with Sec61β (Figure 3.8C), demonstrating the functional relevance of our exogenous expression strategy.

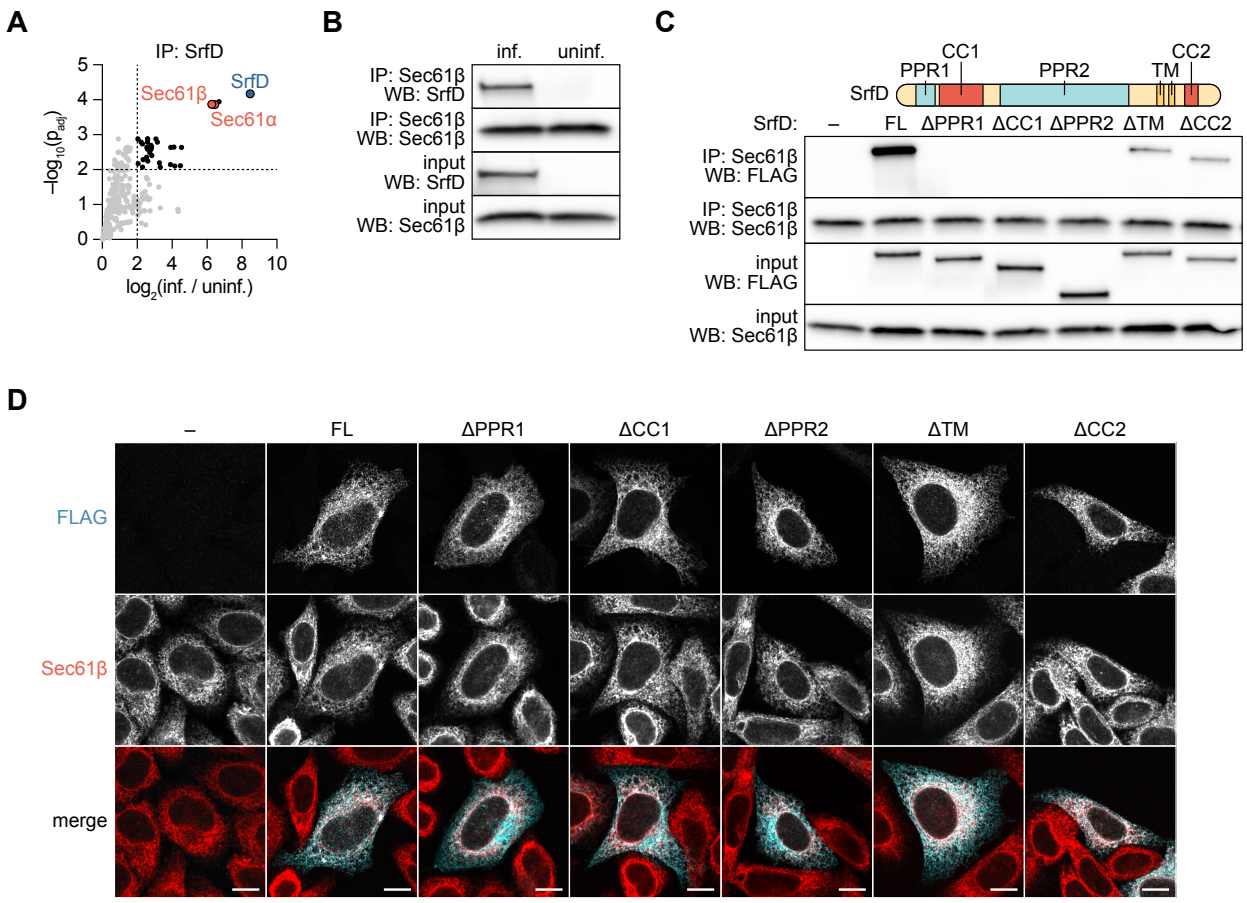

Figure 3.8 – SrfD interacts with host Sec61 and localizes to the ER via multiple domains. (A) Proteins co-enriched following immunoprecipitation (IP) mass spectrometry of SrfD secreted by *R. parkeri* during infection of A549 cells. Protein abundance fold-changes and Benjamini-Hochberg adjusted p-values (p_{adj}) were computed for n = 3 independent infected (inf.) and uninfected (uninf.) samples (unpaired two-tailed t test). SrfD (blue), Sec61α/β (red), and thresholds for fold-change > 4 and $p_{adj} < 0.01$ are indicated. (B) Western blots for SrfD and Sec61β following IP of Sec61β from A549 cells. Samples were prepared from *R. parkeri*-infected (inf.) and uninfected (uninf.) cells. (C) Western blots for FLAG and Sec61β following IP of Sec61β from HEK293T cells transiently transfected with 3xFLAG-tagged SrfD expression constructs. Putative domains and structural motifs are indicated. –, empty vector; FL, full-length SrfD. (D) Images of 3xFLAG-tagged SrfD constructs (cyan) from (C) expressed by transiently transfected HeLa cells (Sec61β, red). Scale bar, 10 μm.

The Sec61 complex forms a channel for protein translocation across the ER membrane (50), and several naturally-occurring small molecules have been identified that bind and inhibit Sec61 (51). Given that SrfD also interacts with Sec61, we tested if SrfD influences protein translocation through Sec61. We transfected 3xFLAG-SrfD into HEK293T cells stably expressing the signal peptide-containing Sec61 substrate *Gaussia* luciferase and then measured luciferase activity in culture supernatants (Figure 3.9) (52). As a control, we treated cells with

brefeldin A, which disrupts ER-Golgi trafficking and thereby blocks luciferase secretion to the cell exterior (53). We found that luciferase secretion was unaffected in SrfD-expressing cells, suggesting that SrfD does not phenocopy the behavior of known Sec61 inhibitors.

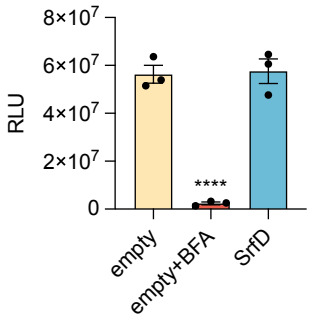

Figure 3.9 – SrfD does not impact secretion of *Gaussia* luciferase. HEK293T cells stably expressing *Gaussia* luciferase were transiently transfected in triplicate ($n = 3$) with either empty vector or 3xFLAG-tagged SrfD and treated with DMSO or brefeldin A (BFA) prior to measuring luciferase activity of the culture supernatants. Relative light units (RLU) from a representative experiment were used to calculate the means ± SD and p-values (one-way ANOVA with *post hoc* Dunnett's test, ****$p < 0.0001$ relative to control).

Multiple domains of SrfD support its interaction with Sec61 and localization to the ER

SrfD does not resemble known components of the Sec61 translocon or associated proteins, but it does harbor several putative protein-protein interaction domains. SrfD is predicted to contain two pentapeptide repeat domains (PPR1 and PPR2) and two coiled coil motifs (CC1 and CC2), which often serve as interfaces for binding protein partners (42, 54). We hypothesized that the interaction between SrfD and Sec61 is mediated by one or more of these domains. To test this hypothesis, we immunoprecipitated Sec61β from HEK293T cells exogenously expressing one of several 3xFLAG-SrfD deletion constructs and assessed pull-down of the constructs (Figure 3.8C). We found that the CC2 domain and predicted C-terminal transmembrane (TM) helices were mostly dispensable for the SrfD-Sec61 interaction. Within the SrfD N-terminus, however, PPR1, CC1, and PPR2 were each independently necessary for this

interaction. These results suggest that the tested domains all contribute to the SrfD-Sec61 interaction, but ablation of any one of the SrfD N-terminal domains fully disrupts the interaction.

Given that SrfD localizes to the ER and interacts with Sec61, we considered two models for how SrfD localizes to the ER. In the first, the N-terminal domains alone drive localization to this compartment via their interaction with Sec61. Alternatively, the combination of the N-terminus and the predicted TM helices confers ER localization, especially because TM helices in other secreted effectors are known to promote insertion into target membranes (55, 56). To test this hypothesis, we exogenously expressed the 3xFLAG-SrfD deletion constructs in HeLa cells and used immunofluorescence microscopy to assess their localization. As expected, full-length 3xFLAG-SrfD localized with Sec61β at the ER (Figure 3.8D). Interestingly, each of the domains we tested was dispensable for ER-targeting: deletion mutants that were unable to interact with Sec61β still localized to the ER, and SrfD lacking its TM domain likewise remained at the ER. These results suggest that targeting of SrfD to the ER is dependent on multiple domains and that its localization is phenotypically separable from the interaction with Sec61.

Discussion

Rickettsia spp. are exquisitely adapted to their host cell niche, but the limited toolkit for studying these bacteria has hindered investigation of the host-pathogen interface. Here, we use cell-selective BONCAT for the first time in an obligate intracellular bacterium and greatly expand the number of experimentally validated rickettsial effectors. The Srfs we identified include *Rickettsia*-specific proteins of unknown function that are structurally diverse, variably conserved, and targeted to distinct host cell compartments. Altogether, our results offer new routes to explore the unique biology of these bacterial pathogens.

The identification of Srf binding partners is an important step towards understanding their functions. For example, we found that SrfD localizes to the ER where it interacts with the host Sec61 translocon. The SrfD-Sec61 interaction was identified during infection and was recapitulated by exogenous SrfD expression in uninfected cells, providing a useful platform for structure-function analysis. Pentapeptide repeats and coiled coils are known to support protein-protein interactions, and our finding that the SrfD PPRs and CC1 are necessary for its interaction with Sec61 agrees with this point. Nevertheless, we cannot exclude the possibility that SrfD interacts indirectly with Sec61 through these domains. We did not identify a candidate protein that could bridge SrfD and Sec61 from our mass spectrometry results, but future studies may reveal if the SrfD-Sec61 interaction can be reconstituted *in vitro*. The functional consequence of the SrfD-Sec61 interaction likewise requires continued investigation. Although SrfD did not impact secretion of a known Sec61 substrate, it is possible that SrfD affects the translocation of other proteins in a client-selective manner. Alternatively, SrfD may influence the role played by the Sec61 translocon in other cellular processes, such as ER stress and calcium homeostasis (57, 58). SrfD may also interact with Sec61 to exert its activity on other host targets at the ER, although we note that SrfD was specifically enriched only with the Sec61 complex.

Of the Srfs we identified, only SrfA has a predicted function. SrfA is likely a functional peptidoglycan amidase *in vivo*, and high abundance of the *R. conorii* SrfA homolog RC0497 during infection makes it a promising biomarker for spotted fever rickettsioses (59). RC0497 has been observed in the periplasm of purified rickettsiae by immunogold labeling (36), despite the absence of a Sec or Tat signal peptide (60). Our detection of SrfA in the infected host cytoplasm and phosphorylation of GSK-tagged SrfA suggest that this protein reaches its final destination outside the bacteria during infection.

For the remaining Srfs, we combined *in silico* predictions and localization analyses to begin characterizing these novel effectors. Curiously, SrfB localized to mitochondria when exogenously expressed, even though it lacks a predicted mitochondrial targeting sequence (61, 62). Once this behavior is validated for the secreted protein, mutational and biochemical studies may identify a cryptic targeting sequence within SrfB or a mitochondrial binding partner of SrfB that mediates its localization. We also showed that the localization pattern for an effector can vary depending on the source of its expression. For example, exogenous SrfC readily colocalized with the ER whereas endogenous, secreted SrfC exhibited perinuclear staining in a minority of infected cells. These results suggest that infection-specific cues dictate effector localization. In contrast to SrfC, both endogenous and exogenous SrfF exhibited similar localization to the host cytoplasm. This congruence suggests that exogenous expression of SrfF serves as a convenient proxy for studying its secreted counterpart. Aside from their localization patterns, the presence and diversification of these unique effectors in bacteria with notoriously streamlined genomes raises exciting questions about rickettsial evolution within the host cell niche (63). We eagerly await the generation of *srf* mutants, the study of which will provide insight into how these effectors contribute to the rickettsial lifestyle and pathogenesis. Furthermore, biochemical characterization of Srf interactions with their targets may uncover novel mechanisms by which bacterial pathogens subvert host processes and yield new tools to probe eukaryotic cell biology.

Rickettsia spp. harbor T4SS and T1SS machinery that may drive Srf translocation to the host cell milieu (44). Our approach to identify effectors is secretion system-agnostic, and future studies should elucidate the mechanisms by which SrfA–G are secreted during infection. Even for well-studied pathogens, however, the signal sequences for substrates of these secretion systems are enigmatic (64–66); the fact that the Srfs were not predicted by *in silico* tools

underscores this limitation. As rickettsial secretion mutants have yet to be reported, heterologous expression or co-immunoprecipitation with components of the secretion apparatus may implicate a cognate secretion system for each Srf (5, 8, 9, 16). Indeed, *srfG* lies immediately upstream of a gene encoding another DUF5410-containing protein, which was identified as an interaction partner of the *R. typhi* T4SS component RvhD4 (8). The gene pair is predicted to have arisen via an ancient duplication event (67), and future studies may reveal if they encode *bona fide* T4SS effectors. Such information will ultimately help define the sequence determinants for rickettsial secretion and improve our ability to predict new effectors.

In this work, we used BONCAT to discover new *R. parkeri* effectors, but our study is by no means exhaustive. First, BONCAT does not provide truly unbiased coverage of the proteome. It has been observed that longer, Met-rich proteins are slightly overrepresented in such pull-downs (28), likely due to greater probabilities for Anl incorporation and peptide detection. Moreover, extensive replacement of amino acids with non-canonical analogues could impact protein folding, stability, secretion, and, ultimately, bacterial physiology. For example, we found that prolonged (24 h) incubation with Anl led to diminished labeling, and our attempts to introduce a PheRS* system for incorporation of the Phe analog azidophenylalanine resulted in minimal labeling and bacterial filamentation (68). Second, our selective lysis strategy precludes extraction of putative effectors that localize to insoluble subcellular compartments (*e.g.*, nuclei), whose transient presence in the host cytoplasm may be insufficient for detection. Third, we labeled infected cells that had already accumulated considerable rickettsial burdens over the course of two days, a timepoint which could theoretically exclude effectors that are only secreted early during infection. Inconsistent detection of the known effector Sca4 (4), combined with

generally low spectral counts for the effectors we did detect, suggest that there is room for further optimization.

Nevertheless, we envision cell-selective BONCAT as a valuable tool for investigating rickettsial biology. For example, pulse-labeling with Anl could reveal the kinetics of effector secretion across the rickettsial life cycle, as was demonstrated for Yop effector secretion during *Yersinia* infection (26). Given that the Srfs we identified are variably conserved across the genus, effector repertoires could be compared between different *Rickettsia* species. BONCAT may also reveal that different suites of effectors are secreted during rickettsial infection of vertebrate host and arthropod vector cell niches. Additionally, arthropods harbor a multitude of microbes that can influence rickettsial biology (69–71), and *in situ* strain-specific labeling could facilitate studies of *Rickettsia* spp. within the broader context of the vector microbiome.

In sum, our work demonstrates that cell-selective BONCAT can uncover novel effectors secreted by an obligate intracellular bacterial pathogen. Proteomics provide a powerful lens through which to interrogate the biology of *Rickettsia* spp. and will complement advances in genetic tool development. The identification of SrfA–G opens new avenues for exploring effector structures, diversification, and secretion by this enigmatic genus. In parallel, mapping the host cell targets of these effectors will help illuminate the host-pathogen interface and offer a handle for studying fundamental cell biological processes. Altogether, a thorough investigation of secreted effectors will enhance our understanding of rickettsial biology and pathogenesis.

Methods

Cell culture

A549 human lung epithelial, HeLa human cervical epithelial, HEK293T human embryonic kidney epithelial, and Vero monkey kidney epithelial cell lines were obtained from the University of California, Berkeley Cell Culture Facility (Berkeley, CA). A549, HeLa, and HEK293T cells were maintained in Dulbecco's modified Eagle's medium (DMEM; Gibco catalog number 11965118) supplemented with 10% fetal bovine serum (FBS). Vero cells were maintained in DMEM supplemented with 5% FBS. Cell lines were confirmed to be mycoplasma-negative in a MycoAlert PLUS assay (Lonza catalog number LT07-710) performed by the Koch Institute High-Throughput Sciences Facility (Cambridge, MA).

Plasmid construction

pRL0128 was made by cloning *E. coli metG(M1-K548)* with mutations *L13N*, *Y260L*, and *H301L* and codon-optimized for *R. parkeri* into pRAM18dSGA[MCS] (kindly provided by Ulrike Munderloh). To enable expression of this gene in *R. parkeri*, a 368 bp fragment upstream of the *R. parkeri metG* (MC1_RS05365) start codon and a 99 bp fragment downstream of the *R. parkeri metG* stop codon were also added. pRL0368–374 were made by cloning the *R. parkeri ompA* promoter, an N-terminal MSGRPRTTSFAESGS sequence (GSK epitope tag underlined), *srfA–G*, and the *ompA* terminator into pRAM18dSGA[MCS]. pRL0375–377 were made by cloning *E. coli* codon-optimized *srfC*, *srfD(ΔF766-N957)*, and *srfF*, respectively, into pGEX6P3 (kindly provided by Matthew Welch) to add an N-terminal GST tag. pRL0378 and pRL0379 were made by cloning *E. coli* codon-optimized *srfD(ΔF766-N957)* and *srfF*, respectively, into His-SUMO-dual strep-TEV-PGT (kindly provided by Barbara Imperiali) (72) to add an N-

terminal 6xHis-SUMO-TwinStrep tag. pRL0381 was made by replacing the Cas9 insert in HP138-puro (kindly provided by Iain Cheeseman) (73) with a MCS downstream of the anhydrotetracycline (aTc)-inducible TRE3G promoter. pRL0382, pRL0385, pRL0387, and pRL0388 were made by cloning an N-terminal MDYKDHDGDYKDHDIDYKDDDDKLIN sequence (3xFLAG epitope tag underlined) and human codon-optimized *srfA*, *srfD*, *srfF*, and *srfG*, respectively, into pRL0381. N-terminally tagged SrfB, SrfC, and SrfE expressed poorly, so pRL0383, pRL0384, and pRL0386 respectively contain a C-terminal GGSGSDYKDHDGDYKDHDIDYKDDDDK sequence instead. FCW2IB-BiP-mNeonGreen-KDEL was generated as previously described (74). pRL0389 was made by replacing the Lifeact-3xTagBFP insert in FCW2IB-Lifeact-3xTagBFP (4) with *Gaussia*-Dura luciferase from pCMV-Gaussia-Dura Luc (Thermo Fisher Scientific catalog number 16191). pRL0390–394 are identical to pRL0385 but *srfD* was replaced with *srfD(ΔA57-Y116)*, *srfD(ΔN126-F257)*, *srfD(ΔF305-D686)*, *srfD(ΔF766-T821)*, and *srfD(ΔK848-D890)*, respectively.

Generation of R. parkeri strains

Parental *R. parkeri* strain Portsmouth (kindly provided by Chris Paddock) and all derived strains were propagated by infection and mechanical disruption of Vero cells grown in DMEM supplemented with 2% FBS at 33°C as previously described (4). Bacteria were clonally isolated and expanded from plaques formed after overlaying infected Vero cell monolayers with agarose as previously described (75). When appropriate, bacteria were further purified by passage through a sterile 2 μm filter (Cytiva catalog number 6783-2520). Bacterial stocks were stored as aliquots at –80°C to minimize variability due to freeze-thaws, and titers were determined by plaque assay (4). Parental *R. parkeri* were transformed with plasmids by small-scale

electroporation as previously described (30). WT and MetRS* *R. parkeri* were generated by transformation with pRAM18dSGA[MCS] and pRL0128, respectively. *R. parkeri* expressing GSK-tagged BFP and RARP-2 were generated as previously described (30). *R. parkeri* expressing GSK-tagged SrfA–G were generated by transformation with pRL0368–374. Spectinomycin (50 μg/mL) was included to select for transformants and to ensure plasmid maintenance during experiments.

Infectious focus assays

Infectious focus assays were performed as previously described (30). For each strain, 15 foci were imaged, and the number of infected cells and bacteria per focus was calculated.

BONCAT microscopy validation

Confluent A549 cells (approximately 3.5 x 10^5 cells/cm^2) were grown on 12-mm coverslips in 24-well plates and were infected with WT or MetRS* *R. parkeri* at a multiplicity of infection (MOI) of 0.001-0.004, centrifuged at 200 x g for 5 min at room temperature (RT), and incubated at 33°C. After 45 h, infected cells were treated with or without 1 mM azidonorleucine (Anl, Iris Biotech catalog number HAA1625) for 3 h, washed three times with phosphate-buffered saline (PBS), and fixed with 4% paraformaldehyde (PFA) in PBS for 10 min at RT. Fixed samples were incubated with 100 mM glycine in PBS for 10 min at RT to quench residual PFA. Samples were then washed three times with PBS, permeabilized with 0.5% Triton X-100 in PBS for 5 min at RT, and washed again with PBS. Samples were incubated with blocking buffer (2% bovine serum albumin [BSA] and 10% normal goat serum in PBS) for 30 min at RT. Primary and secondary antibodies were diluted in blocking buffer and incubated for 1 h each at

RT with three 5-min PBS washes after each incubation step. The following antibodies and stains were used: mouse anti-*Rickettsia* 14-13 (kindly provided by Ted Hackstadt), goat anti-mouse conjugated to Alexa Fluor 488 (Invitrogen catalog number A-11001), and Hoechst stain (Invitrogen catalog number H3570) to detect host nuclei. To perform the click reaction, coverslips were subsequently fixed with 4% PFA in PBS for 5 min at RT, quenched with 0.1 M glycine in PBS for 10 min at RT, washed three times with PBS, incubated with lysozyme reaction buffer (0.8X PBS, 50 mM glucose, 5 mM EDTA, 0.1% Triton X-100, 5 mg/mL lysozyme [Sigma-Aldrich catalog number L6876]) for 20 min at 37°C to permeabilize bacteria, and then washed five times with PBS. Samples were incubated with click reaction staining cocktail (50 mM sodium phosphate buffer [pH 7.4], 4 mM copper (II) sulfate [Sigma-Aldrich catalog number 209198], 20 mM tris-(3-hydroxypropyltriazolylmethyl)amine [THPTA, Sigma-Aldrich catalog number 762342], 5 µM AZDye 647 alkyne [Click Chemistry Tools catalog number 1301], 10 mM sodium ascorbate [Sigma-Aldrich catalog number A4034]) for 30 min at RT and washed five times with PBS. Coverslips were mounted using ProLong Gold Antifade mountant (Invitrogen catalog number P36934) and images were acquired using a 100X UPlanSApo (1.35 NA) objective on an Olympus IXplore Spin microscope system. Image analysis was performed with ImageJ.

BONCAT Western blot validation

Confluent A549 cells (approximately 3.5 x 10^5 cells/cm^2) were grown in 6-well plates and were infected with WT or MetRS* *R. parkeri* at a MOI of 0.006-0.02, centrifuged at 200 x g for 5 min at RT, and incubated at 33°C. After 45 h, infected cells were treated with or without 1 mM Anl for 3 h, washed with PBS, lifted with trypsin-EDTA, and centrifuged at 2,400 x g for 5

min at RT. Infected cell pellets were washed three times with PBS, resuspended in selective lysis buffer (50 mM HEPES [pH 7.9], 150 mM NaCl, 10% glycerol, 1% IGEPAL) supplemented with protease inhibitors (Sigma-Aldrich catalog number P1860), incubated on ice for 20 min, and centrifuged at 11,300 x g for 10 min at 4°C. The resulting supernatants were passed through a 0.22-µm cellulose acetate filter (Thermo Fisher Scientific catalog number F2517-1) by centrifugation at 6,700 x g for 10 min at 4°C. The resulting pellets were resuspended in total lysis buffer (50 mM HEPES [pH 7.9], 150 mM NaCl, 10% glycerol, 2% sodium dodecyl sulfate [SDS]) supplemented with 2 mM $MgCl_2$ and 0.1 units/µL Benzonase (Sigma catalog number E1014), incubated for 5 min at 37°C, and clarified by centrifugation at 21,100 x g for 1 min at RT. Lysate protein content was determined by bicinchoninic acid assay (Thermo Fisher Scientific catalog number 23227) and 45 µg cytoplasmic lysate was used as input for a click reaction at 1 mg/mL protein. An equivalent volume of pellet lysate was used as input. Lysates were incubated with click reaction biotin-alkyne cocktail (50 mM sodium phosphate buffer [pH 7.4], 2 mM copper (II) sulfate, 10 mM THPTA, 40 µM biotin-alkyne [Click Chemistry Tools catalog number 1266], 5 mM aminoguanidine [Sigma-Aldrich catalog number 396494], 20 mM sodium ascorbate) for 90 min at RT and proteins were precipitated with chloroform/methanol. Clicked protein precipitates were boiled in loading buffer (50 mM Tris-HCl [pH 6.8], 2% SDS, 10% glycerol, 0.1% bromophenol blue, 5% β-mercaptoethanol) and detected by Western blotting using StrepTactin-HRP (Bio-Rad catalog number 1610381). To prevent signal saturation, only 10% of the pellet precipitate was loaded.

BONCAT pull-downs

Confluent A549 cells (approximately 3.5 x 10^5 cells/cm^2) were grown in 10 cm^2 dishes and were infected with MetRS* *R. parkeri* at a MOI of 0.3, gently rocked at 37°C for 50 min, and incubated at 33°C. After 48 h, infected cells were treated with or without 1 mM Anl (n = 2 dishes per condition) for 5 h, washed with PBS, lifted with trypsin-EDTA, and centrifuged at 2,400 x g for 5 min at RT. Cytoplasmic lysates were harvested as described in the BONCAT Western blot validation section, SDS was added to 4.2 mg lysate input to a final concentration of 1.7%, and the mixture was heated at 70°C for 10 min. Denatured lysates were diluted to 1 mg/mL protein and 0.4% SDS with click reaction biotin-alkyne cocktail, incubated for 90 min at RT, and precipitated with 20% trichloroacetic acid. Clicked protein precipitates were washed with acetone, resuspended to 1.4 mg/mL protein in 1% SDS in PBS, and carryover acid was neutralized with 118 mM Tris-HCl (pH 8). To stabilize streptavidin tetramers during pull-down and washes, crosslinked streptavidin resin was prepared following a previously described resin cross-linking strategy (76). Briefly, streptavidin resin (Cytiva catalog number 17511301) was incubated with cross-linking buffer (20 mM sodium phosphate [pH 8], 150 mM NaCl) supplemented with 1.2 mM bis(sulfosuccinimidyl)suberate (BS3, Thermo Fisher Scientific catalog number A39266) for 30 min at RT. Unreacted BS3 was quenched with 40 mM Tris-HCl (pH 8) for 15 min at RT and the cross-linked streptavidin resin was washed twice with resin wash buffer (25 mM Tris-HCl [pH 7.4], 137 mM NaCl, 0.1% Tween 20) and once with PBS. Clicked protein suspensions were incubated with 200 µL cross-linked streptavidin resin for 2 h at RT, washed four times with 1% SDS in PBS, once with 6 M urea in 250 mM ammonium bicarbonate, once with 1 M NaCl, twice with 0.1% SDS in PBS, and five times with PBS. Resin-

bound proteins were submitted to the Whitehead Institute Proteomics Core Facility (Cambridge, MA) for sample workup and mass spectrometry analysis.

GSK secretion assays

GSK secretion assays were performed as previously described (30).

Srf protein purification

GST-tagged constructs were expressed in *E. coli* BL21 by overnight induction with 0.3 mM IPTG at 18°C. Pelleted cells were resuspended in protein lysis buffer (50 mM HEPES [pH 8.0], 150 mM NaCl, 0.1% Triton X-100, 1 mM PMSF, 6 units/mL Benzonase, 6 mM $MgCl_2$) supplemented with protease inhibitor tablets (Sigma-Aldrich catalog number 11836153001), lysed using a LM20 Microfluidizer (Microfluidizer) at 18,000 PSI for three passes, and clarified by centrifugation at 40,000 x g for 1 h at 4°C. Proteins were purified using glutathione sepharose resin (Cytiva catalog number 17075601), eluted by step gradient (50 mM HEPES [pH 8], 200 mM NaCl, 1 to 10 mM reduced glutathione), and concentrated using Amicon Ultra concentrators (Sigma-Aldrich). 6xHis-SUMO-TwinStrep-tagged constructs were expressed in *E. coli* BL21(DE3) and harvested as described for the GST-tagged proteins, purified using nickel sepharose resin (Cytiva catalog number 17531802), eluted by step gradient (50 mM HEPES [pH 8], 200 mM NaCl, 100 to 500 mM imidazole), and cleaved with ULP1 protease (kindly provided by Barbara Imperiali) while dialyzing overnight at 4°C (into 50 mM HEPES [pH 8], 200 mM NaCl). TwinStrep-tagged proteins were further purified using nickel sepharose resin followed by size-exclusion chromatography using a HiLoad 16/600 Superdex 200 pg column (Cytiva catalog number 28989335) and then concentrated.

Srf antibody purification

GST-tagged proteins were used for immunization by Labcorp (Denver, PA) according to their standard 77-day rabbit polyclonal antibody protocol. To affinity purify anti-Srf antibodies, NHS-activated sepharose resin (1 mL, Cytiva catalog number 17090601) was activated with 1 mM HCl, drained, and incubated with TwinStrep-tagged proteins (1.4 mg) for 1 h at RT. The resin was washed twice with alternating ethanolamine (500 mM ethanolamine [pH 8.3], 500 mM NaCl) and acetate (100 mM sodium acetate [pH 4.5], 500 mM NaCl) buffers and then equilibrated (with 20 mM Tris [pH 7.5] first with and then without 500 mM NaCl) before incubating with 2 mL filtered (0.22 µm) SrfD or SrfF antisera for 1 h at RT. The resin was washed (20 mM Tris [pH 7.5] first without and then with 500 mM NaCl), and antibodies were eluted with 100 mM glycine (pH 2.8), neutralized with 65 mM Tris-HCl (pH 8.8), dialyzed overnight at 4°C (into 50 mM HEPES [pH 8], 150 mM NaCl, 10% glycerol), and concentrated. For retrieval of anti-SrfC antibodies, filtered SrfC antisera were purified by sequential incubation with GST tag and GST-tagged SrfC conjugated separately to NHS-activated sepharose resin. Antibodies were validated by Western blotting using purified *R. parkeri*, uninfected A549 cell lysates, and purified recombinant Srfs.

Secreted Srf immunoblotting

Selective lysis fractions from infection of A549s with parental *R. parkeri* were prepared as previously described (30). Lysates were analyzed by Western blotting using Srf antisera and mouse anti-RpoA (BioLegend catalog number 663104).

Secreted Srf immunofluorescence assays

Confluent A549 cells (approximately 3.5 x 10^5 cells/cm^2) were grown on 12-mm coverslips in 24-well plates and were infected with WT *R. parkeri* at a MOI of 0.1 or 0.2, centrifuged at 200 x g for 5 min at RT, and incubated at 33°C for 47 h until fixation with 4% PFA in PBS for 1 h at RT. Fixed samples were processed as described in the BONCAT microscopy validation section, except primary antibodies were incubated for 3 h at 37°C. The following antibodies and stains were used: purified rabbit anti-Srf antibodies, goat anti-rabbit conjugated to Alexa Fluor 647 (Invitrogen catalog number A-21245), and Hoechst stain to detect host nuclei.

Exogenous Srf immunofluorescence assays

HeLa cells (4 x 10^4 cells/cm^2) were plated on 12-mm coverslips in 24-well plates and were transfected the next day with 500 ng DNA using Lipofectamine 3000 (Thermo Fisher Scientific catalog number L3000001) following the manufacturer's instructions. The following day, the media was replaced and supplemented with 1 µg/mL aTc (Clontech catalog number 631310). After 24 h induction, cells were fixed with 4% PFA in PBS for 10 min at RT. Fixed samples were quenched, washed, and permeabilized and then incubated with blocking buffer (2% BSA in PBS) for 30 min at RT. Primary and secondary antibodies were diluted in blocking buffer and incubated for 1 h each at RT with three 5-min PBS washes after each incubation step. The following antibodies and stains were used: mouse anti-FLAG (Sigma-Aldrich catalog number F1804), goat anti-mouse conjugated to Alexa Fluor 488 or to Alexa Fluor 647 (Invitrogen catalog number A-21235), rabbit anti-AIF (Cell Signaling Technology catalog number 5318S), goat anti-rabbit conjugated to Alexa Fluor 488 (Invitrogen catalog number A-11008), and Hoechst stain to detect nuclei. To assess colocalization of 3xFLAG-SrfC or

3xFLAG-SrfD with ER-targeted mNeonGreen, the same procedure was followed except 250 ng each of pRL0384 or pRL0385 and FCW2IB-BiP-mNeonGreen-KDEL were co-transfected and the cells were fixed for 1 h.

Secreted SrfD immunoprecipitation assays

Confluent A549 cells (approximately 3.5 x 10^5 cells/cm^2) were grown in triplicate in 10 cm^2 dishes and were infected with WT *R. parkeri* at a MOI of 0.3, gently rocked at 37°C for 50 min, and incubated at 33°C. Triplicate dishes were infected with bacteria in brain heart infusion media (BHI) or mock-infected with BHI as uninfected controls. After 45 h, cells were washed with ice-cold PBS, scraped into selective lysis buffer supplemented with protease inhibitors and 1 mM EDTA, incubated on ice for 20 min, and centrifuged at 11,300 x g for 10 min at 4°C. The resulting supernatants were filtered as described in the BONCAT Western blot validation section, pre-cleared with Protein A magnetic resin (Thermo Fisher Scientific catalog number 88846) for 30 min at 4°C, and incubated with 15 µg/mL purified rabbit anti-SrfD overnight at 4°C. Immune complexes were precipitated with Protein A magnetic resin for 1 h at 4°C, washed four times with supplemented selective lysis buffer, eluted by incubation with 100 mM glycine (pH 2.8) for 20 min at RT, and neutralized with 115 mM Tris-HCl (pH 8.5). The neutralized eluates were submitted to the Koch Institute Biopolymers & Proteomics Core Facility for sample workup and mass spectrometry analysis.

Mass spectrometry

For identification of secreted effectors from BONCAT, resin-bound proteins were denatured, reduced, alkylated, and digested with trypsin/Lys-C overnight at 37°C. The resulting

peptides were purified using styrene-divinylbenzene reverse phase sulfonate StageTips as previously described (77). LC-MS/MS data were acquired using a Vanquish Neo nanoLC system coupled with an Orbitrap Exploris mass spectrometer, a FAIMS Pro interface, and an EASY-Spray ESI source (Thermo Fisher Scientific). Peptide separation was carried out using an Acclaim PepMap trap column (75 µm x 2 cm; Thermo Fisher Scientific) and an EASY-Spray ES902 column (75 µm x 250 mm, 100 Å; Thermo Fisher Scientific) using standard reverse-phase gradients. Data analysis was performed using PEAKS Studio 10.6 software (Bioinformatics Solutions) and analyzed as previously described (78). RefSeq entries for *R. parkeri* strain Portsmouth (taxonomy ID 1105108) were downloaded from NCBI. Variable modifications for Anl and biotin-Anl were included. Peptide identifications were accepted with a false discovery rate of ≤ 1% and a significance threshold of 20 ($-10\log_{10}P$). Protein identifications were accepted with two unique peptides. Proteins that were present in both replicates of the Anl-treated infection lysate pull-down were called as hits.

For identification of proteins in the secreted SrfD immunoprecipitation eluates, peptides were prepared using S-Trap micro spin columns (ProtiFi) following the manufacturer's instructions, except 10 mM DTT was used instead of TCEP, samples were reduced for 10 min at 95°C, 20 mM iodoacetamide was used instead of MMTS, and samples were alkylated for 30 min at RT. LC-MS/MS data were acquired using an UltiMate 3000 HPLC system coupled with an Orbitrap Exploris mass spectrometer (Thermo Fisher Scientific). Peptide separation was carried out using an Acclaim PepMap RSLC C18 column (75 µm x 50 cm; Thermo Fisher Scientific) using standard reverse-phase gradients. Data analysis was performed using Sequest HT in Proteome Discoverer (Thermo Fisher Scientific) against human (UniProt) and *R. parkeri* (RefSeq) databases with common contaminants removed. Normalized intensities from the top

three precursors were computed with Scaffold (Proteome Software) and filtered to require a non-zero value for at least two of the three replicates in at least one condition. Zero values were then imputed to the minimum intensity within each sample. Mean fold-changes and Benjamini-Hochberg adjusted p-values were computed for log-transformed intensities between infected and uninfected conditions.

Sec61 immunoprecipitation assays

For immunoprecipitation of Sec61 during infection, confluent A549 cells (approximately 3.5 x 10^5 cells/cm^2) were grown in 10 cm^2 dishes and were infected with WT *R. parkeri* at a MOI of 0.25, gently rocked at 37°C for 50 min, and incubated at 33°C. After 53 h, lysates were harvested, filtered, and pre-cleared as described in the secreted SrfD immunoprecipitation assays section, and incubated with 0.18 µg/mL rabbit anti-Sec61β (Cell Signaling Technology catalog number 14648S) overnight at 4°C. Immune complexes were precipitated and washed, eluted by boiling in loading buffer, and detected by Western blotting using purified rabbit anti-SrfD and rabbit anti-Sec61β. For immunoprecipitation of Sec61 following SrfD transfection, HEK293T cells (5 x 10^4 cells/cm^2) were grown in 6-well plates and transfected the next day with 2.5 µg DNA with TransIT-LT1 (Mirus Bio catalog number MIR-2304) following the manufacturer's instructions. To ensure comparable expression levels of the SrfD constructs, 2 µg pRL0385, 2 µg pRL0390, 2 µg pRL0391, 2 µg pRL0392, 2.5 µg pRL0393, and 1.5 µg pRL0394 were brought up to 2.5 µg total DNA with pRL0381. The following day, the media was replaced and supplemented with 200 ng/mL aTc. After 24 h induction, lysates were harvested (without filtering), pre-cleared, and incubated with rabbit anti-Sec61β. Immune complexes were

precipitated, washed, eluted, and detected by Western blotting using mouse anti-FLAG and rabbit anti-Sec61β.

Luciferase secretion assays

HEK293T cells stably expressing *Gaussia* luciferase were generated with pRL0389 by lentiviral transduction as previously described (4), except 300 µL filtered viral supernatant was used and selection was performed with 5 µg/mL blasticidin. Cells (5 x 10^4 cells/cm^2) were grown in triplicate in 24-well plates pre-coated with 6 µg fibronectin (Sigma-Aldrich catalog number FC010) and transfected the next day with 500 ng pRL0381 or pRL0385 with TransIT-LT1. The following day, the media was first replaced and supplemented with 200 ng/mL aTc to prime expression of SrfD. After 8 h, the media was replaced and supplemented with 200 ng/mL aTc and either DMSO or 6 µg/mL brefeldin A (Sigma-Aldrich catalog number B6542). After an additional 16 h, culture supernatants were assayed for luciferase activity on a Varioskan plate reader (Thermo Fisher Scientific) using the Pierce Gaussia Luciferase Glow Assay Kit (Thermo Fisher Scientific catalog number 16161) following the manufacturer's instructions.

Bioinformatic analyses

Protein-protein BLAST (79) E-values were computed using the default BLOSUM62 scoring matrix to evaluate similarity between *R. parkeri* SrfA–G and homologs in representative members of the *Rickettsia* genus. Srf structures were predicted with ColabFold (37) and searched against the AlphaFold, PDB, and GMGCL databases using FoldSeek (38) in 3Di/AA mode with an E-value cutoff of 0.001. HHpred (39) with an E-value cutoff of 0.001 was used to search Srf sequences against the PDB and Pfam databases. Phyre2 (40) with a 95% confidence cutoff was

also used for Srf homolog prediction. Putative secondary structure features were identified using the MPI Bioinformatics Toolkit (39). The *R. parkeri* proteome was searched for type IV effectors using OPT4e (22) and S4TE (45). SrfA was searched for Sec and Tat signal peptides using SignalP (60). SrfB was searched for a mitochondrial targeting sequence using TargetP (61) and MitoFates (62).

Statistical analyses

Statistical analysis was performed using Prism 9 (GraphPad Software). Graphical representations, statistical parameters, and significance are reported in the figure legends. Unless otherwise specified, data were considered to be statistically significant when $p < 0.05$.

Data Availability

Mass spectral data and the protein sequence databases used for searches have been deposited in the public proteomics repository MassIVE (https://massive.ucsd.edu, MSV000093380 and MSV000093381).

Acknowledgements

We are grateful to Michael Laub and Brandon Sit for critical review of the manuscript. We thank Ulrike Munderloh, Matthew Welch, Barbara Imperiali, Iain Cheeseman, Chris Paddock, and Ted Hackstadt for reagents and Roberto Vazquez Nunez and Seychelle Vos for assistance with protein purification. We also thank Fabian Schulte at the Whitehead Institute Proteomics Core Facility and Richard Schiavoni at the Koch Institute Biopolymers & Proteomics Core Facility for experimental support. Work in the Lamason laboratory is supported in part by

the National Institutes of Health (R01 AI155489) and by the Office of the Assistant Secretary of Defense for Health Affairs through the Tick-Borne Disease Research Program (TB200032). Opinions, interpretations, conclusions, and recommendations are those of the authors and are not necessarily endorsed by the Department of Defense. This work was also supported by the NIH Institutional Training Grants for AGS and HKM (T32 GM007287 and GM136540) and by the National Science Foundation Graduate Research Fellowship to HKM (2141064).

References

1. Walker DH, Ismail N. 2008. Emerging and re-emerging rickettsioses: endothelial cell infection and early disease events. Nature Reviews Microbiology 6:375.

2. Parola P, Paddock CD, Socolovschi C, Labruna MB, Mediannikov O, Kernif T, Abdad MY, Stenos J, Bitam I, Fournier P-E, Raoult D. 2013. Update on Tick-Borne Rickettsioses around the World: a Geographic Approach. Clin Microbiol Rev 26:657–702.

3. McGinn J, Lamason RL. 2021. The enigmatic biology of rickettsiae: recent advances, open questions and outlook. Pathog Dis 79:ftab019.

4. Lamason RL, Bastounis E, Kafai NM, Serrano R, del Álamo JC, Theriot JA, Welch MD. 2016. Rickettsia Sca4 Reduces Vinculin-Mediated Intercellular Tension to Promote Spread. Cell 167:670-683.e10.

5. Lehman SS, Noriea NF, Aistleitner K, Clark TR, Dooley CA, Nair V, Kaur SJ, Rahman MS, Gillespie JJ, Azad AF, Hackstadt T. 2018. The Rickettsial Ankyrin Repeat Protein 2 Is a Type IV Secreted Effector That Associates with the Endoplasmic Reticulum. mBio 9:e00975-18.

6. Aistleitner K, Clark T, Dooley C, Hackstadt T. 2020. Selective fragmentation of the trans-Golgi apparatus by Rickettsia rickettsii. PLoS Pathog 16:e1008582.

7. Borgo GM, Burke TP, Tran CJ, Lo NTN, Engström P, Welch MD. 2022. A patatin-like phospholipase mediates Rickettsia parkeri escape from host membranes. 1. Nat Commun 13:3656.

8. Voss OH, Gillespie JJ, Lehman SS, Rennoll SA, Beier-Sexton M, Rahman MS, Azad AF. 2020. Risk1, a Phosphatidylinositol 3-Kinase Effector, Promotes *Rickettsia typhi* Intracellular Survival. mBio 11:e00820-20, /mbio/11/3/mBio.00820-20.atom.

9. Rennoll-Bankert KE, Rahman MS, Gillespie JJ, Guillotte ML, Kaur SJ, Lehman SS, Beier-Sexton M, Azad AF. 2015. Which Way In? The RalF Arf-GEF Orchestrates Rickettsia Host Cell Invasion. PLOS Pathogens 11:e1005115.

10. Rennoll-Bankert KE, Rahman MS, Guillotte ML, Lehman SS, Beier-Sexton M, Gillespie JJ, Azad AF. 2016. RalF-Mediated Activation of Arf6 Controls Rickettsia typhi Invasion by Co-Opting Phosphoinositol Metabolism. Infection and Immunity https://doi.org/10.1128/iai.00638-16.

11. Bumann D, Aksu S, Wendland M, Janek K, Zimny-Arndt U, Sabarth N, Meyer TF, Jungblut PR. 2002. Proteome Analysis of Secreted Proteins of the Gastric Pathogen Helicobacter pylori. Infect Immun 70:3396–3403.

12. Galka F, Wai SN, Kusch H, Engelmann S, Hecker M, Schmeck B, Hippenstiel S, Uhlin BE, Steinert M. 2008. Proteomic Characterization of the Whole Secretome of Legionella pneumophila and Functional Analysis of Outer Membrane Vesicles. Infect Immun 76:1825–1836.

13. Eshraghi A, Kim J, Walls AC, Ledvina HE, Miller C, Ramsey KM, Whitney JC, Radey MC, Peterson SB, Ruhland BR, Tran BQ, Goo YA, Goodlett DR, Dove SL, Celli J, Veesler D, Mougous JD. 2016. Secreted Effectors Encoded Within and Outside of the Francisella Pathogenicity Island Promote Intramacrophage Growth. Cell Host Microbe 20:573–583.

14. Luo Z-Q, Isberg RR. 2004. Multiple substrates of the Legionella pneumophila Dot/Icm system identified by interbacterial protein transfer. Proceedings of the National Academy of Sciences 101:841–846.

15. Geddes K, Worley M, Niemann G, Heffron F. 2005. Identification of New Secreted Effectors in Salmonella enterica Serovar Typhimurium. Infection and Immunity 73:6260–6271.

16. VieBrock L, Evans SM, Beyer AR, Larson CL, Beare PA, Ge H, Singh S, Rodino KG, Heinzen RA, Richards AL, Carlyon JA. 2015. Orientia tsutsugamushi ankyrin repeat-containing protein family members are Type 1 secretion system substrates that traffic to the host cell endoplasmic reticulum. Front Cell Infect Microbiol 4.

17. Whitaker N, Berry TM, Rosenthal N, Gordon JE, Gonzalez-Rivera C, Sheehan KB, Truchan HK, VieBrock L, Newton ILG, Carlyon JA, Christie PJ. 2016. Chimeric Coupling Proteins Mediate Transfer of Heterologous Type IV Effectors through the Escherichia coli pKM101-Encoded Conjugation Machine. Journal of Bacteriology 198:2701–2718.

18. McCaslin PN, Andersen SE, Icardi CM, Faris R, Steiert B, Smith P, Haider J, Weber MM. 2023. Identification and Preliminary Characterization of Novel Type III Secreted Effector Proteins in Chlamydia trachomatis. Infection and Immunity 91:e00491-22.

19. Samudrala R, Heffron F, McDermott JE. 2009. Accurate Prediction of Secreted Substrates and Identification of a Conserved Putative Secretion Signal for Type III Secretion Systems. PLOS Pathogens 5:e1000375.

20. Burstein D, Amaro F, Zusman T, Lifshitz Z, Cohen O, Gilbert JA, Pupko T, Shuman HA, Segal G. 2016. Genomic analysis of 38 Legionella species identifies large and diverse effector repertoires. 2. Nat Genet 48:167–175.

21. McClure EE, Oliva Chávez AS, Shaw DK, Carlyon JA, Ganta RR, Noh SM, Wood DO, Bavoil PM, Brayton KA, Martinez JJ, McBride JW, Valdivia1 RH, Munderloh UG, Pedra JHF. 2017. Engineering of obligate intracellular bacteria: progress, challenges and paradigms. Nat Rev Microbiol 15:544–558.

22. Esna Ashari Z, Brayton KA, Broschat SL. 2019. Prediction of T4SS Effector Proteins for Anaplasma phagocytophilum Using OPT4e, A New Software Tool. Front Microbiol 10:1391.

23. Dieterich DC, Link AJ, Graumann J, Tirrell DA, Schuman EM. 2006. Selective identification of newly synthesized proteins in mammalian cells using bioorthogonal noncanonical amino acid tagging (BONCAT). Proceedings of the National Academy of Sciences 103:9482–9487.

24. Ngo JT, Champion JA, Mahdavi A, Tanrikulu IC, Beatty KE, Connor RE, Yoo TH, Dieterich DC, Schuman EM, Tirrell DA. 2009. Cell-selective metabolic labeling of proteins. 10. Nat Chem Biol 5:715–717.

25. Grammel M, Zhang MM, Hang HC. 2010. Orthogonal Alkynyl Amino Acid Reporter for Selective Labeling of Bacterial Proteomes during Infection. Angewandte Chemie International Edition 49:5970–5974.

26. Mahdavi A, Szychowski J, Ngo JT, Sweredoski MJ, Graham RLJ, Hess S, Schneewind O, Mazmanian SK, Tirrell DA. 2014. Identification of secreted bacterial proteins by noncanonical amino acid tagging. PNAS 111:433–438.

27. Chande AG, Siddiqui Z, Midha MK, Sirohi V, Ravichandran S, Rao KVS. 2015. Selective enrichment of mycobacterial proteins from infected host macrophages. Scientific Reports 5:13430.

28. Franco M, D'haeseleer PM, Branda SS, Liou MJ, Haider Y, Segelke BW, El-Etr SH. 2018. Proteomic Profiling of Burkholderia thailandensis During Host Infection Using Bio-Orthogonal Noncanonical Amino Acid Tagging (BONCAT). Frontiers in Cellular and Infection Microbiology 8.

29. Schmidt F, Völker U. 2011. Proteome analysis of host–pathogen interactions: Investigation of pathogen responses to the host cell environment. PROTEOMICS 11:3203–3211.

30. Sanderlin AG, Hanna RE, Lamason RL. 2022. The Ankyrin Repeat Protein RARP-1 Is a Periplasmic Factor That Supports Rickettsia parkeri Growth and Host Cell Invasion. Journal of Bacteriology 204:e00182-22.

31. Rahman MS, Gillespie JJ, Kaur SJ, Sears KT, Ceraul SM, Beier-Sexton M, Azad AF. 2013. Rickettsia typhi Possesses Phospholipase A2 Enzymes that Are Involved in Infection of Host Cells. PLOS Pathogens 9:e1003399.

32. Blanc G, Ngwamidiba M, Ogata H, Fournier P-E, Claverie J-M, Raoult D. 2005. Molecular Evolution of Rickettsia Surface Antigens: Evidence of Positive Selection. Mol Biol Evol 22:2073–2083.

33. Riley SP, Goh KC, Hermanas TM, Cardwell MM, Chan YGY, Martinez JJ. 2010. The Rickettsia conorii Autotransporter Protein Sca1 Promotes Adherence to Nonphagocytic Mammalian Cells. Infection and Immunity 78:1895–1904.

34. Noriea NF, Clark TR, Hackstadt T. 2015. Targeted Knockout of the Rickettsia rickettsii OmpA Surface Antigen Does Not Diminish Virulence in a Mammalian Model System. mBio 6:e00323-15.

35. Nock AM, Aistleitner K, Clark TR, Sturdevant D, Ricklefs S, Virtaneva K, Zhang Y, Gulzar N, Redekar N, Roy A, Hackstadt T. 2023. Identification of an autotransporter peptidase of Rickettsia rickettsii responsible for maturation of surface exposed autotransporters. PLOS Pathogens 19:e1011527.

36. Patel JG, Narra HP, Sepuru KM, Sahni A, Golla SR, Sahni A, Singh A, Schroeder CLC, Chowdhury IH, Popov VL, Sahni SK. 2020. Evolution, purification, and characterization of RC0497: a peptidoglycan amidase from the prototypical spotted fever species Rickettsia conorii. Biological Chemistry 401:249–262.

37. Mirdita M, Schütze K, Moriwaki Y, Heo L, Ovchinnikov S, Steinegger M. 2022. ColabFold: making protein folding accessible to all. 6. Nat Methods 19:679–682.

38. van Kempen M, Kim SS, Tumescheit C, Mirdita M, Lee J, Gilchrist CLM, Söding J, Steinegger M. 2023. Fast and accurate protein structure search with Foldseek. Nat Biotechnol 1–4.

39. Zimmermann L, Stephens A, Nam S-Z, Rau D, Kübler J, Lozajic M, Gabler F, Söding J, Lupas AN, Alva V. 2018. A Completely Reimplemented MPI Bioinformatics Toolkit with a New HHpred Server at its Core. Journal of Molecular Biology 430:2237–2243.

40. Kelley LA, Mezulis S, Yates CM, Wass MN, Sternberg MJE. 2015. The Phyre2 web portal for protein modeling, prediction and analysis. 6. Nat Protoc 10:845–858.

41. Lynch MJ, Levenson R, Kim EA, Sircar R, Blair DF, Dahlquist FW, Crane BR. 2017. Co-Folding of a FliF-FliG Split Domain Forms the Basis of the MS:C Ring Interface within the Bacterial Flagellar Motor. Structure 25:317–328.

42. Zhang R, Kennedy MA. 2021. Current Understanding of the Structure and Function of Pentapeptide Repeat Proteins. Biomolecules 11:638.

43. Schmidt H, Hensel M. 2004. Pathogenicity Islands in Bacterial Pathogenesis. Clinical Microbiology Reviews 17:14–56.

44. Gillespie JJ, Kaur SJ, Rahman MS, Rennoll-Bankert K, Sears KT, Beier-Sexton M, Azad AF. 2015. Secretome of obligate intracellular Rickettsia. FEMS Microbiol Rev 39:47–80.

45. Noroy C, Lefrançois T, Meyer DF. 2019. Searching algorithm for Type IV effector proteins (S4TE) 2.0: Improved tools for Type IV effector prediction, analysis and comparison in proteobacteria. PLOS Computational Biology 15:e1006847.

46. Delepelaire P. 2004. Type I secretion in gram-negative bacteria. Biochimica et Biophysica Acta (BBA) - Molecular Cell Research 1694:149–161.

47. Torruellas Garcia J, Ferracci F, Jackson MW, Joseph SS, Pattis I, Plano LRW, Fischer W, Plano GV. 2006. Measurement of Effector Protein Injection by Type III and Type IV Secretion Systems by Using a 13-Residue Phosphorylatable Glycogen Synthase Kinase Tag. Infect Immun 74:5645–5657.

48. Weber MM, Chen C, Rowin K, Mertens K, Galvan G, Zhi H, Dealing CM, Roman VA, Banga S, Tan Y, Luo Z-Q, Samuel JE. 2013. Identification of Coxiella burnetii Type IV Secretion Substrates Required for Intracellular Replication and Coxiella-Containing Vacuole Formation. Journal of Bacteriology 195:3914–3924.

49. Keeble AH, Khan Z, Forster A, James LC. 2008. TRIM21 is an IgG receptor that is structurally, thermodynamically, and kinetically conserved. Proceedings of the National Academy of Sciences 105:6045–6050.

50. Gemmer M, Förster F. 2020. A clearer picture of the ER translocon complex. J Cell Sci 133.

51. Itskanov S, Wang L, Junne T, Sherriff R, Xiao L, Blanchard N, Shi WQ, Forsyth C, Hoepfner D, Spiess M, Park E. 2023. A common mechanism of Sec61 translocon inhibition by small molecules. 9. Nat Chem Biol 19:1063–1071.

52. Tannous BA, Kim D-E, Fernandez JL, Weissleder R, Breakefield XO. 2005. Codon-Optimized Gaussia Luciferase cDNA for Mammalian Gene Expression in Culture and in Vivo. Molecular Therapy 11:435–443.

53. Helms JB, Rothman JE. 1992. Inhibition by brefeldin A of a Golgi membrane enzyme that catalyses exchange of guanine nucleotide bound to ARF. 6402. Nature 360:352–354.

54. Lupas AN, Bassler J. 2017. Coiled Coils – A Model System for the 21st Century. Trends in Biochemical Sciences 42:130–140.

55. Weigele BA, Orchard RC, Jimenez A, Cox GW, Alto NM. 2017. A systematic exploration of the interactions between bacterial effector proteins and host cell membranes. 1. Nat Commun 8:532.

56. Krampen L, Malmsheimer S, Grin I, Trunk T, Lührmann A, de Gier J-W, Wagner S. 2018. Revealing the mechanisms of membrane protein export by virulence-associated bacterial secretion systems. 1. Nat Commun 9:3467.

57. Li X, Sun S, Appathurai S, Sundaram A, Plumb R, Mariappan M. 2020. A Molecular Mechanism for Turning Off IRE1α Signaling during Endoplasmic Reticulum Stress. Cell Reports 33:108563.

58. Schäuble N, Lang S, Jung M, Cappel S, Schorr S, Ulucan Ö, Linxweiler J, Dudek J, Blum R, Helms V, Paton AW, Paton JC, Cavalié A, Zimmermann R. 2012. BiP-mediated closing of the Sec61 channel limits Ca2+ leakage from the ER. The EMBO Journal 31:3282–3296.

59. Zhao Y, Fang R, Zhang J, Zhang Y, Bechelli J, Smalley C, Valbuena G, Walker DH, Oteo JA, Brasier AR. 2020. Quantitative Proteomics of the Endothelial Secretome Identifies RC0497 as Diagnostic of Acute Rickettsial Spotted Fever Infections. The American Journal of Pathology 190:306–322.

60. Teufel F, Almagro Armenteros JJ, Johansen AR, Gíslason MH, Pihl SI, Tsirigos KD, Winther O, Brunak S, von Heijne G, Nielsen H. 2022. SignalP 6.0 predicts all five types of signal peptides using protein language models. 7. Nat Biotechnol 40:1023–1025.

61. Armenteros JJA, Salvatore M, Emanuelsson O, Winther O, Heijne G von, Elofsson A, Nielsen H. 2019. Detecting sequence signals in targeting peptides using deep learning. Life Science Alliance 2.

62. Fukasawa Y, Tsuji J, Fu S-C, Tomii K, Horton P, Imai K. 2015. MitoFates: Improved Prediction of Mitochondrial Targeting Sequences and Their Cleavage Sites. Mol Cell Proteomics 14:1113–1126.

63. Andersson SGE, Zomorodipour A, Andersson JO, Sicheritz-Pontén T, Alsmark UCM, Podowski RM, Näslund AK, Eriksson A-S, Winkler HH, Kurland CG. 1998. The genome sequence of Rickettsia prowazekii and the origin of mitochondria. 6707. Nature 396:133–140.

64. Voth DE, Broederdorf LJ, Graham JG. 2012. Bacterial Type IV Secretion Systems: Versatile Virulence Machines. Future Microbiol 7:241–257.

65. McDermott JE, Corrigan A, Peterson E, Oehmen C, Niemann G, Cambronne ED, Sharp D, Adkins JN, Samudrala R, Heffron F. 2011. Computational Prediction of Type III and IV Secreted Effectors in Gram-Negative Bacteria. Infection and Immunity 79:23–32.

66. Spitz O, Erenburg IN, Kanonenberg K, Peherstorfer S, Lenders MHH, Reiners J, Ma M, Luisi BF, Smits SHJ, Schmitt L. 2022. Identity Determinants of the Translocation Signal for a Type 1 Secretion System. Front Physiol 12:804646.

67. Lehman SS, Verhoeve VI, Driscoll TP, Beckmann JF, Gillespie JJ. 2024. Metagenome diversity illuminates the origins of pathogen effectors. mBio:e0075923.

68. Yuet KP, Doma MK, Ngo JT, Sweredoski MJ, Graham RLJ, Moradian A, Hess S, Schuman EM, Sternberg PW, Tirrell DA. 2015. Cell-specific proteomic analysis in Caenorhabditis elegans. Proc Natl Acad Sci U S A 112:2705–2710.

69. Macaluso KR, Sonenshine DE, Ceraul SM, Azad AF. 2002. Rickettsial infection in Dermacentor variabilis (Acari: Ixodidae) inhibits transovarial transmission of a second Rickettsia. J Med Entomol 39:809–813.

70. Gall CA, Reif KE, Scoles GA, Mason KL, Mousel M, Noh SM, Brayton KA. 2016. The bacterial microbiome of Dermacentor andersoni ticks influences pathogen susceptibility. ISME J 10:1846–1855.

71. Maitre A, Wu-Chuang A, Mateos-Hernández L, Foucault-Simonin A, Moutailler S, Paoli J-C, Falchi A, Díaz-Sánchez AA, Banović P, Obregón D, Cabezas-Cruz A. 2022. Rickettsia helvetica infection is associated with microbiome modulation in Ixodes ricinus collected from humans in Serbia. Sci Rep 12:11464.

72. Dodge GJ, Bernstein HM, Imperiali B. 2023. A generalizable protocol for expression and purification of membrane-bound bacterial phosphoglycosyl transferases in liponanoparticles. Protein Expression and Purification 207:106273.

73. McKinley KL, Cheeseman IM. 2017. Large-Scale Analysis of CRISPR/Cas9 Cell-Cycle Knockouts Reveals the Diversity of p53-Dependent Responses to Cell-Cycle Defects. Dev Cell 40:405-420.e2.

74. Acevedo-Sánchez Y, Woida PJ, Kraemer S, Lamason RL. 2023. An obligate intracellular bacterial pathogen forms a direct, interkingdom membrane contact site. bioRxiv https://doi.org/10.1101/2023.06.05.543771.

75. Lamason RL, Kafai NM, Welch MD. 2018. A streamlined method for transposon mutagenesis of Rickettsia parkeri yields numerous mutations that impact infection. PLOS ONE 13:e0197012.

76. Ivanov KI, Bašić M, Varjosalo M, Mäkinen K. 2014. One-step Purification of Twin-Strep-tagged Proteins and Their Complexes on Strep-Tactin Resin Cross-linked With Bis(sulfosuccinimidyl) Suberate (BS3). JoVE 51536.

77. Rappsilber J, Mann M, Ishihama Y. 2007. Protocol for micro-purification, enrichment, pre-fractionation and storage of peptides for proteomics using StageTips. 8. Nat Protoc 2:1896–1906.

78. Schulte F, Hasturk H, Hardt M. 2019. Mapping Relative Differences in Human Salivary Gland Secretions by Dried Saliva Spot Sampling and nanoLC–MS/MS. PROTEOMICS 19:1900023.

79. Boratyn GM, Camacho C, Cooper PS, Coulouris G, Fong A, Ma N, Madden TL, Matten WT, McGinnis SD, Merezhuk Y, Raytselis Y, Sayers EW, Tao T, Ye J, Zaretskaya I. 2013. BLAST: a more efficient report with usability improvements. Nucleic Acids Res 41:W29–W33.

CHAPTER 4: DISCUSSION

Rickettsia spp. are exquisitely adapted to the host cell niche, and their success hinges on surface proteins and secreted protein effectors that allow them to manipulate host cell processes. The limited genetic toolkit for probing rickettsial biology has precluded a thorough investigation of the host-pathogen interface; indeed, much of our knowledge about these proteins stems from comparisons between strains and the fortuitous insertion of transposons (1, 2). Given the state of tool development in the field, perhaps it is not surprising that so few secreted effectors have been characterized. In Chapter 2, I leveraged a *rarp-1*::Tn mutant to test the hypothesis that RARP-1 is a secreted effector. My work supported a model whereby RARP-1 remains in the periplasm to facilitate invasion and growth in the host cell cytoplasm. With one less protein in the already short list of secreted effectors, I developed a cell-selective proteomic screen in Chapter 3 to flesh out the rickettsial secretome. In addition to identifying known secreted effectors, this approach revealed novel effectors that are unique to the *Rickettsia* genus, variably conserved, structurally diverse, and targeted to distinct host cell compartments. One of these novel effectors, SrfD, appears to interact with the host Sec61 translocon, but its function was not determined. In the following chapter, I discuss the implications of this work and propose directions for further study.

RARP-1 as a periplasmic regulator of the rickettsial life cycle

Using multiple orthogonal approaches, I found no evidence for RARP-1 secretion by *R. parkeri*. GSK-RARP-1 was not phosphorylated, indicating that it did not access the host cytoplasm. Despite their ability to complement the *rarp-1*::Tn infectious focus defects, 3xFLAG-RARP-1 and 3xFLAG-Ty1-RARP-1 were not detectable in the host cytoplasm by blotting. Using immunofluorescence microscopy, 3xFLAG-RARP-1 was only observable along the periphery of

lysozyme-permeabilized bacteria, suggestive of periplasmic localization; indeed, co-immunoprecipitation mass spectrometry (co-IP/MS) identified putative 3xFLAG-RARP-1 binding partners that access the periplasm. Finally, endogenous, untagged RARP-1 was not detectable in the host cytoplasm by blotting.

How can these results be reconciled with the study by Kaur *et al*. (3)? The most generous explanation is that *R. parkeri* RARP-1 (RpRARP-1) and *R. typhi* RARP-1 (RtRARP-1) have different secretion behaviors. RpRARP-1 and RtRARP-1 only have 70% sequence similarity (Figure 4.1; note that most differences occur in the central intrinsically disordered region), and these differences may confer distinct fates for the two proteins. If true, this model raises interesting questions about protein structure-function diversification between two species with different lifestyles (addressed in Chapter 1). An alternative explanation is that neither RpRARP-1 nor RtRARP-1 are secreted during infection. Using an antibody against RtRARP-1, Kaur *et al*. detected unique cytoplasmic speckles in host cells infected with *R. typhi*. Nevertheless, absent a *R. typhi rarp-1* mutant, the specificity of this staining pattern to RtRARP-1 *per se* (and not some other infection-specific protein) cannot be determined. Using the same antibody, Kaur *et al*. observed a unique band in the cytoplasmic lysate fraction of infected cells that they noted was a different size from the doublet of bands observed in the bacterial pellet fraction. Again, without a *R. typhi rarp-1* mutant, the specificity of any of these bands cannot be determined. Alternative secretion assays with *R. typhi* that do not rely on such a mutant (*e.g.*, GSK tag phosphorylation, epitope tag detection, or BONCAT pull-down) could provide much-needed clarity.

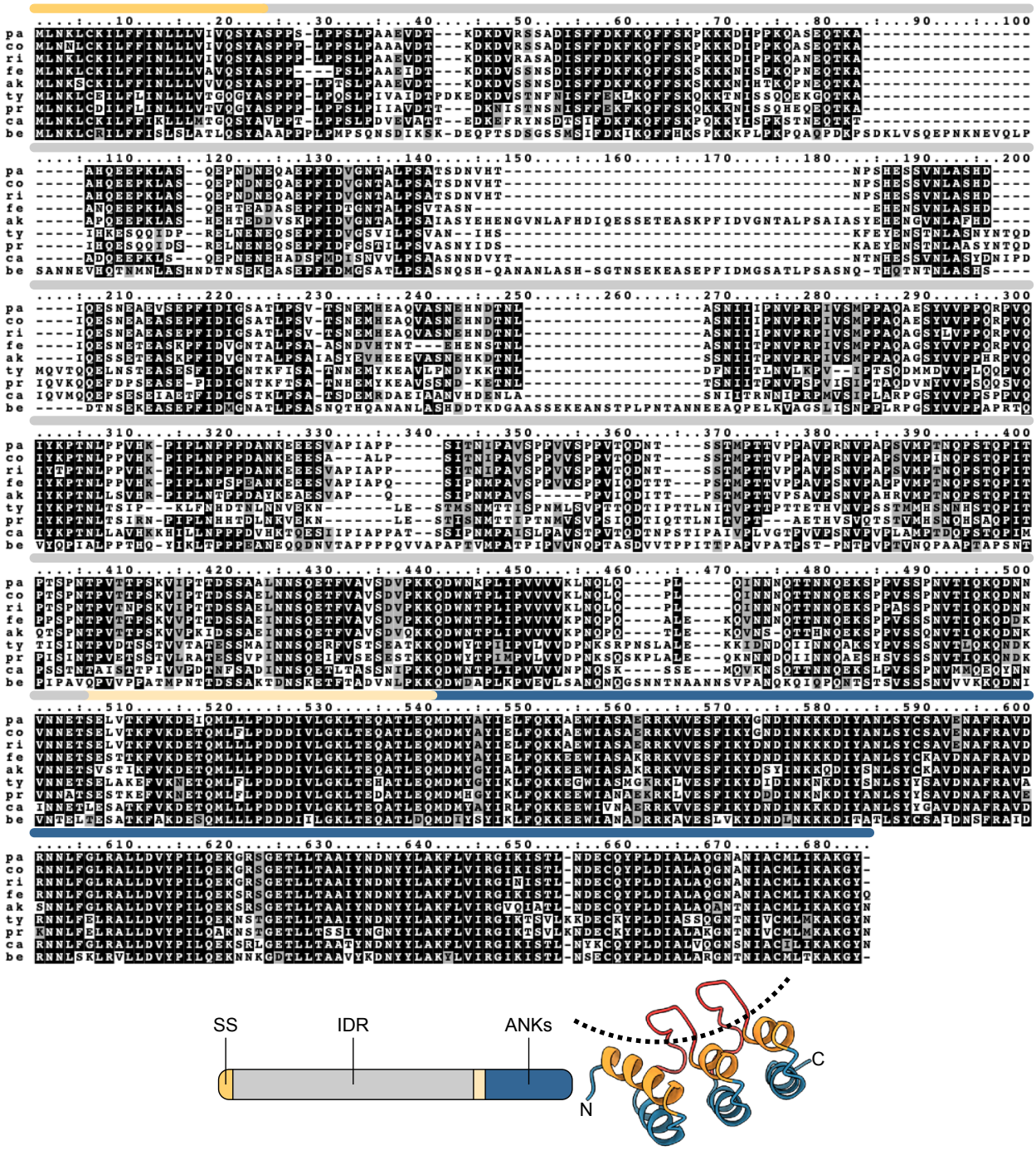

Figure 4.1 – RARP-1 conservation and ANKs. Scheme and sequence alignment of RARP-1 from representative members of the *Rickettsia* genus. Identical (black) and similar (grey) residues are shaded. *pa*, *R. parkeri*; *co*, *R. conorii*; *ri*, *R. rickettsii*; *fe*, *R. felis*; *ak*, *R. akari*; *ty*, *R. typhi*; *pr*, *R. prowazekii*; *ca*, *R. canadensis*; *be*, *R. bellii*; SS, Sec signal sequence; IDR, intrinsically disordered region; ANKs, ankyrin repeats. AlphaFold model of the RARP-1 ANKs showing the putative target recognition surface (dashed line) formed by the inner helices (yellow) and loops (red).

This work also calls into question the *E. coli* secretion assay used by Kaur *et al*. Following the same methodology described in that work, I failed to detect RpRARP-1 or RtRARP-1 in *E. coli* culture supernatants but successfully detected a known secreted protein (YebF). Although it is formally possible that the different *E. coli* K-12 strain (BW25113 versus C600) used in this work is responsible for the discrepancy, the fact remains that this secretion assay is not robust to its use by different laboratories. Furthermore, the model that periplasmic RARP-1 is secreted in a TolC-dependent manner raises interesting questions about secretion. As described in Chapter 1, the only proteins known to follow this non-canonical Sec-TolC route to the extracellular space are small (< 10 kDa) enterotoxins (4, 5). Passage through TolC would require that RARP-1 either remain unfolded in the periplasm or become unfolded immediately prior to its secretion through the activity of unknown chaperones (6). Moreover, the energy for opening the TolC aperture and translocating RARP-1 would have to be provided by unknown adaptor proteins. At least for the enterotoxin STII, the MacAB T1SS components appear to perform this role (5, 7); the functionality of the putative rickettsial T1SS (TolC-AprDE) and its ability to accommodate a much larger protein like RARP-1 (> 65 kDa) remains to be determined. A more parsimonious explanation is that RARP-1 simply remains in the periplasm.

What does RARP-1 do? The results from this work indicate that RARP-1 supports *R. parkeri* invasion and growth in the host cell niche. These steps of the life cycle are shared across all *Rickettsia* spp., in agreement with the conservation of RARP-1 across the genus. Nevertheless, the *rarp-1*::Tn mutant was still competent for both behaviors, suggesting that this conserved protein is not essential under the conditions tested. With advances in genetic tools to manipulate host cell biology (*e.g.*, genome-wide CRISPR screening), it would be interesting to see if there are unique host mutants that fail to support invasion and/or growth of the *rarp-1*::Tn

mutant. We might anticipate that the *rarp-1*::Tn mutant is hypersensitive to genetic ablation of particular host surface proteins or metabolic pathways that support rickettsial invasion or growth, respectively.

In parallel to this host-directed approach, a structure-function analysis of RARP-1 may provide insights into its mechanism of action. RARP-1 contains a large central intrinsically disordered region (IDR) and several C-terminal ankyrin repeats (ANKs). As discussed in Chapter 2, IDRs do not form ordered structures on their own (8); instead, their structural plasticity can support passage through protein channels and binding of diverse protein partners (8–11). It is possible that the RARP-1 IDR facilitates its translocation to the periplasm by maintaining the protein in a predominately unfolded state. Alternatively (or additionally), the IDR may mediate dynamic interactions between RARP-1 and other proteins in the periplasm (*e.g.*, the factors identified by co-IP/MS). To test these models, one could generate a *rarp-1*::Tn strain harboring 3xFLAG-RARP-1 construct lacking some or all of its IDR and then assess its ability to complement the *rarp-1*::Tn defects, localize to the rickettsial periphery and poles, and interact with proteins that co-purified with the full-length construct. A similar structure-function analysis could be performed with a RARP-1 mutant construct lacking its ANKs, since ANKs are among the most common protein-protein interaction modules (12). If such a fully disordered construct cannot be expressed (*i.e.*, is targeted for proteolysis), point mutations within the ANKs may be necessary. Of particular interest are residues predicted to form the target recognition surface that are also conserved across the genus (Figure 4.1) (13, 14). It should be noted, however, that ANKs can also bind sugars and lipids (15, 16); these interaction partners would not be identifiable by co-IP/MS, and testing the RARP-1 ANKs for such behavior would require extensive *in vitro* characterization. Finally, it would be interesting to test a divergent RARP-1 (*e.g.*, RARP-1 from

R. bellii) for complementation of the *rarp-1*::Tn mutant to see if the function of RARP-1 is conserved across the genus.

The above structure-function analyses may help narrow down the list of RARP-1 binding partners for further study. Sca2 was the only hit that had been previously characterized in *R. parkeri* (17), and yet Sca2 expression, localization, and actin tail formation were not affected in the *rarp-1*::Tn mutant. These results suggest that RARP-1 is dispensable for Sca2 function, but it is still possible that Sca2 promotes RARP-1 function. For example, polarization of Sca2 may drive RARP-1 to the rickettsial poles; expression of 3xFLAG-RARP1 by the *sca2*::Tn mutant should address this hypothesis. Nevertheless, since the loss of Sca2 does not cause a growth defect (18), it is unclear how Sca2 would act upstream of RARP-1 to support its activity. Other conspicuous hits in the co-IP/MS dataset include RvhB9 and RvhB10, components of the T4SS outer membrane core complex (19). We might anticipate that RARP-1 could support the assembly, localization, or effector export of the T4SS apparatus. As discussed in Chapter 1, no rickettsial T4SS substrates have been conclusively identified, but several candidates have been proposed based on their interactions with RvhD4 (20–22). Thus, it would be interesting to test for effector secretion (*e.g.*, GSK-tagged RARP-2 or Risk1) by the *rarp-1*::Tn mutant, especially given the potential roles of these effectors in the *R. parkeri* life cycle. The remaining putative binding partners include hypothetical porins and lipoproteins; given the role of these proteins in nutrient exchange and bacterial physiology, it is possible that RARP-1 modulates their activities to support infection. Using RNA-Seq to compare WT and *rarp-1*::Tn mutant transcriptomic profiles may provide clues about why the *rarp-1*::Tn mutant is defective in growth and invasion. Furthermore, the development of tools for targeted genetic manipulation (*e.g.*, CRISPRi-

mediated knockdown) in *Rickettsia* spp. could enable epistasis analysis for RARP-1 and these as-of-yet uncharacterized periplasmic binding partners.

BONCAT: optimization and future uses

Cell-selective BONCAT permitted the identification of both known and novel effectors secreted by *R. parkeri*. As discussed in Chapter 3, however, this list of effectors is not exhaustive: effector coverage is limited by both biological and technical constraints. Biologically, the efficiency and tolerance of Anl incorporation by MetRS* as well as the timing and extent of effector production and secretion all dictate effector capture. As an alternative strategy, I piloted cell-selective BONCAT through incorporation of the Phe analog azidophenylalanine (Azf) by PheRS* (23). Unfortunately, Azf labeling was inefficient and coincided with rickettsial filamentation and altered surface staining (Figure 4.2). Technically, the efficiency of effector protein extraction, click-tagging, pulldown, digestion, and peptide identification likewise influence how much of the secretome is detected. I attempted to optimize many of the technical aspects (*e.g.*, lysis buffers, click reaction conditions, clickable tags, precipitation and solubilization approaches, resins, washes, and cleavage methods) in pilot experiments, but there is plenty of room for improving the efficiency and simplicity of the method. As it stands, cell-selective BONCAT with MetRS* *R. parkeri* can provide a qualitative snapshot of the secretome; methodological innovations will be necessary for quantitative coverage of the secretome.

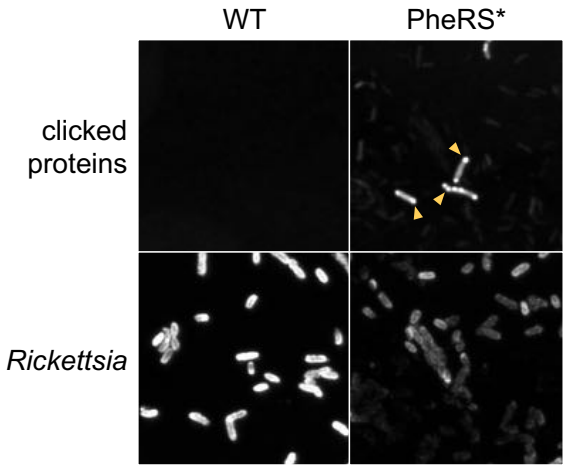

Figure 4.2 – Cell-selective BONCAT using PheRS*. Images of WT and PheRS* *R. parkeri* treated with azidophenylalanine (Azf) during infection of A549 cells. Bacteria were permeabilized and stained, and Azf-labeled proteins were detected by tagging with an alkyne-functionalized fluorescent dye. Note the filamentation, poor labeling relative to background, puncta of labeled proteins (arrowheads), and uneven surface staining of the PheRS* strain.

Even as a qualitative approach, however, cell-selective BONCAT has the potential to address important questions in rickettsial biology (Figure 4.3). For example, how is the secretome modulated by environmental cues? Perturbing host metabolism can have a dramatic impact on rickettsial physiology (24, 25), and it stands to reason that the rickettsial secretome is likewise affected under such conditions. With sufficiently high bacterial burdens, pulse-labeling with Anl may reveal temporal regulation of the secretome, as has been demonstrated for *Yersinia enterocolitica* (26). Different effectors may be secreted at different steps of the life cycle (*e.g.*, immediately following invasion or in the hours before and after Sca2 tail formation), and such an approach would complement transcriptomic data. Although this work analyzed effector secretion during infection of human host cells, it is possible that the repertoire of secreted effectors is tuned for infection of the tick cell niche; to that end, cell-selective BONCAT during *R. parkeri* infection of a tick cell line (*e.g.*, ISE6) should be straightforward. Furthermore, the fact that the MetRS* system is plasmid-based should facilitate cell-selective BONCAT in other *R. parkeri* strains (*e.g.*, transposon mutants) or even other *Rickettsia* spp. (*e.g.*, *R. bellii*). Comparing such

effector profiles could help identify regulators of secretion or highlight core and unique effector sets across the genus. Finally, the feasibility of this method should lend itself to effector identification in similarly intractable systems; indeed, several labs have discussed implementing cell-selective BONCAT in *Anaplasma*, *Wolbachia*, and other intracellular bacteria.

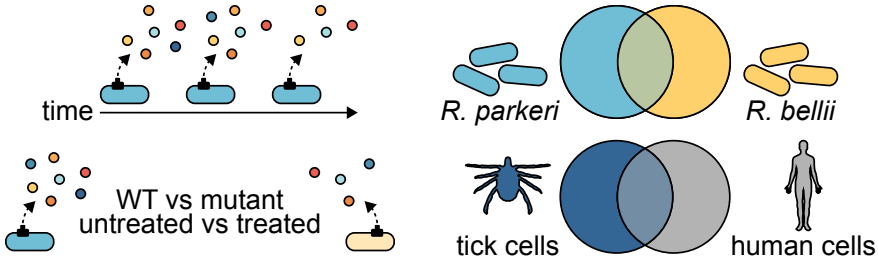

Figure 4.3 – Future uses for cell-selective BONCAT. Future work could leverage BONCAT to explore how the rickettsial secretome changes over the course of infection, in response to genetic or chemical perturbation, and across different species and host cell niches.

Exploring Srf function

SrfA–G present exciting new opportunities to investigate effector function. In general, future efforts to characterize these Srfs would benefit from the workflow used to study SrfD: generation of antibodies against the endogenous protein, co-IP/MS for binding partners during infection, validation of interactions, and domain analyses. High-quality anti-Srf antibodies are of particular importance given the unpredictability of expressing tagged effectors in *R. parkeri*. For example, I was unable to detect expression of GSK-tagged SrfB or SrfE; 3xFLAG-tagged SrfB, SrfC, SrfE, and SrfF expressed poorly, if at all; and 3xFLAG-, Ty1-, Myc-, or HA-tagged SrfD failed to yield transformants. Such failures may be due to interference from the epitope tags or from ectopic production of the Srfs above endogenous levels; regardless, they highlight the value of studying the "ground truth" of the untagged, endogenous effector. Similarly, identifying and validating binding partners during infection is cumbersome but closer to the "ground truth" than performing pull-downs with uninfected Srf-expressing host cells. On a related note, the vector

cell context should not be ignored. Although this work focused on the interface between rickettsiae and mammalian host cells, the activity of each Srf may be different in the arthropod vector cell niche. Again, co-IP/MS for Srf binding partners during infection of a tick cell line could yield valuable insights into Srf function. It was fortuitous that the SrfD-Sec61 interaction could be recapitulated in an uninfected setting, but it is possible that infection-specific cues (*e.g.*, a host response or other rickettsial effector) are required for interactions between the other Srfs and their cognate binding partners. In cases where Srfs can be studied exogenously, structure-function analyses should be straightforward. Finally, genetic or biochemical perturbation of a host cell target could serve as a proxy for studying Srf function during infection.

Generation of *srf* mutants will ultimately be necessary for understanding the role of each Srf during infection. As discussed in Chapter 1, targeted mutagenesis of rickettsiae is still in its infancy (27), and thus random transposon mutants have been the mainstay of mechanistic studies. If a Srf is essential for infection, however, a transposon mutant will not be recoverable. Moreover, many of the Srfs are located within potential operons, and polar effects may obfuscate Srf function even if such mutants are viable. The advent of tools for inducible knockdown (*i.e.*, CRISPRi) may provide a workaround for isolated Srfs for which transposon mutants do not exist. Alternatively, gain-of-function studies with *Rickettsia* spp. lacking particular Srfs (*e.g.*, *R. bellii*) may be possible for Srfs that can be expressed ectopically by these bacteria. Indeed, ectopic RARP-2 expression by *R. rickettsii* str. Iowa (which encodes a truncated RARP-2) confers a lytic plaque phenotype similar to the plaques produced by *R. rickettsii* str. Shiela Smith (which encodes full-length RARP-2) (22).

Characterization of Srf structures could inform these functional studies. As discussed in Chapter 3, SrfB–G have limited or no sequence homology outside the *Rickettsia* genus.

Consequently, AlphaFold models for these proteins are replete with low-confidence regions, even when those regions are not predicted to be disordered (Figure 4.4) (13, 14). SrfG is a notable exception to this rule in that, aside from its N-terminus, it is modelled with high confidence. Comparison of the SrfG model against the AlphaFold Database using Dali yielded putative structural homology to GTPase-activating proteins (GAPs) (Figure 4.5) (28). GAPs typically inactivate their cognate GTP-binding proteins by accelerating GTP hydrolysis using an Arg finger (29), and other bacterial pathogens secrete GAP domain-containing effectors to manipulate host cell signaling (30–32). The SrfG model retains this conserved Arg finger, but SrfG is not cytotoxic when exogenously expressed in host cells. Further characterization is needed to confirm or refute the hypothesis that SrfG behaves as a GAP. Regardless, obtaining structures for the Srfs could reveal new ways rickettsiae employ molecular mimicry or uncover hitherto uncharacterized protein folds that are not readily predicted by *in silico* tools.

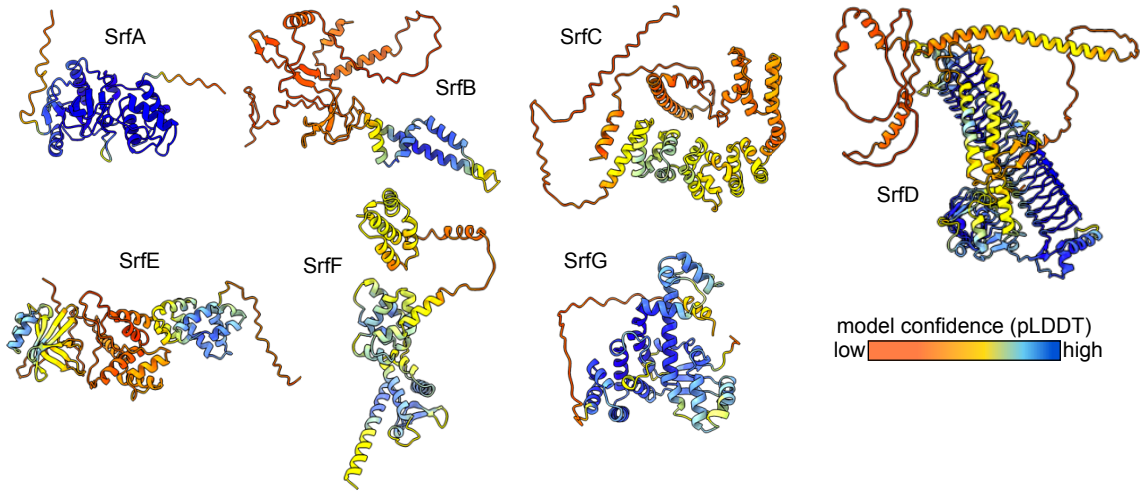

Figure 4.4 – Srf AlphaFold models. AlphaFold models for SrfA–G colored by per-residue confidence score (pLDDT). Note the extensive regions of low confidence (yellow and orange, pLDDT < 70) for most Srfs.

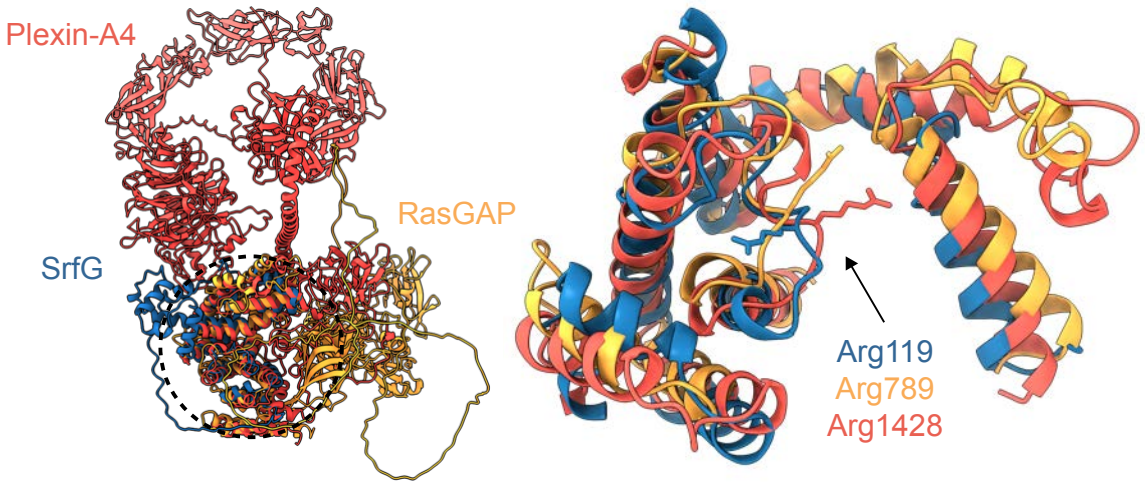

Figure 4.5 – SrfG has putative structural homology to GAPs. Left, AlphaFold models for SrfG (blue) superimposed on the human GAP domain-containing proteins RasGAP (yellow, P20936, Dali Z-score = 9.1) and Plexin-A4 (red, Q9HCM2, Dali Z-score = 8.4). Dotted circle, region of interest shown at right. Right, discontinuous structural alignment with conserved Arg finger indicated (arrow).

This work raises numerous questions about the Srfs and rickettsial biology, only a sample of which are included below. What mediates Srf secretion? The Srfs are not obvious T1SS or T4SS effectors by *in silico* predictions, and yet they are presumably translocated by these systems. Even the C-termini of the Srfs (where such secretion signal sequences are often located) have unique characteristics: SrfD has a positively charged C-terminal tail (like Risk1), but the remaining Srfs have acidic C-termini (like RARP-2). Moreover, SrfC, SrfD, and SrfF appear to be secreted with different efficiencies or otherwise have different stabilities in the infected host cytoplasm (see Figure 3.5B). What selective pressures have acted on the Srfs? SrfE and SrfG are found across the genus, and yet SrfA, SrfB, and SrfD are absent from TG rickettsiae (see Figure 3.2). Likewise, the C-terminus of SrfF is divergent across different groups, whereas even the regions of SrfD outside of the low-complexity pentapeptide repeats are highly conserved. What is the benefit to secreting an amidase (SrfA) into the host cytoplasm? *Rickettsia* spp. appear to encode some components of the peptidoglycan recycling pathway (33), but the extent to which these bacteria release peptidoglycan during infection (either during normal growth and division

or from lysis) is unknown. It is tempting to speculate that SrfA could act against other bacteria in the vector microbiome or help limit the activation of cytoplasmic peptidoglycan sensors (*e.g.*, Nod1) in the event that peptidoglycan is released. How do SrfB and SrfC localize to the mitochondria and ER, respectively? Neither contain canonical targeting signals or transmembrane helices, and so it is possible that they are targeted to those compartments by interactions with their cognate binding partners. Where does SrfE localize? The SrfE puncta observed from exogenous expression do not colocalize with early endosomes or lysosomes, and it is unknown if this localization pattern recapitulates that of endogenous SrfE secreted during infection. How have the activities of SrfG and its DUF5410-containing paralog diverged? This paralog was identified as an interaction partner of RvhD4 (21, 34), but it is unknown if this protein is a *bona fide* effector or if SrfG is a T4SS effector. This list of questions is by no means exhaustive, and each Srf presents opportunities to explore aspects of rickettsial biology, evolution, and interactions with the host cell.

SrfD as a regulator of Sec61 activity

SrfD is the best characterized of the Srfs thus far and yet many questions remain. As discussed in Chapter 3, SrfD localizes to the ER and interacts with the host Sec61 translocon. Curiously, these phenotypes are separable: the N-terminal pentapeptide repeat (PPR1 and PPR2) and coiled coil (CC1) domains are individually necessary for the SrfD-Sec61 interaction, but no single domain is necessary for targeting to the ER. How does SrfD localize to the ER? Although it is formally possible that SrfD secreted during infection is recognized as a Sec61 substrate, post-translational translocation in higher eukaryotes is generally reserved for short secretory proteins (reviewed in Chapter 1). Furthermore, for this model to be true, the N-terminal domains

of SrfD would have to clog or otherwise promote a stable interaction with Sec61 that is dispensable for ER localization. Depleting Sec62, which is required for efficient post-translational translocation (35), and then evaluating SrfD localization could address if SrfD is a Sec61 substrate. Alternatively, multiple domains of SrfD may redundantly drive ER localization from the cytoplasm or a cryptic targeting signal outside of the tested domains may be responsible for this behavior. Further structure-function experiments could provide clarity.

Is the interaction between SrfD and Sec61 direct or indirect? SrfD does not resemble any known Sec61 accessory factor, and yet I did not detect a putative bridging factor (host or bacterial) by co-IP/MS. Reconstituting SrfD with the Sec61 translocon *in vitro* would be non-trivial, but it could help distinguish between these two models. If the interaction is direct, it is unclear if SrfD binds a particular subunit of Sec61. In co-IP/MS experiments where I pulled down on SrfD secreted during infection, the α and β subunits were robustly co-enriched; thus, SrfD may interact directly with both subunits or one subunit may be pulled down with the other. Curiously, in preliminary co-IP/MS experiments where I pulled down on Sec61β from SrfD-expressing cells, Sec61α was only co-enriched with Sec61β when full-length SrfD was present (Figure 4.6): Sec61α was not pulled down with Sec61β following transfection of an empty vector control or SrfD mutants (ΔPPR1 and ΔCC1) that fail to co-IP with Sec61β (see Figure 3.8). These results suggest that SrfD may somehow strengthen the interaction between the α and β subunits, which is otherwise disrupted by the lysis conditions I use for this assay. Ultimately, crosslinking experiments could help determine which (if any) subunits of Sec61 bind to SrfD.

Hit	empty vector	3xFLAG-		
		SrfD	SrfDΔPPR1	SrfDΔCC1
SrfD	0	163	0	0
Sec61α	0	22	0	0
Sec61β	20	23	24	21

Figure 4.6 – Sec61 spectral counts from Sec61β co-IP/MS. Sec61β was immunoprecipitated from HEK293Ts transfected with an empty vector control or 3xFLAG-tagged SrfD constructs. Note the absence of Sec61α in conditions where SrfD is absent (empty vector) or otherwise fails to interact with Sec61β (SrfDΔPPR1 and SrfDΔCC1 mutants).

Interestingly, an AlphaFold model containing SrfD and Sec61 predicts (albeit with low confidence for SrfD-Sec61 residue pairs) an interface between CC1 and the cytosolic face of Sec61α (Figure 4.7). This model is thus far consistent with my characterization efforts. Ablation of CC1 would eliminate the SrfD-Sec61 interaction, and it is possible that removal of PPR1 or PPR2 prevents the proper positioning of CC1 at this interface. Meanwhile, the (poorly modeled) transmembrane helices could root SrfD at the ER membrane even when the SrfD-Sec61 interaction is disrupted. The cytosolic N-terminus of Sec61β is largely unstructured and thus not predicted to interact with SrfD, but it stands to reason that binding of SrfD to Sec61α could stabilize its interactions with the other subunits even if SrfD does not also bind Sec61β. If the AlphaFold model is correct, more precise mutations within CC1 should disrupt the SrfD-Sec61 interaction. Again, crosslinking experiments (coupled with MS) or a structure of the SrfD-Sec61 complex could address the validity of this model.

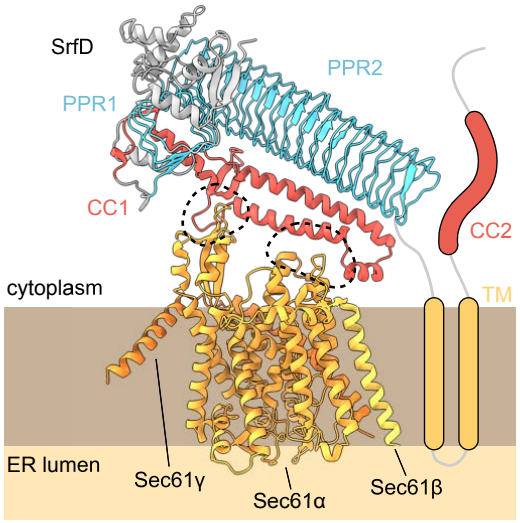

Figure 4.7 – AlphaFold model of SrfD with Sec61. Putative interface (black dotted circles) between the SrfD N-terminal domains (blue, PPR1 and PPR2; red, CC1) and Sec61 heterotrimer (light orange, α; yellow, β; dark orange, γ). The putative C-terminal transmembrane helices (yellow, TM) and CC2 (red) of SrfD were poorly modeled, but their predicted topology is included for clarity. The disordered N-terminal tail of Sec61β was also poorly modeled, but it was omitted for clarity.

What is the functional consequence of the SrfD-Sec61 interaction? Expression of SrfD had no impact on secretion of *Gaussia* luciferase, which harbors a canonical Sec signal peptide. As discussed in Chapter 1, known small molecule inhibitors of Sec61 bind deep within Sec61α to stabilize the closed state (36). Assuming SrfD binds a different interface, perhaps it is not surprising that SrfD fails to phenocopy these inhibitors. The luciferase assay results suggest that SrfD does not disrupt (or promote) co-translational translocation of a secreted protein, but it is possible that SrfD affects co-translational translocation of other secreted proteins (*i.e.*, in a client-selective manner) or membrane proteins, post-translational translocation, or other behaviors of Sec61. Using other clients (*e.g.*, a multi-pass transmembrane protein, glycoprotein, or short secretory protein) to report on Sec61 activity in the presence of SrfD could address the first two models. Alternatively, proteomics approaches could offer a more unbiased view of client-selective effects. In a preliminary quantitative label-free proteomics experiment, I failed to detect any proteomic changes in response to exogenous SrfD expression; nevertheless, a pulse-labeling

proteomics approach (*e.g.*, BONCAT or SILAC) could provide a readout for protein abundance changes that would otherwise be masked by slow turnover. Since the conditions I use for co-IP/MS appear to disrupt the translocon complex (at least in the absence of SrfD), crosslinking before lysis could reveal if SrfD interacts with a particular subset of translocons or otherwise changes the composition of the translocon. Live-cell imaging with calcium reporters or monitoring IRE1 activity could help determine if SrfD influences the role of Sec61 in ER homeostasis. In a pilot experiment where I co-transfected SrfD with an IRE1 reporter (wherein *XBP1* splicing by active IRE1 yields a frameshift that permits translation of mNeonGreen) (37), I did not observe obvious induction or suppression of IRE1 activity by SrfD (Figure 4.8). Blotting for phosphorylated IRE1 in the presence of SrfD could provide a direct confirmation of this null result. Curiously, expression of the SrfD N-terminal domains is highly toxic to yeast (Figure 4.9); assuming SrfD still interacts with Sec61 in this context, the yeast expression system may offer a more tractable means to study the impact of SrfD on fundamental cell biological processes (38). A final possibility is that SrfD does not impact Sec61 activity, but that it instead interacts with the translocon to act on other host targets at the ER. Although I cannot rule out this model, only the Sec61 complex was specifically co-enriched with SrfD during infection.

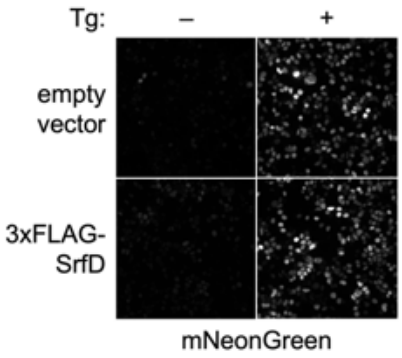

Figure 4.8 – IRE1 reporter activity in SrfD-expressing cells. HEK293Ts were co-transfected with an IRE1 reporter (*XBP1* splice-responsive mNeonGreen targeted to the nucleus) and either an empty vector control of

3xFLAG-SrfD and then treated with (+) or without (–) the ER stress inducer thapsigargin (Tg). Nuclear mNeonGreen is shown for a representative field of cells.

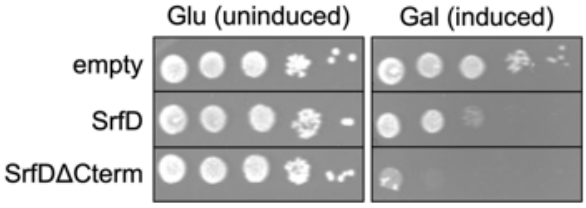

Figure 4.9 – Yeast toxicity assay for SrfD. Ten-fold serial dilutions of yeast harboring a galactose-inducible empty vector, 6xHis-SrfD, or 6xHis-SrfD lacking the C-terminal transmembrane helices and CC2.

The conservation of SrfD in bacteria with such streamlined genomes suggests that it provides at least some benefit. How does the SrfD-Sec61 interaction promote rickettsial infection? It is tempting to speculate that SrfD could antagonize Sec61 to block the display of adhesion or immune signaling molecules or otherwise disrupt secretory protein homeostasis: weakened cell-cell junctions, dampened immune responses, and excess free amino acids could all support rickettsial infection. In a pilot experiment where I treated infected cells with a sub-cytotoxic dose of the Sec61 inhibitor ipomoeassin F, I did not observe an obvious impact on rickettsial burdens (Figure 4.10). Nevertheless, SrfD may have a different mode of action than ipomoeassin F (in agreement with the luciferase assay results), or this particular assay may not capture the influence of Sec61 on infection. Ultimately, the generation of a *srfD* mutant will be necessary to determine what benefit (if any) SrfD provides to rickettsial infection and in what cellular contexts it acts.

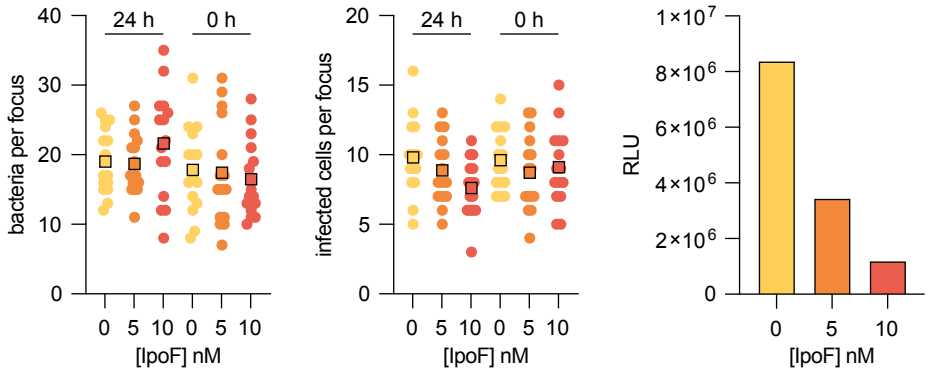

Figure 4.10 – Infectious focus assays with ipomoeassin F treatment. A549 host cells were treated with ipomoeassin F (IpoF) at the indicated concentrations 24 or 0 h before infection with *R. parkeri*. Bacteria (left) and infected cells (middle) were counted for 15 foci after infecting for 28 h (raw counts, circles; means, squares). Treatment with IpoF for 16 h was sufficient to reduce luciferase secretion by A549 cells stably expressing *Gaussia* luciferase (right).

References

1. Clark TR, Noriea NF, Bublitz DC, Ellison DW, Martens C, Lutter EI, Hackstadt T. 2015. Comparative Genome Sequencing of Rickettsia rickettsii Strains That Differ in Virulence. Infect Immun 83:1568–1576.

2. Lamason RL, Kafai NM, Welch MD. 2018. A streamlined method for transposon mutagenesis of Rickettsia parkeri yields numerous mutations that impact infection. PLOS ONE 13:e0197012.

3. Kaur SJ, Rahman MS, Ammerman NC, Ceraul SM, Gillespie JJ, Azad AF. 2012. TolC-Dependent Secretion of an Ankyrin Repeat-Containing Protein of Rickettsia typhi. J Bacteriol 194:4920–4932.

4. Yamanaka H, Nomura T, Fujii Y, Okamoto K. 1998. Need for TolC, anEscherichia coliouter membrane protein, in the secretion of heat-stable enterotoxin I across the outer membrane. Microbial Pathogenesis 25:111–120.

5. Yamanaka H, Kobayashi H, Takahashi E, Okamoto K. 2008. MacAB Is Involved in the Secretion of Escherichia coli Heat-Stable Enterotoxin II. J Bacteriol 190:7693–7698.

6. Delepelaire P. 2004. Type I secretion in gram-negative bacteria. Biochimica et Biophysica Acta (BBA) - Molecular Cell Research 1694:149–161.

7. Fitzpatrick AWP, Llabrés S, Neuberger A, Blaza JN, Bai X, Okada U, Murakami S, van Veen HW, Zachariae U, Scheres SHW, Luisi BF, Du D. 2017. Structure of the MacAB-TolC ABC-type tripartite multidrug efflux pump. Nat Microbiol 2:17070.

8. Dyson HJ, Wright PE. 2005. Intrinsically unstructured proteins and their functions. Nat Rev Mol Cell Biol 6:197–208.

9. Rodgers L, Gamez A, Riek R, Ghosh P. 2008. The Type III Secretion Chaperone SycE Promotes a Localized Disorder-to-Order Transition in the Natively Unfolded Effector YopE *. Journal of Biological Chemistry 283:20857–20863.

10. Housden NG, Hopper JTS, Lukoyanova N, Rodriguez-Larrea D, Wojdyla JA, Klein A, Kaminska R, Bayley H, Saibil HR, Robinson CV, Kleanthous C. 2013. Intrinsically Disordered Protein Threads through the Bacterial Outer Membrane Porin OmpF. Science 340:10.1126/science.1237864.

11. Holmes JA, Follett SE, Wang H, Meadows CP, Varga K, Bowman GR. 2016. Caulobacter PopZ forms an intrinsically disordered hub in organizing bacterial cell poles. PNAS 113:12490–12495.

12. Mosavi LK, Cammett TJ, Desrosiers DC, Peng Z. 2004. The ankyrin repeat as molecular architecture for protein recognition. Protein Sci 13:1435–1448.

13. Mirdita M, Schütze K, Moriwaki Y, Heo L, Ovchinnikov S, Steinegger M. 2022. ColabFold: making protein folding accessible to all. 6. Nat Methods 19:679–682.

14. Pettersen EF, Goddard TD, Huang CC, Meng EC, Couch GS, Croll TI, Morris JH, Ferrin TE. 2021. UCSF ChimeraX: Structure visualization for researchers, educators, and developers. Protein Sci 30:70–82.

15. Woodford CR, Thoden JB, Holden HM. 2015. A New Role for the Ankyrin Repeat Revealed by the Study of the N-formyltransferase from Providencia alcalifaciens. Biochemistry 54:631–638.

16. Kim DH, Park M-J, Gwon GH, Silkov A, Xu Z-Y, Yang EC, Song S, Song K, Kim Y, Yoon HS, Honig B, Cho W, Cho Y, Hwang I. 2014. Chloroplast targeting factor AKR2 evolved from an ankyrin repeat domain coincidentally binds two chloroplast lipids. Dev Cell 30:598–609.

17. Reed SCO, Lamason RL, Risca VI, Abernathy E, Welch MD. 2014. Rickettsia Actin-Based Motility Occurs in Distinct Phases Mediated by Different Actin Nucleators. Current Biology 24:98–103.

18. Kleba B, Clark TR, Lutter EI, Ellison DW, Hackstadt T. 2010. Disruption of the Rickettsia rickettsii Sca2 Autotransporter Inhibits Actin-Based Motility. Infect Immun 78:2240–2247.

19. Gillespie JJ, Phan IQH, Driscoll TP, Guillotte ML, Lehman SS, Rennoll-Bankert KE, Subramanian S, Beier-Sexton M, Myler PJ, Rahman MS, Azad AF. 2016. The Rickettsia type IV secretion system: unrealized complexity mired by gene family expansion. Pathog Dis 74:ftw058.

20. Rennoll-Bankert KE, Rahman MS, Gillespie JJ, Guillotte ML, Kaur SJ, Lehman SS, Beier-Sexton M, Azad AF. 2015. Which Way In? The RalF Arf-GEF Orchestrates Rickettsia Host Cell Invasion. PLOS Pathogens 11:e1005115.

21. Voss OH, Gillespie JJ, Lehman SS, Rennoll SA, Beier-Sexton M, Rahman MS, Azad AF. 2020. Risk1, a Phosphatidylinositol 3-Kinase Effector, Promotes Rickettsia typhi Intracellular Survival. mBio https://doi.org/10.1128/mBio.00820-20.

22. Lehman SS, Noriea NF, Aistleitner K, Clark TR, Dooley CA, Nair V, Kaur SJ, Rahman MS, Gillespie JJ, Azad AF, Hackstadt T. 2018. The Rickettsial Ankyrin Repeat Protein 2 Is a Type IV Secreted Effector That Associates with the Endoplasmic Reticulum. mBio 9:e00975-18.

23. Yuet KP, Doma MK, Ngo JT, Sweredoski MJ, Graham RLJ, Moradian A, Hess S, Schuman EM, Sternberg PW, Tirrell DA. 2015. Cell-specific proteomic analysis in Caenorhabditis elegans. Proc Natl Acad Sci U S A 112:2705–2710.

24. Ahyong V, Berdan CA, Burke TP, Nomura DK, Welch MD. 2019. A Metabolic Dependency for Host Isoprenoids in the Obligate Intracellular Pathogen *Rickettsia parkeri* Underlies a Sensitivity to the Statin Class of Host-Targeted Therapeutics. mSphere 4:e00536-19, /msphere/4/6/mSphere536-19.atom.

25. Sun H, Luu AP, Danielson M, Vo TT, Burke TP. 2023. Host glutathione is required for Rickettsia parkeri to properly septate, avoid ubiquitylation, and survive in macrophages. bioRxiv https://doi.org/10.1101/2023.10.02.560592.

26. Mahdavi A, Szychowski J, Ngo JT, Sweredoski MJ, Graham RLJ, Hess S, Schneewind O, Mazmanian SK, Tirrell DA. 2014. Identification of secreted bacterial proteins by noncanonical amino acid tagging. PNAS 111:433–438.

27. McClure EE, Oliva Chávez AS, Shaw DK, Carlyon JA, Ganta RR, Noh SM, Wood DO, Bavoil PM, Brayton KA, Martinez JJ, McBride JW, Valdivia1 RH, Munderloh UG, Pedra JHF. 2017. Engineering of obligate intracellular bacteria: progress, challenges and paradigms. Nat Rev Microbiol 15:544–558.

28. Holm L. 2022. Dali server: structural unification of protein families. Nucleic Acids Res 50:W210–W215.

29. Kötting C, Kallenbach A, Suveyzdis Y, Wittinghofer A, Gerwert K. 2008. The GAP arginine finger movement into the catalytic site of Ras increases the activation entropy. Proceedings of the National Academy of Sciences 105:6260–6265.

30. Frithz-Lindsten E, Du Y, Rosqvist R, Forsberg A. 1997. Intracellular targeting of exoenzyme S of Pseudomonas aeruginosa via type III-dependent translocation induces phagocytosis resistance, cytotoxicity and disruption of actin microfilaments. Mol Microbiol 25:1125–1139.

31. Fu Y, Galán JE. 1999. A salmonella protein antagonizes Rac-1 and Cdc42 to mediate host-cell recovery after bacterial invasion. Nature 401:293–297.

32. Von Pawel-Rammingen U, Telepnev MV, Schmidt G, Aktories K, Wolf-Watz H, Rosqvist R. 2000. GAP activity of the Yersinia YopE cytotoxin specifically targets the Rho pathway: a mechanism for disruption of actin microfilament structure. Mol Microbiol 36:737–748.

33. Oyler BL, Rennoll-Bankert KE, Verhoeve VI, Rahman MS, Azad AF, Gillespie JJ, Goodlett DR. 2022. Rickettsia typhi peptidoglycan mapping with data-dependent tandem mass spectrometry. bioRxiv https://doi.org/10.1101/2022.03.10.483817.

34. Lehman SS, Verhoeve VI, Driscoll TP, Beckmann JF, Gillespie JJ. 2024. Metagenome diversity illuminates the origins of pathogen effectors. mBio:e0075923.

35. Lang S, Benedix J, Fedeles SV, Schorr S, Schirra C, Schäuble N, Jalal C, Greiner M, Haßdenteufel S, Tatzelt J, Kreutzer B, Edelmann L, Krause E, Rettig J, Somlo S, Zimmermann R, Dudek J. 2012. Different effects of Sec61α, Sec62 and Sec63 depletion on transport of polypeptides into the endoplasmic reticulum of mammalian cells. J Cell Sci 125:1958–1969.

36. Itskanov S, Wang L, Junne T, Sherriff R, Xiao L, Blanchard N, Shi WQ, Forsyth C, Hoepfner D, Spiess M, Park E. 2023. A common mechanism of Sec61 translocon inhibition by small molecules. 9. Nat Chem Biol 19:1063–1071.

37. Nougarède A, Tesnière C, Ylanko J, Rimokh R, Gillet G, Andrews DW. 2018. Improved IRE1 and PERK Pathway Sensors for Multiplex Endoplasmic Reticulum Stress Assay Reveal Stress Response to Nuclear Dyes Used for Image Segmentation. Assay Drug Dev Technol 16:350–360.

38. Faris R, Weber MM. 2019. Identification of Host Pathways Targeted by Bacterial Effector Proteins using Yeast Toxicity and Suppressor Screens. JoVE 60488.